SKAT

Harnessing Water Power on a Small Scale

Volume 2

# Hydraulics Engineering Manual

Alex Arter / Ueli Meier

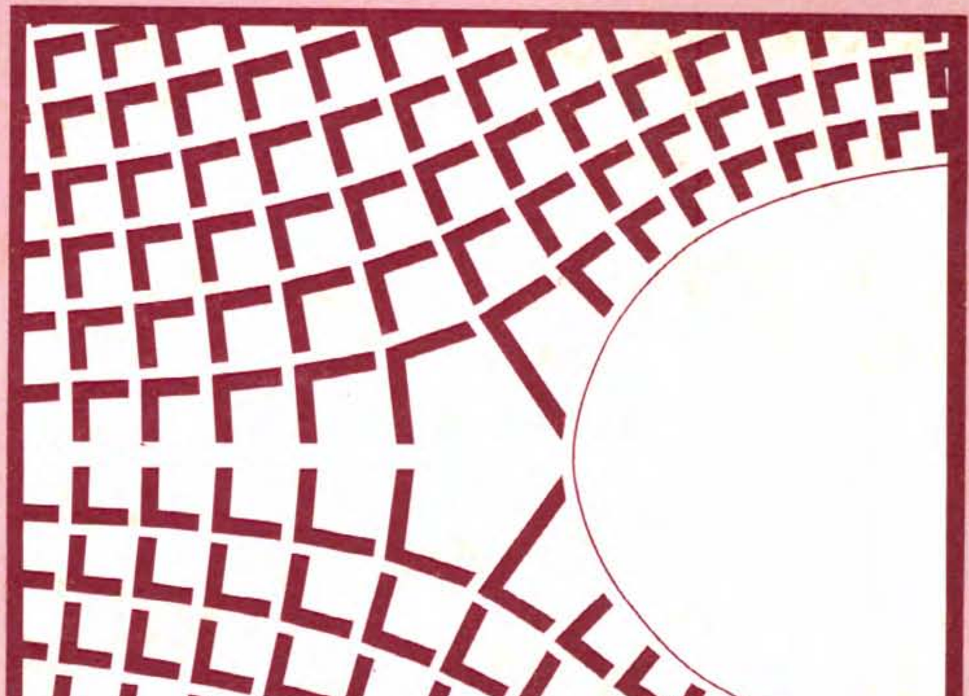

Harnessing Water Power on a Small Scale

# Hydraulics Engineering Manual

Volume 1 : Local Experience with Micro-Hydro Technology

Volume 2 : Hydraulics Engineering Manual

Volume 3 : Cross Flow Turbine Design and Equipment Engineering

Volume 4 : Cross Flow Turbine Fabrication

Volume 5 : Village Electrification

Volume 6 : The Heat Generator

Volume 7 : MHP Information Package

Volume 8 : Governor Product Information

First edition: 1990 by SKAT, Swiss Center for Appropriate Technology

Authors : Alex Arter, Head Hydropower Projects
Ueli Meier, Director SKAT

Published by : SKAT, Swiss Center for Appropriate Technology, St.Gallen, Switzerland

Layout : Werner Fuchs, Head Publications Department SKAT

Cover: F.Hartmann, Design, St.Gallen



Comments: Please send any comments concerning this publication to:
SKAT
Tigerbergstr. 2
CH - 9000 St.Gallen, Switzerland

Printed by : H. Harrer, St.Gallen, Switzerland

ISBN : 3-908001-13-7

---

**Distribution by:**

From 01.01.1993:
**SKAT**
Vadianstrasse 42,
CH-9000 St.Gallen, Switzerland
Tel: +41 (0)71 23 74 75
Fax: +41 (0)71 23 75 45

**and**

# Preface

It is well recognized today that the development of small hydropower resources in rural areas of less developed countries may be an important contribution to overall development, but also, that it is often a difficult task, given the many constraints existing. Nepal, on the slopes of the Himalayan range, has experienced a significant development in this field and the objective of the series HARNESSING WATER POWER ON A SMALL SCALE is to share this experience, for the benefit of many regions with undeveloped potential, in a large number of Third World countries.

Since the publication of the handbook "Local Experience with Micro-Hydropower Technology" (volume 1) in 1981, there have been substantial further developments in the adaptation and application of hydropower technology in less developed countries.

There has also been a steady process of development of relevant engineering skills in Nepal, where the local engineering firm Balaju Yantra Shala (BYS) has built up know-how progressively. In its history of small water turbine development and micro hydropower implementation, BYS has come a long way. It started with the production and installation of small turbine-mills of simple design, and, in a long learning process, moved on to design, manufacture and implement schemes for more complex village electrification projects.

Volume 1 of the series HARNESSING WATER POWER ON A SMALL SCALE, mentioned above, had the objective of giving an introduction to local micro hydropower technology, and of showing what was achieved by that time in Nepal. The publication met with profound interest and we have therefore made an effort in documenting what progress has been made since then. We felt that in order to do so it is necessary to also deal with the underlying theory as a prerequisite to full understanding and the transfer of the technology. The present volume 2, entitled HYDRAULICS ENGINEERING MANUAL, contains this theory and many tools for hydraulics design in the form of diagrams and nomograms. Among the various turbine types applicable, solely the theory of the Cross Flow turbine is given in detail, since this is the turbine type on which work of the past years concentrated. Laboratory testing of small turbines is also treated with material from actual tests conducted at the Hongkong Polytechnic Institute on machines designed and built in Nepal.

The series Harnessing Water Power on a Small Scale is further to be continued. Volume 3 and 4 shall be devoted to optimized Cross Flow turbine designs, equipment engineering and turbine fabrication and Volume 5 shall illustrate village electrification schemes implemented. Volume 6, which was published in 1983, deals with a mechanical heat generating device and thus represents a manual on the subject of energy application. Volume 7, being printed at present, is an annotated bibliography of literature and documents in the specific field of micro hydropower, and finally, volume 8 is going to be a handbook on governing systems for small scale hydropower.

SKAT, the Swiss Center for Appropriate Technology, is actively engaged in technology dissemination. Micro hydropower is one of our target areas and in addition to publishing activities, our information-, documentation- and consulting-services are available to those who plan to, or are engaged in, developing and implementing this technology with the chief objective of overall rural development.

St. Gallen, January 1990

# Acknowledgment

As in the past, the work on this publication has been made possible with financing by the Directorate for Development Cooperation and Humanitarian Aid of the Government of Switzerland (DEH/SDC). Actual development work in the field, which provided the practical experience upon which most of the contents of this manual are based, has been initiated and carried out by Balaju Yantra Shala (BYS), a private engineering firm in Kathmandu, Nepal, in cooperation with the Small Hydel Development Board (SHDB) of the Nepal government and was sponsored by His Majesty's Government, and jointly by the Nepal Industrial Development Corporation (NIDC) and Helvetas, a Swiss Organization for Development, over the past 15 years. In addition, Helvetas has also supported the work of the authors, in a material sense and otherwise, over many years.

The authors, both of which look back on many years of fruitful cooperation with BYS in Nepal, would like to gratefully acknowledge their thanks to all the institutions who made the past development work and the present publishing activity possible.

In the course of compiling material for the present volume, we have received support and cooperation from many sides. Our sincere thanks go to S. Devkota, General Manager of BYS for his support and the permission to use competition-sensitive materials of the company, to K.B. Nakarmi, Design Engineer of BYS for his excellent drawing work, to M. Pomfret, Senior Lecturer at the Hongkong Polytechnic for writing the chapter on laboratory testing and to M. Eisenring, of Eisenring Engineering, for the part on the water-hammer effect and to W. Roth who provided us with hard to come by photographs illustrating consequences of this hydraulic phenomena.

Many others have helped us in different ways and it is impossible to name all individuals and institutions. We wish to thank them all for their spirit of cooperation.

Finally, our thanks go to M. Weyermann who has done much of the typing and editing and to W. Fuchs who was responsible for desktop publishing and all other work related to getting this manual printed.

The Authors

St. Gallen, January 1990

# Nomenclature

| | |
|---|---|
| a | channel width, velocity of sound, coefficient of linear expansion |
| A | cross-sectional flow area, work, substitution used in formulae |
| b | inlet width, channel bottom width, crest width of weir |
| B | channel width (rectangular channel), substitution used in formulae |
| c | absolute velocity, coefficient, distance |
| $c_m$ | absolute velocity component in meridional direction |
| $c_u$ | absolute velocity component in peripheral direction |
| C | substitution used in formulae |
| d | grain size diameter, distance |
| D | diameter of penstock, nominal rotor diameter of turbine |
| E | YOUNG's modulus of elasticity |
| g | gravitational constant |
| h | headloss, water depth, hour, piezometric head |
| H | energy head |
| $H_{net}$ | net head |
| HP | horse power |
| k | friction coefficient (STRICKLER) |
| K | empirical coefficient, constant |
| L | length, wave length |
| n | rotative speed, safety factor, number, side wall slope |
| $n_s$ | specific speed (based on HP) |
| $N_s$ | specific speed (based on kW) |
| p | pressure |
| P | power, point, weir height |
| Q | flow rate, discharge |
| R,r | radius, hydraulic radius |
| rpm | revolutions per minute |
| s | slope, gradient |
| S | full load operating hours, stagnation point |
| t | time, running time, pitch, thickness of penstock |
| T | torque, time span, duration, period, cost per ton, temperature |
| u | peripheral velocity |
| U | wetted perimeter |
| v | velocity |
| w | relative velocity |
| $w_u$ | relative velocity component in peripheral direction |
| W | weight |
| z | blade number, geodetic head |
| $Z^2$ | ALLIEVI pressure rise factor |

## Greek symbols

| | | |
|---|---|---|
| $\alpha$ | (alpha) | absolute velocity angle |
| $\beta$ | (beta) | relative velocity angle |
| $\gamma$ | (gamma) | specific weight of water |
| $\Delta,\delta$ | (delta ) | difference, angle |
| $\varepsilon$ | (epsilon) | angle |
| $\zeta$ | (zeta) | head loss coefficient |
| $\eta$ | (eta) | efficiency |
| $\theta$ | (theta) | angle, ALLIEVI valve operation parameter |
| $\kappa$ | (kappa) | ratio, substitution used in formulae |
| $\lambda$ | (lambda) | ratio, substitution used in formulae |
| $\xi$ | (ksi) | angle |
| $\mu$ | (mu) | discharge coefficient |
| $\pi$ | (phi) | 3.14... |
| $\rho$ | (rho) | density, ALLIEVI penstock parameter |
| $\sigma$ | (sigma) | cavitation index, stress |
| $\phi$ | (phi) | flow factor |
| $\omega$ | (omega) | angular velocity |

## Subscripts

| | |
|---|---|
| ax | axial |
| b | blade |
| c | closing / opening |
| cr | critical |
| dyn | dynamic |
| e | energy |
| el | electrical |
| i | input, intermediate value |
| m | mean, average, meridional |
| max | maximum |
| min | minimum |
| net | net |
| o | output |
| opt | optimal |
| p | pitch circle |
| P | pump |
| perm | permissible |
| Q | flow, discharge |
| R | rotor |
| r | radial |
| s | suction, closing, specific |
| sp | specific |
| st | static |
| syn | synchronous |
| T | turbine |
| tot | total |
| th | theoretical |
| w | water |
| wc | wave cycle |
| u | peripheral |
| 0,1,2... | index |
| 0 | channel inlet |
| 1 | cascade inlet, machine inlet |
| 2, 4 | cascade exit |
| 3 | cascade inlet, machine exit |

# Contents

## Chapter 3: Performance tests on Cross Flow turbines

# Chapter 1 : Introduction to Cross Flow turbine theory

## 1.1 Definitions and fundamental relations

(Illustrations and text are based on [9])

### 1.1.1 Steady state flow

Flow is steady or at equilibrium if the relationship of two different values of velocity observed at different points remains constantly the same. This is the case if the flow rate of a fluid through both cross-sectional areas A and B in fig. 1.1 are equal. Flow through a pipe, from an overhead tank with constant water level to a lower point, is steady. If the cross-sectional area of the pipe outlet is changed, flow will reach steady state only after reaching a new equilibrium.

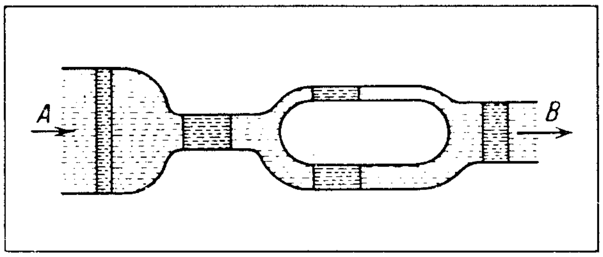


**Fig. 1.1: Steady state flow**

### 1.1.2 The equation of continuity

If Q [m³/s] is the flow rate of a fluid through a cross-sectional area A [m²], with an equal velocity c [m/s] at all points, the equation of continuity holds true for steady state flow:

$$\{1.1\} \quad \boxed{Q = c \cdot A = \text{constant}}$$

The observed cross-sectional area A must be perpendicular to all stream lines of the flow. For all practical purposes this is the case if the cross-sectional area is perpendicular to the axis of the conduit.

### 1.1.3 BERNOULLI's equation

The flow energy in all elements of a flowing fluid is composed of three components:

a) the potential energy component, which takes the value:

$$W \cdot h$$

where W is the weight of the liquid and h is the perpendicular distance or head above a reference level.

b) the pressure energy component, which takes the value of :

$$\frac{W \cdot p}{\gamma}$$

where p is the pressure [kg/m²] and $\gamma$ [kg/m³] is the density of the fluid (e.g. the pressure head $p/\gamma$), and

c) the velocity (or kinetic) energy component, which results from the velocity head :

$$\frac{c^2}{2\,g}$$

(according to the law of TORICELLI, $c = \sqrt{2\,g\,h}$), where g is the gravitational constant and h is the head, and the weight W of the fluid, at a value of

$$\frac{W\,c^2}{2\,g}$$

The energy head contained in 1 kg of fluid is therefore:

$$\{1.2\} \quad \boxed{H_e = h + \frac{p}{\gamma} + \frac{c^2}{2\,g} \quad [\text{mkg/kg}]}$$

For practical purposes of the study of flow, we may assume that all fluid elements contain equal amounts of energy at the entry point into the observed system, so that equation {1.2} is valid for the entire system. If no energy is fed into the system or extracted, we have the condition:

$$\{1.3\} \quad \boxed{h + \frac{p}{\gamma} + \frac{c^2}{2\,g} = \text{constant}}$$

Equation {1.3} is BERNOULLI's equation, expressing that no energy losses occur in a steady state flow system with inviscid (free of friction) fluids. Under the condition of h = constant, and for flow perpendicular to the cross-sectional area of reference, we have:

$$\{1.4\} \qquad \frac{p}{\gamma} + \frac{c^2}{2\,g} = \text{constant}$$

It is possible to derive from equation {1.4} that at points of lower pressure, higher velocities must exist, and vice versa. In a conduit of continuously decreasing cross-sectional area, where flow velocity increases according to equation {1.1} in proportion to the decrease of the cross-sectional area, pressure drops continuously. However, if velocity increases too much, resulting in excessive pressure decrease, separation of the fluid may result. In this situation, vapor bubbles form in the water as soon as the pressure has decreased to a point below the vapor pressure of the fluid. This phenomenon is called cavitation, and is usually accompanied by sound generated by vapor bubbles collapsing. Beginning cavitation results in a crackling or light rustling noise, or noise as if gravel is passing through the machine. In case of complete flow separation, noise increases to sounds like machine gun fire or thunder.

## 1.1.4 Dynamic pressure and stagnation point

If flow passes by an imerged object (such as in fig. 1.2), there will be a stream line which is divided at the leading edge of the object and which unites again at the downstream edge of the object.

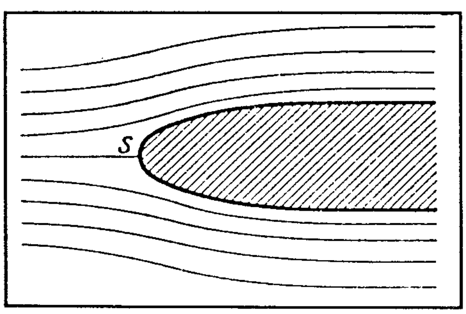


**Fig. 1.2: Rounded leading edge of an object imerged in a flowing fluid.
S = stagnation point**

The points at which this happens are named upstream and downstream stagnation point, respectively (notation S in fig. 1.2), because relative to the object, flow velocity at point S is zero. The dynamic pressure $h_{dyn}$ [meters of fluid column], resulting from the stagnated flow is:

$$\{1.5\} \qquad h_{dyn} = \frac{c^2}{2g} \qquad [m]$$

The dynamic pressure $p_{dyn}$ in pressure units [kg/m²] takes the value of:

$$\{1.6\} \qquad P_{dyn} = \frac{\gamma\, c^2}{2\,g} = \frac{\rho\, c^2}{2} \qquad [kg/m^2]$$

where the density is:

$$\rho = \frac{\gamma}{g}$$

## 1.1.5 Angular momentum equation

For purely rotational flow, the law of angular momentum is applied:

$$\{1.7\} \qquad r_1 \cdot c_1 = r_2 \cdot c_2 = r \cdot c = \text{constant}$$

Rotational flow is characterized by fluid elements moving vortex-like on a plane with a common center. We may determine from this equation, which is the equation of an equal-sided hyperbola, that the velocity c increases quickly with decreasing radius **r** (refer to fig. 1.3)

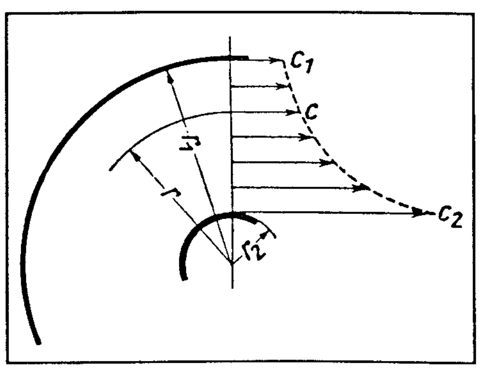


**Fig. 1.3: Velocity distribution according to the law of angular momentum**

Flow with these characteristics is called rotational or vortex flow. Velocity decrease towards the periphery and the related rise in pressure is explained by the increasing centrifugal forces. Rotational flow contained in a circular enclosure such as a pipe, requires in its center a solid core, because theoretically, an infinitely high velocity and therefore infinitely small pressure exists at the core, which in reality is a void as may be observed in a vortex.

## 1.1.6 The velocity triangle

An imaginary observer sitting on the blade of a revolving runner, would observe flow through the runner as if looking at a stationary rectangular closed conduit. In contrast to flow through a stationary conduit, flow in the observed runner has the relative velocity **w** in respect to the runner blade. However, a stationary observer outside the runner, observes the absolute velocity **c** of the moving fluid. The two velocities described are different by the peripheral velocity **u** of the runner, with **c** taking the higher value. The absolute velocity **c** is the result of the geometrical addition of the relative velocity **w** and the peripheral velocity **u**, according to the formula: **c = u + w**.
This situation is shown graphically in fig. 1.4 where the relative velocity **w**, flowing in the direction of the blade, and the peripheral velocity **u** in tangential direction, form a paralellogram as shown, or, together with the absolute velocity **c**, are forming velocity triangles.

In the velocity triangle shown, vectors **u** and **w** enclose the blade angle $\beta$ and vectors **c** and **u** enclose the absolute flow angle $\alpha$. The relative path of a fluid element is determined by the shape of the blade.

The widely accepted conventions for notations used in velocity triangles are:

c = absolute velocity
w = relative velocity
u = peripheral velocity
$\alpha$ = absolute velocity angle
$\beta$ = relative velocity angle

index 0 = channel inlet
index 1 = cascade inlet, blade channel entrance
index 2 = cascade exit

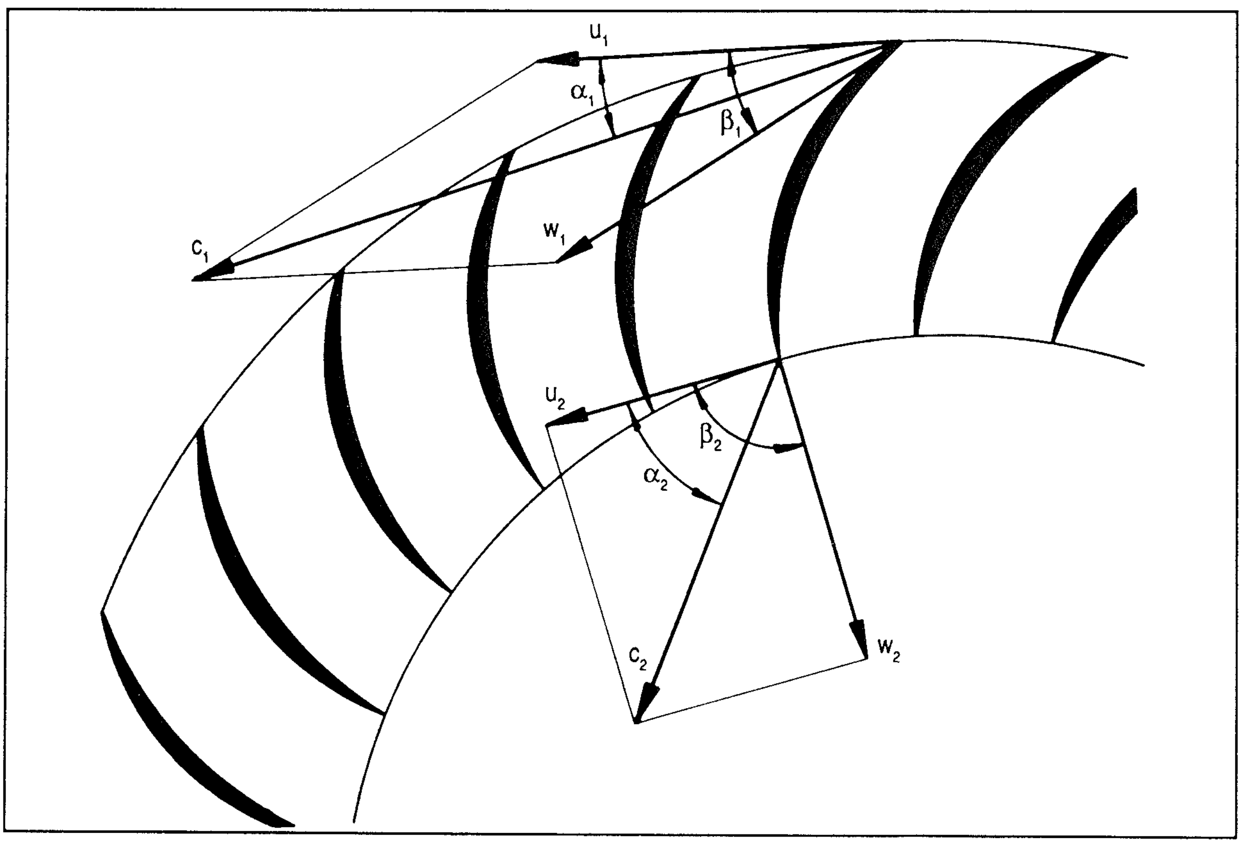


Fig. 1.4: Velocity triangles in a runner with peripheral blades

Further, it is essential to know the following terms shown in fig. 1.5:

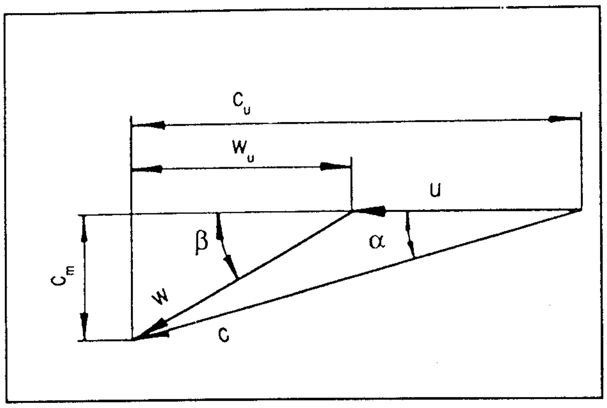


**Fig. 1.5: Terms used in velocity triangles**

$c_u = c \cos\alpha$ = absolute velocity component in peripheral direction
$w_u = w \cos\beta$ = relative velocity component in peripheral direction
$c_m = c \sin\alpha$ = absolute velocity component in meridional direction

Note: It is a general convention to not calculate with actual velocity values U,W,C, but with dimensionless expressions u,w,c, which represent the ratio of actual speed to free jet velocity, thus:

$$u = \frac{U}{\sqrt{2\,g\,H}}$$

where: g = gravitational constant = 9.81 [m/s²]
H = pressure head [m]

$$w = \frac{W}{\sqrt{2\,g\,H}}$$

$$c = \frac{C}{\sqrt{2\,g\,H}}$$

## 1.1.7 EULER equation

The precondition for an energy exchange between a moving fluid and a moving runner blade of a hydraulic machine is that the runner blade causes the fluid to change its velocity. In the case where the fluid is accelerated by the runner blade, energy is imparted by the runner blades to the fluid as happens in pumps. In the opposite case, where the fluid is retarded by the runner blade, energy is imparted to the runner of the machine by the moving fluid, which is the operating principle of all water turbines.

Speaking in terms of velocity triangles, energy exchange between the moving fluid and the blades of a turbine runner takes place, if the entrance velocity triangle is different from the exit velocity triangle. Since the entrance as well as the exit velocity triangles are composed of the three velocity vectors **c, u** and **w**, the value of each term needs to be compared between entrance and exit, and the following energy terms are thus established:

$$\{1.8\} \quad \boxed{\frac{c_1^2 - c_2^2}{2\,g}}$$

static pressure difference due to change of absolute velocity

$$\{1.9\} \quad \boxed{\frac{u_1^2 - u_2^2}{2\,g}}$$

static pressure difference due to centrifugal forces

$$\{1.10\} \quad \boxed{\frac{w_1^2 - w_2^2}{2\,g}}$$

dynamic pressure difference due to change of relative velocity

Based on this, the theoretical energy head $H_{th}$ of a runner system, transferring flow energy without loss into power, may be written in the form of the EULER equation:

$$\{1.11\} \quad \boxed{H_{th} = \frac{c_1^2 - c_2^2}{2\,g} + \frac{u_1^2 - u_2^2}{2\,g} - \frac{w_1^2 - w_2^2}{2\,g}}$$

The law of cosine makes the following expression implicit:

$$\{1.12\} \quad \boxed{w^2 = u^2 + c^2 - 2\,u\,c\cos\alpha}$$

where: α = the angle between the absolute and the peripheral velocity vectors

With:

{1.13} $$c \cos \alpha = c_u$$

where: $c_u$ = the absolute velocity vector in peripheral direction, $w^2$ may be expressed as:

{1.14} $$w^2 = u^2 + c^2 - 2\,u\,c_u$$

and therefore:

{1.15} $$H_{th} = \frac{u_1\,c_{u1} - u_2\,c_{u2}}{g}$$

where: $u$ = peripheral runner velocity
$c_u$ = the component of the absolute velocity acting in peripheral direction.

Equation {1.15} represents the EULER equation in its general form. The theoretically obtainable energy head $H_{th}$ is nothing else but the algebraic difference of the inlet moment of momentum and the exit moment of momentum of the system in question.

## 1.2. The concept of the Cross Flow turbine

The initial work of developing Cross Flow turbines in Nepal was based on the theory of professor Donat BANKI, who patented this novel concept around 1920. BANKI's papers have remained a very useful source of information and the present chapter is devoted to reproducing a free translation of his work by C.A. Mockmore and F. Merryfield, which was published many years ago by the Oregon State College in the U.S.A.

With kind permission of the Oregon State University, the most important passages of this publication, containing the full theory of BANKI, are reproduced here in its original, without any changes of wording or notation, as a basis for the understanding of subsequent chapters. In chapter 1.3, further theoretical and design aspects are presented, which are not found in the work of BANKI. Since notations, equations and figure numbering of the present originial text are not compatible with chapter 1.3., no further reference is made later on. Chapter 1.2 stands for itself as a fundamental basis.

# The Banki Water Turbine

By

C.A. MOCKMORE
Professor of Civil Engineering
and
FRED MERRYFIELD
Professor of Civil Engineering

Bulletin Series No.25
February 1949

Engineering Experiment Station
Oregon State System of Higher Education
Oregon State College
Corvallis

# The Banki Water Turbine

By
C.A. MOCKMORE
Professor of Civil Engineering
and
FRED MERRYFIELD
Professor of Civil Engineering

## I. INTRODUCTION

**1. Introductory statement.** The object of this Bulletin is to present a free translation of Donat Banki's paper "Neue Wasserturbine", and to show the results of a series of tests on a laboratory turbine built according to the specifications of Banki.

The Banki turbine is an atmospheric radial flow wheel which derives its power from the kinetic energy of the water jet. The caracteristic speed of the turbine places it between the so-called Pelton tangential water turbine and the Francis mixed-flow wheel. There are some unusual characteristics not found in most water wheels, which are displayed by the Banki turbine and should be of interest to most engineers, especially those of the Mountain States.

Included in this bulletin are diagrams of two Banki turbine nozzles as patented and used in Europe.

## II. THEORY OF THE BANKI TURBINE

**1.Description of turbine.** The Banki Turbine consists of two parts, a nozzle and a turbine runner. The runner is built up of two parallel circular disks joined together at the rim with a series of curved blades. The nozzle, whose cross-sectional area is rectangular, discharges the jet the full width of the wheel and enters the wheel at an angle of 16 degrees to the tangent of the periphery of the wheel. The shape of the jet is rectangular, wide, and not very deep. The water strikes the blades on the rim of the wheel (Figure 2), flows over the blade, leaving it, passing through the empty space beween the inner rims, enters a blade on the inner side of the rim, and discharges at the outer rim. The wheel is therefore an inward jet wheel and because the flow is essentially radial, the diameter of the wheel is practically independent of the amount of water impact, and the desired wheel breadth can be given independent of the quantity of water.

2. **Path of jet through turbine.** Assuming that the center of the jet enters the runner at point *A* (Figure 2) at an angle of $\alpha_1$ with the tangent to the periphery, the velocity of the water before entering would be

$$V_1 = C(2gH)^{1/2} \tag{1}$$

$V_1$ = Absolute velocity of water
$H$ = Head at the point
$C$ = Coefficient dependent upon the nozzle

The relative velocity of the water at entrance, $v_1$, can be found if $u_1$, the peripheral velocity of the wheel at that point, is known. $\beta_1$ would be the angle between the forward directions of the two latter velocities.

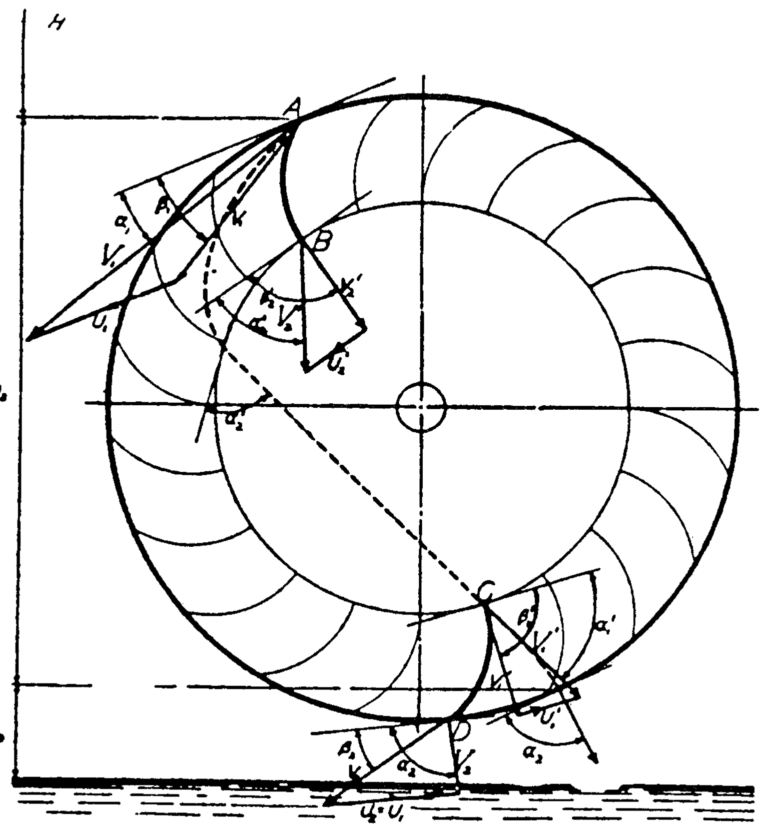


Figure 2. Path of water through turbine

For maximum efficiency, the angle of the blade should equal $\beta_1$. If *AB* represents the blade, the relative velocity at exit, $v_2'$, forms $\beta_2'$ with the peripheral velocity of the wheel at that point. The absolute velocity of the water at exit to the blade, $V_2'$, can be determined by means of $v_2'$, $\beta_2'$, and $u_2$. The angle between this absolute velocity and the velocity of the wheel at this point is $\alpha_2'$. The absolute path of the water while flowing over the blade *AB* can be determined as well as the actual point at which the water leaves the blade. Assuming no change in absolute velocity $V_2'$, the point *C*, where the water again enters the rim, can be found. $V_2'$ at this point becomes $V_1'$, and the absolute path of the water over the blade *CD* from point *C* to point *D* at discharge can be ascertained.

Accordingly
$$\alpha_1' = \alpha_2'$$
$$\beta_1' = \beta_2'$$
$$\beta_1 = \beta_2$$
since they are corresponding angles of the same blade.

It is apparent that the whole jet cannot follow these paths, since the paths of some particles of water tend to cross inside the wheel, as shown in Figure 3. The deflection angles $\theta$ and $\theta_1$ will be a maximum at the outer edge of each jet. Figure 3 shows the approximate condition.

3. **Efficiency.** The following equation for brake horsepower is true:

$$HP = (wQ/g)(V_1 \cos\alpha_1 + V_2 \cos\alpha_2)u_1 \tag{2}$$

Part of the formula (2) can be reduced by plotting all the velocity triangles as shown in Figure 3.

$$V_2 \cos \alpha_2 = v_2 \cos \beta_2 - u_1 \tag{3}$$

Neglecting the increase in velocity of water due to the fall $h_2$ (Figure 2) which is small in most cases,

$$v_2 = \psi v_1 \tag{4}$$

where $\psi$ is an empirical coefficient less than unity (about 0.98). From the velocity diagram Figure 4,

$$v_1 = (V_1 \cos\alpha_1 - u_1)/(\cos\beta_1) \tag{5}$$

Substituting equations (3), (4) and (5) in the horsepower equation (2)

$$HP_{\text{output}} = (WQu_1/g)(V_1\cos\alpha_1 - u_1)\cdot(1+\psi\cos\beta_2/\cos\beta_1) \tag{6}$$

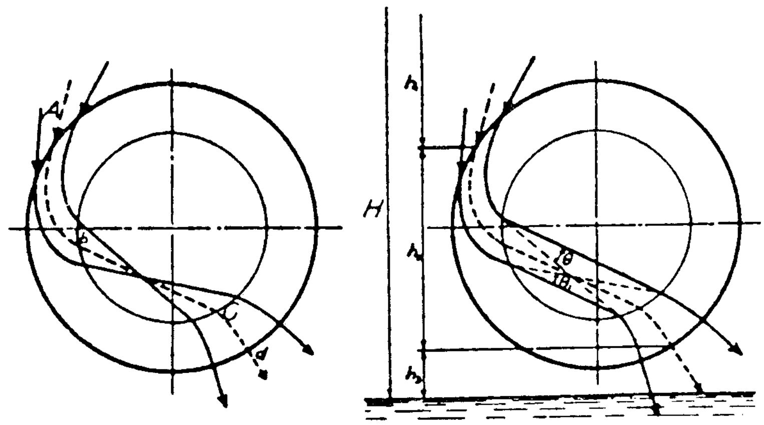


Figure 3. Interference of filaments of flow through wheel

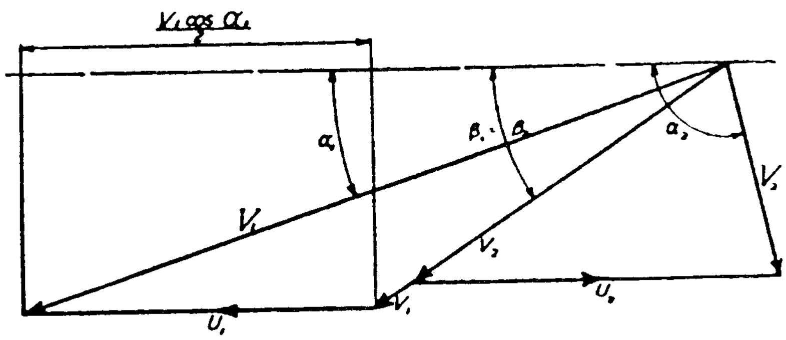

Figure 4. Velocity diagram

The theoretical horsepower input due to the head $H_1$

$$HP = wQH/g = wQV_1^2/C^2 2g \qquad (7)$$

The efficiency, $e$ , is equal to the ratio of the output and input horsepower,

$$e = (2C^2 u_1/V_1)\,(1 + \psi\cos\beta_2/\cos\beta_1)\cdot(\cos\alpha_1 - u_1/V_1) \qquad (8)$$

when

$$\beta_2 = \beta_1, \text{ then efficiency}$$
$$e = (2C^2 u_1/V_1)(1 + \psi)(\cos\alpha_1 - u_1/V_1) \qquad (9)$$

Considering all variables as constant except efficiency and $u_1/V_1$ and differentiating and equating to zero, then

$$u_1/V_1 = \cos \alpha_1/2 \tag{10}$$

and for maximum efficiency

$$e_{max} = 1/2C^2(1 + \psi) \cos^2\alpha_1 \tag{11}$$

It is noticeable (see Figure 4) that the direction of $V_2$ when $u_1 = 1/2V_1 cos\alpha_1$, does not become radial. The outflow would be radial with

$$u_1 = [C/(1 + \psi)] (V_1 \cos\alpha_1) \tag{12}$$

only when $\psi$ and $C$ are unity, that is, assuming no loss of head due to friction in nozzle or on the blades. To obtain the highest mechanical efficiency, the entrance angle $\alpha_1$ should be as small as possible, and an angle of 16° can be obtained for $\alpha_1$ without difficulty. For this value cos $\alpha_1 = 0.96$, $cos^2\alpha_1 = 0.92$.

Substituting in equation (11), $C = 0{,}98$ and $\psi = 0.98$, the maximum efficiency would be 87.8 per cent. Since the efficiency of the

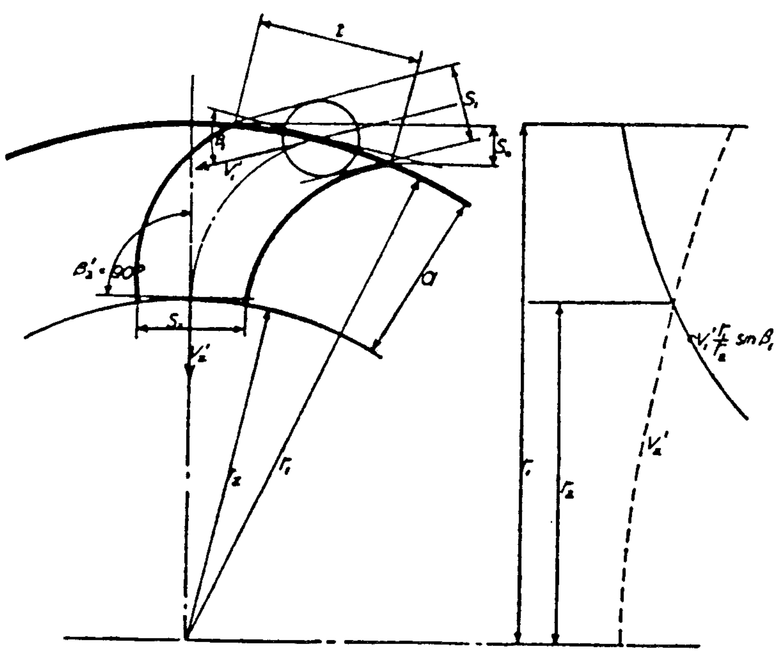

Figure 5. Blade spacing

nozzle varies as the square of the coefficient, the greatest care should be taken to avoid loss here. There are hydraulic losses due to water striking the outer and inner periphery. The latter loss is small, for according to computations to be made later, the original thickness of the jet $s_0$, Figure 5, increases to 1.90, which means that about 72 per cent of the whole energy was given up by the water striking the blade from the outside and 28 per cent was left in the water prior to striking the inside periphery. If the number of blades is correct and they are as thin and smooth as possible the coefficient $\psi$ may be obtained as high as 0.98.

## 4. Construction proportions

(A) Blade angle: The blade angle $\beta_1$, can be determined from $\alpha_1$, $V_1$ and $u_1$ in Figures 2 and 4. (10)

If $u_1 = 1/2V_1 \cos\alpha_1$ (13)

then $\tan\beta_1 = 2\tan\alpha_1$

assuming $a_1 = 16°$

then $\beta_1 = 29°50'$ or $30°$ approx.

The angle between the blade on the inner periphery and the tangent to the inner periphery $\beta_2$ can be determined by means of the following as shown in Figure 6. Draw the two inner velocity triangles together by moving both blades together so that point $C$ falls on point $B$ and the tangents coincide. Assuming that the inner absolute exit and entrance velocities are equal and because $\alpha_2' = \alpha_1'$ the triangles are congruent and $v_2'$ and $v_1'$ fall in the same direction.

Assuming no shock loss at entrance at point $C$ then $\beta_2' = 90°$, that is, the inner tip of the blade must be radial. On account of the difference in elevation between points $B$ and $C$ (exit and entrance to the inner periphery) $V_1'$ might differ from $V_2'$ if there were no losses between these points. (14)

$$V_1' = [2gh_2 + (V_2')^2]^{1/2}$$

Assuming $\beta_2' = 90°$ (Figure 7a) $v_1'$ would not coincide with the blade angle and therefore shock loss would be experienced. In order to avoid this $\beta_2$ must be grater than 90°. The difference in $V_2'$ and $V_1'$ however is usually small because $h_2$ is small, so $\beta_2$ might be 90° in all cases.

(B) Radial rim width: Neglecting the blade thickness, the thickness ($s_1$) Figure 5, of the jet entrance, measured at right angles to the relative velocity, is given by the blade spacing ($t$).

$$s_1 = t\sin\beta_1 \qquad (15)$$

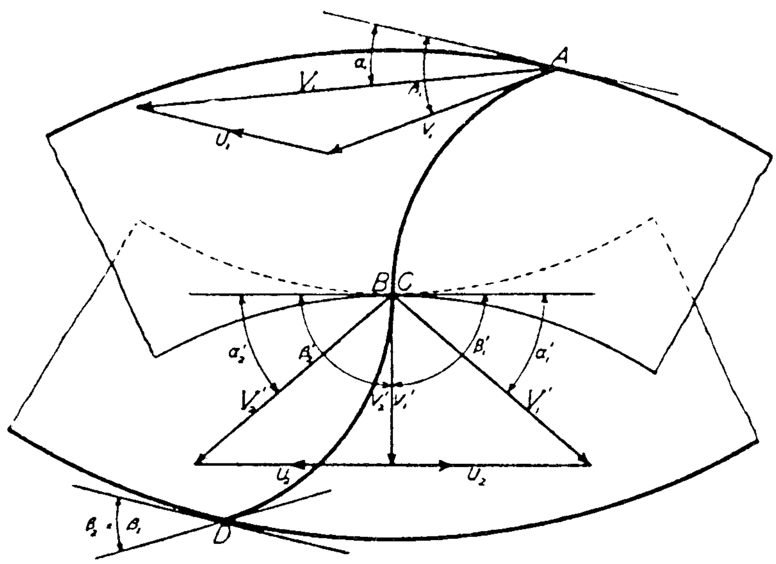

Figure 6. Composite velocity diagram

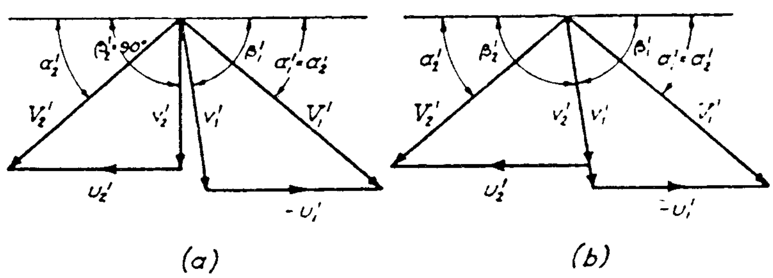

Figure 7. Velocity diagrams

Assuming $\beta_2 = 90°$ the inner exit blade spacing is known for every rim width, (a),

$$s_2 = t(r_2/r_1) \tag{16}$$

As long as ($a$) is small the space between the blades will not be filled by the jet. As ($a$) increases $s_2$ decreases so ($a$) will be limited by

$$s_2 = v_1 s_1 / v_2' \tag{17}$$

It is not advisable to increase the rim width *(a)* over this limit because the amount of water striking it could not flow through so small a cross-section and back pressure would result. Moreover, a rim width which would be under this limit would be inefficient since separated jets would flow out of the spacing between the blades at the inner periphery.

In order to determine the width *(a)* it is necessary to know the velocity $v_2'$, which is affected by the centrifugal force (see Figure 5).

$$(v_1)^2 - (v_2')^2 = (u_1)^2 - (u_2')^2 \qquad (18)$$

or $$(v_2')^2 = (u_2')^2 - (u_1)^2 + (v_1)^2$$

but $$v_2' = v_1(s_1/s_2) = v_1(r_1/r_2)\sin\beta_1 \qquad (19)$$

and $$u_2' = u_1(r_2/r_1)$$

calling $$x = (r_2/r_1)^2$$

$$x_2 - [\,1 - (v_1/u_1)^2\,]x - (v_1/u_I)^2 \sin^2\beta_1 = 0 \qquad (20)$$

If the ideal velocity of the wheel $u_1 = 1/2V_1\cos\alpha_1$

then $$v_1/u_I = 1/\cos\beta_1 \qquad (21)$$

Assuming: $$\alpha_1 = 16°,\ \beta_I = 30°$$

then $$v_1/u_1 = 1/0.866 = 1.15$$

$$(v_1/u_1)^2 = 1.33, \text{ approx.}$$

$$1 - (v_1/u_1)^2 = -0.33;\ \sin^2\beta_1 = 1/4$$

Then equation 20 becomes

$$x_2 + 0.33x - 0.332 = 0$$

$$x = 0.435$$

$$x^{1/2} = r_2/r_1 = 0.66$$

$$2r_1 = D_1$$

Therefore $a = 0.17\,D_1$ = radial rim width. (22)

$D_1$ = the outside diameter of the wheel.

This value of (a), the radial rim width, was graphically ascertained from the intersection of the two curves (Figure 5).

$$(v_2')^2 = (r_2/r_1)^2(u_1)^2 + (v_1)^2 - (u_1)^2 \qquad (18)$$

and $$v_2' = v_1(r_1/r_2)\sin\beta_1 \qquad (19)$$

The central angle *bOC*, Figure 8, can be determined from equation (18) and

$$\alpha_2' = bOC/2$$
$$v_1 = u_1/\cos B_1 = u_1/0.866$$
$$r_2/r_1 = 0.66$$
$$v_2' = u_1 [ (0.66)^2 + 1.33 - 1 ]^{1/2}$$
$$= 0.875\, u_1 \qquad (23)$$
$$\tan\alpha_2' = v_2'/u_2' \qquad (24)$$
$$= 0.875\, u_1/0.66\, u_1$$
$$=1.326$$
$$\alpha_2' = 53°$$
$$\text{angle } bOC = 106° \qquad (25)$$

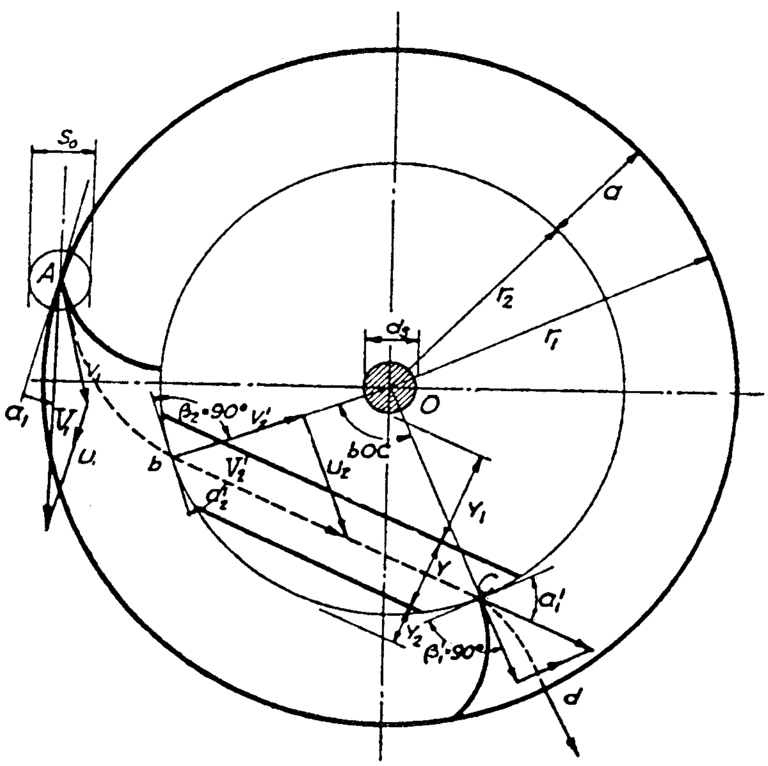


Figure 8. Path of jet inside wheel

The thickness of the jet (y) in the inner part of the wheel can be computed from the continuity equation of flow (Figure 8),

$$V_1 s_0 = V_2' y \quad (26)$$

$$V_2'\cos\alpha_2' = u_2' = (r_2/r_1)u_1$$

$$= (r_2/r_1)V_1/2\ \cos\alpha_1$$

therefore,

$$y = 2\cos\alpha_2' s_0/(r_2/r_1)\cos\alpha_1 \quad (27)$$

$$= (3.03)\ (0.6)s_0/0.961$$

$$= 1.89s_0 \quad (28)$$

The distance between the inside edge of the inside jet as it passes through the wheel and the shaft of the wheel, $y_1$ (Figure 8),

$$y_1 = r_2\sin(90 - a_2') - 1.89s_0/2 - d./2 \quad (29)$$

since $s_1 = kD_1$

then $y_1 = (0.1986 - 0.945\ k)D_1 - d./2$ (30)

In a similar manner the distance $y_2$, the distance between the outer edge of the jet and the inner periphery, can be determined.

$$y_2 = (0.1314 - 0.945k)D_1 \quad (31)$$

For the case where the shaft does not extend through the wheel, the only limit will be $y_2$.

For most cases $k = 0.075$ to $0.10$

then $y_1 + d./2 = 0.128D_1$ to $0.104\ D_1$

$y_2 = 0.0606D_1$ to $0.0369D_1$

(C) Wheel diameter and axial wheel breadth: The wheel diameter can be determined from the following equation:

$$u_1 = \pi D_1 N/(12)(60) \quad (32)$$

$$(1/2)V_1\cos\alpha_1 = \pi D_1 N/(12)(60)$$

$$(1/2)C(2gH)^{1/2}\cos\alpha_1 = \pi D_1 N/(60)(12)$$

$$D_1 = 360C(2gH)^{1/2}\cos\alpha_1/\pi N \quad (33)$$

Where $D_1$ is the diameter of the wheel in inches and $\alpha_1 = 16°$, $C = 0.98$

$$D_1 = 862H^{1/2}/N \quad (34)$$

The thickness $s_0$ of the jet in the nozzle is dependent upon a compromise of two conditions. A large value for $s_0$ would be advantageous because the loss caused by the filling and emptying of the wheel would be small. However, it would not be satisfactory because the angle of attack of the outer filaments of the jet would vary considerably from $a_l = 16°$, thereby increasing these losses as the thickness increases. The thickness should be determined by experiment.

In finding the breadth of the wheel (L), the following equations are true:

$$Q = (Cs_0L/144)(2gH)^{1/2} \quad (35)$$
$$= C(kD_1L/144)(2gH)^{1/2}$$
$$D_1 = 144Q/CkL(2gH)^{1/2}$$
$$= (862/N)H^{1/2} \quad (34)$$
$$144Q/CkL(2gH)^{1/2} = (862/N)H^{1/2}$$
$$L = 144QN/862H^{1/2}Ck(2gH)^{1/2}$$
$$= 0.283\ QN//H \text{ to } 0.212\ QN/H \quad (36)$$

where $k = 0.075$ and $0.10$ respectively

(D) Curvature of the blade: The curve of the blade can be chosen from a circle whose center lies at the intersection of two perpendiculars, one to the direction of relative velocity $v_l$ at ($A$) and the other to the tangent to the inner periphery intersecting at ($B$) (Figure 9).

From triangles $AOC$ and $BOC$, $\overline{CO}$ is common,

then $$(\overline{OB})^2 + (\overline{BC})^2 = (\overline{AO})^2 + (\overline{AC})^2 - 2\overline{AO}\,\overline{AC}\cos\beta_1$$

but $$\overline{AO} = r_1$$
$$\overline{OB} = r_2$$
$$\overline{AC} = \overline{BC} = \rho$$
$$\rho = [(r_1)^2 - (r_2)^2)]/2r_1 \cos\beta_1$$

When $$r_2 = (0.66r_1);\ \text{and } \cos\beta_1 = \cos 30° = 0.866,$$
$$\rho = 0.326r_1 \quad (37)$$

(E) Central angle:

$$r_1/r_2 = \sin(180°-1/2\delta)/\sin(90°-(1/2\delta+\beta_1))$$
$$= \sin 1/2\delta/\cos(1/2\delta+\beta_1)$$
$$\tan 1/2\delta = \cos\beta_1/(\sin\beta_1 + r_2/r_1)$$
$$\delta = 73°\ 28'$$

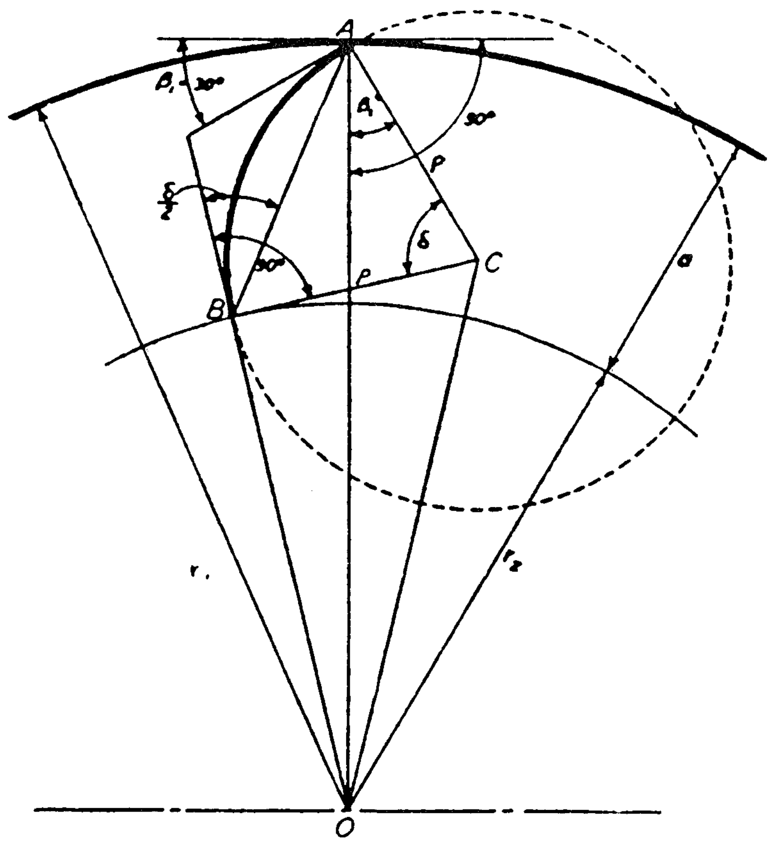


Figure 9. Curvature of blade

# 1.3 The Cross Flow runner and inlet theory

## 1.3.1 Summary of the runner theory

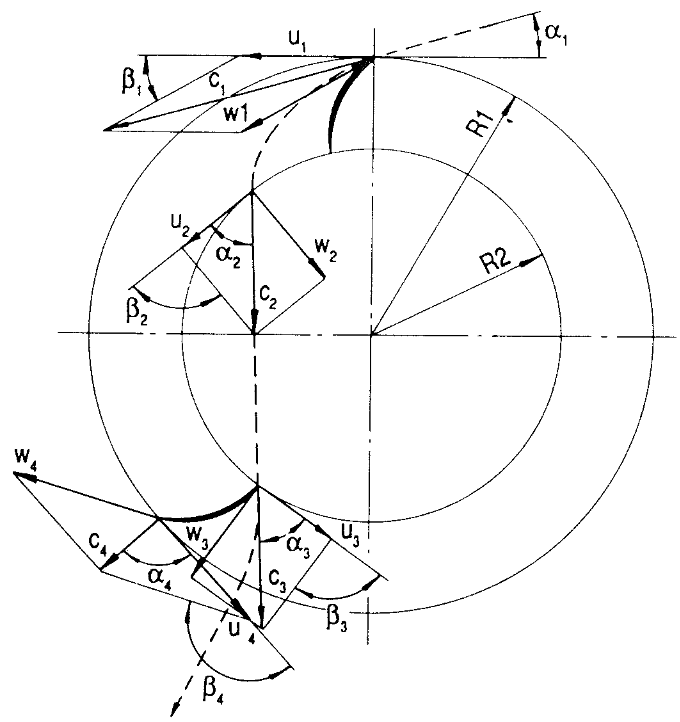


$c_1 = \sqrt{2gH} = 1\ ;\ \alpha_1 = 16°$

$u_3 = u_2\ ;\ u_4 = u_1\ ;\ c_3 = c_2$

$\alpha_3 = \alpha_2\ ;\ \beta_4 = 180° - \beta_1$

$\beta_3 = \beta_2 = 90°$

$w_2 = w_3\ ;\ w_4 = w_1$

$+\quad c_1 \cos\alpha_1 = u_1 + w_1 \cos\beta_1$

$c_4 \cos\alpha_4 = u_4 - w_4 \cos(180 - \beta_4)$

$-\quad c_4 \cos\alpha_4 = u_1 - w_1 \cos\beta_1$

$\rightarrow\ g\,\eta\,H = 2\,u_1\,w_1 \cos\beta_1$

$$g\,H = \frac{c_1^{\,2}}{2}$$

$$\eta = \frac{4u_1}{c_1}\left(\cos\alpha_1 - \frac{u_1}{c_1}\right)$$

$$\frac{d\eta}{d\frac{u_1}{c_1}} = 0 \Rightarrow u_1 = \frac{c_1 \cos\alpha_1}{2}$$

$\tan\beta_1 = 2\tan\alpha_1$ $\qquad \boxed{\eta_{max} = \cos^2\alpha_1}$

$w_1^{\,2} - u_1^{\,2} = w_2^{\,2} - u_2^{\,2}\ ;\ w_2 = \sqrt{w_1^{\,2} - u_1^{\,2} + u_2^{\,2}}$

$w_1^2 - w_2^2 = u_1^2 - u_2^2$

$w_2 = w_1\ \dfrac{R_1}{R_2}\ \sin\beta_1$

$\Big\}$ with $\beta_1 = 30° \Rightarrow \dfrac{R_2}{R_1} = 0{,}666$

$\tan\alpha_2 = \dfrac{w_2}{u_2}\ ;\ u_2 = \dfrac{R_1}{R_2}\ u_1\ ;$

with $\beta_1 = 30° \Rightarrow \tan\alpha_2 = 1{,}148\ \dfrac{w_1}{u_1}$

$w_1 = 0{,}555\ c_1\ ;\quad u_1 = 0{,}481\ c_1\ ;\quad \tan\alpha_2 = 1{,}3 \Rightarrow \alpha_2 = 53°\ ;\ c_2 = \dfrac{u_2}{\cos\alpha_2} = 0{,}528\ c_1$

$c_4 = \dfrac{c_1 \sin\alpha_1}{\sin\alpha_4}\ ;\ \text{with } u_1 = \dfrac{c_1 \cos\alpha_1}{2} \Rightarrow \alpha_4 = 90°\ ;\ c_4 = 0{,}276\ c_1$

Fig. 1.6 : Velocity triangles and related formulae for a Cross Flow turbine

### 1.3.2 Development of the absolute flow path

Based on the velocity triangles and the related formulae as described in the foregoing sections, the flow path through the runner can be traced. However, in this section, the absolute flow path through the first stage of the runner shall be discussed in detail in an explanatory manner, as a basis for further studies.

During the time needed by a fluid element to travel along the turbine blade from the entrance edge to the exit edge, the runner itself rotates. To locate the exact exit point of an absolute stream line, it is therefore of interest to calculate the angle of rotation of the runner during the passing time of a fluid element through the first stage of the runner. The task at hand is to determine intermediate velocity triangles between the entrance and the exit point of the runner blade. The entrance velocity is defined as follows:

$$c_1 = 1$$

$$\alpha_1 = 16°$$

$$u_{1\,opt} = \frac{c_1 \cos \alpha_1}{2} = 0.48063$$

$$\beta_1 = 30°$$

$$w_{1opt} = \frac{c_1 \cos \alpha_1}{\cos \beta_1} = \frac{u_1}{\cos \beta_1} = 0.55498$$

The outer runner radius shall be denoted as $R_1$, the inner runner radius as $R_2$ and any radius in between as $R_i$; therefore, the peripheral velocity at the outer runner radius is $u_1$, the peripheral velocity at the inner runner radius is $u_2$ and any peripheral velocity in between is $u_i$.

The relative velocity component at any point between the outer and the inner radius can be expressed as:

$$w_i = \sqrt{w_1^2 - u_1^2 + u_i^2} \tag{1.16}$$

and with the substitution:

$$w_1^2 - u_1^2 = \kappa \Rightarrow w_i = \sqrt{\kappa + u_i^2} \tag{1.17}$$

with: $\left.\begin{array}{l} u_1 = 0.48063 \\ w_1 = 0.55498 \end{array}\right\} \kappa = 0.0770$

The relative velocity angle $\beta$ at any point between the outer and the inner runner radius can be expressed as:

$$\beta_i = \arcsin \frac{\sin \beta_1 \, u_1^2}{u_i^2} \tag{1.18}$$

and with the substitution:

$$\sin \beta_1 \, u_1^2 = \lambda \Rightarrow \sin \beta_i = \frac{\lambda}{u_i^2} \tag{1.19}$$

with: $\left.\begin{array}{l} \beta_1 = 30° \\ u_1 = 0.48063 \end{array}\right\} \lambda = 0.1155$

The absolute velocity component in meridional direction at any point between the outer and the inner runner radius is the product of the relative velocity component and the sinus of the relative velocity angle at that point:

$$c_{m_i} = w_i \sin \beta_i \Rightarrow c_{m_i} = \lambda \frac{\sqrt{\kappa + u_i^2}}{u_i^2} \tag{1.20}$$

The mean absolute velocity component in meridional direction between the outer runner radius and the inner runner radius and any other radius in between the two, corresponds to the integral of the absolute velocity component in meridional direction along the two radii:

$$\overline{c_{m_i}} = \frac{1}{u_1 - u_i} \int_{u_i}^{u_1} \frac{\lambda \sqrt{\kappa + u_i^2}}{u_i^2} \, d_{u_i} \tag{1.21}$$

The angle of rotation of the runner during the travel of a fluid element from the outer runner radius to the inner runner radius, or to any radius in between the two, is:

$$\gamma\,[\,°\,] = \frac{\left[1 - \left(\frac{R_i}{R_1}\right)\right] u_1 \, 360°}{\overline{c_{m_i}} \quad 2\pi} \tag{1.22}$$

where: $\gamma\,[°]$ = the angle of rotation of the runner in degrees.

The calcualtion of the mean absolute velocity component in meridional direction $\overline{c_{m_i}}$ requires the application of a numerical integration method. It is recommended to use the SIMPSON formula below {1.23}.

**Example:**

The mean absolute velocity component in meridional direction $\overline{c_{m_i}}$ is to be calculated along $R_1$ to $R_{i1}$ as well as the angle of rotation of the runner $\gamma_{i1}$. The following values are given:

$$
\begin{aligned}
R_1 &= 100\ [\mathrm{mm}] \\
R_{i1} &= 88.88\ [\mathrm{mm}] \\
b &= u_1 = 0.48063 \\
\kappa &= 0.0770 \\
\lambda &= 0.1155 \\
n &= 4
\end{aligned}
$$

Step 1: calculation of $a = u_i$:

$$u_{i1} = u_1 \frac{R_{i1}}{R_1} = 0.48063 \frac{88.88}{100} = 0.42723$$

Step 2: dividing the intervall of $u_1$ to $u_i$ into $n = 4$ sections:

$$
\begin{aligned}
u_{i1} &= u_{y_a} = 0.42723 \\
u_{y1} &= 0.44058 \\
u_{y2} &= 0.45393 \\
u_{y3} &= 0.46728 \\
u_1 &= u_{y_b} = 0.48063
\end{aligned}
$$

Step 3: calculating the value y for each value of $u_y$:

$$y_a = c_{mi} = \frac{\lambda \sqrt{\kappa + u_{y_a}^2}}{u_{y_a}^2}$$

$$= \frac{0.1155 \sqrt{0.077 + 0.42723^2}}{0.42723^2} = 0.32237$$

$$
\begin{aligned}
y_1 &\text{ with } u_{y_1} = 0.44058 \Rightarrow 0.30982 \\
y_2 &= 0.29822 \\
y_3 &= 0.28747 \\
y_b &= c_{m_1} = 0.27748
\end{aligned}
$$

Step 4: numerical integration with the SIMPSON rule:

$$\int_a^b y\,dx = \frac{b-a}{3n} (y_a + 4y_1 + 2y_2 + 4y_3 + y_b)$$

$$= \frac{0.48063 - 0.42723}{3 \cdot 4} (0.32237 + 4 \cdot 0.30982 +$$

$$+ 2 \cdot 0.29822 + 4 \cdot 0.28747 + 0.27748 = 0.01596$$

Step 5: calculation of $\overline{c_{m_i}}$:

$$c_{mi} = \frac{1}{u_1 - u_i} \int_{u_i}^{u_1} \frac{\lambda \sqrt{\kappa + u_i^2}}{u_i^2}\, d_{u_i}$$

$$= \frac{1}{0.48063 - 0.42723} \cdot 0.01596 = 0.29888$$

Step 6: calculation of the angle of rotation $\gamma_{Ri1}$ of the runner:

$$\gamma\,[°] = \frac{\left[1 - \left(\frac{R_i}{R_1}\right)\right] u_1 \cdot 360°}{\overline{c_{m_i}}\ 2\pi}$$

$$= \frac{\left[1 - \left(\frac{88.88}{100}\right)\right] 0.48063 \cdot 360°}{0.29888 \cdot 2\pi} = 10.24°$$

**The SIMPSON formula :**

$$\int_a^b y\,dx = \frac{b-a}{3n} (y_a + 4y_1 + 2y_2 + 4y_3 + 2y_4 + \ldots + 2y_{n-2} + 4y_{n-1} + y_b) \qquad (n = 2k;\ k \in N) \tag{1.23}$$

where: $a = u_i$ $\quad y_a = c_{m_i}$

$b = u_1$ $\quad y_b = c_{m_1}$

$n$ = number of values

Fig. 1.7 shows the absolute flow path of a single stream line through the first stage of a Cross Flow runner. The values given, and the velocity triangles shown, correspond to the calculations described in the foregoing section.

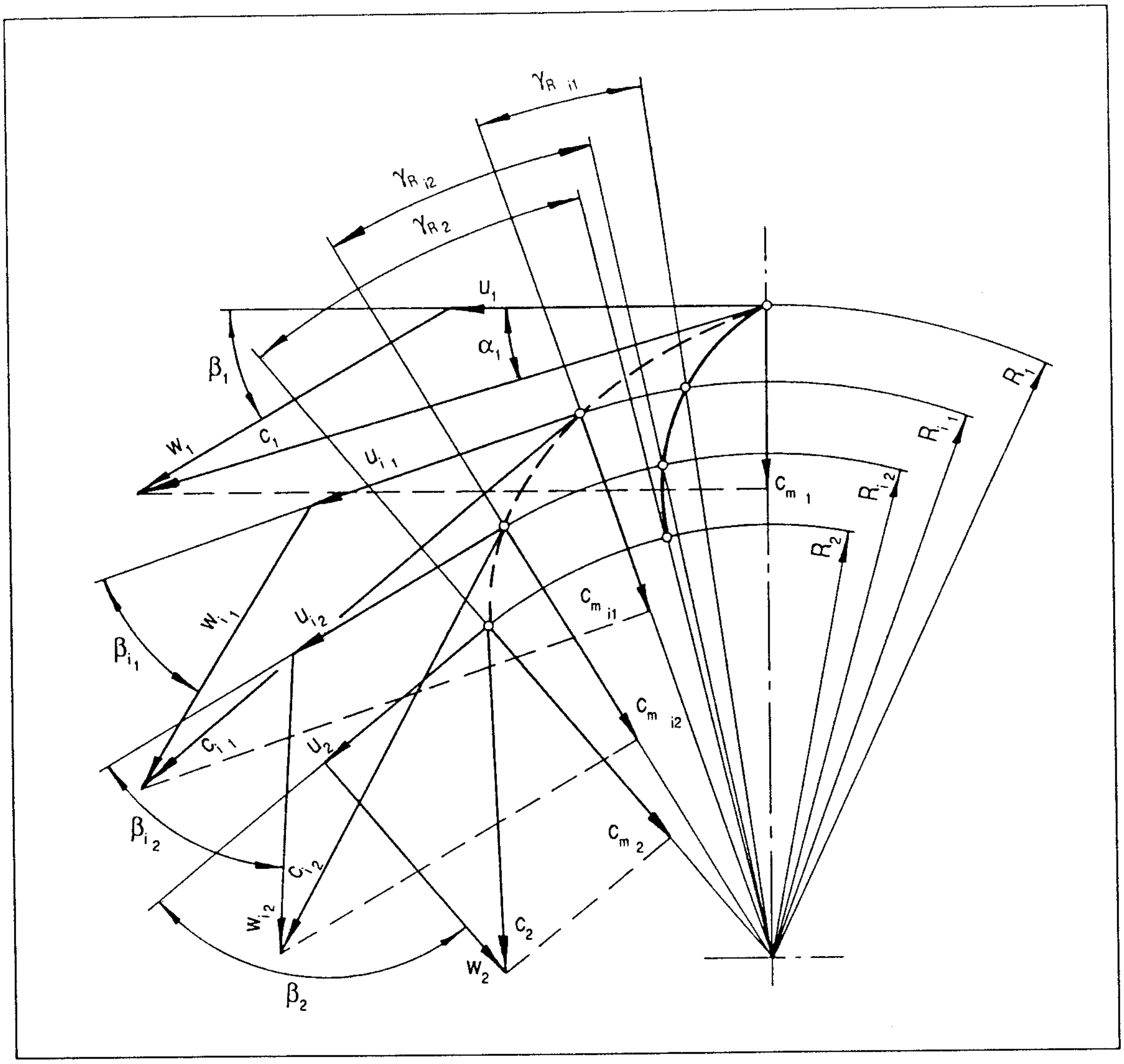


**Fig. 1.7:Design of the absolute flow path in the first stage of a Cross Flow runner**

| | $c_i$ | $w_i$ | $u_i$ | $\beta_i$ | $c_{m_i}$ | $\int_{u_i}^{u_1}$ | $\overline{c_{m_i}}$ | $\gamma_{R_i}$ |
|---|---|---|---|---|---|---|---|---|
| $R_1$ = 100 [mm] | 1.00000 | 0.55498 | 0.48063 | 30° | 0.27748 | 0 | - | 0 |
| $R_{i_1}$ = 88,88 [mm] | 0.88269 | 0.50944 | 0.42723 | 39.25° | 0.32237 | 0.01596 | 0.29888 | 10.24° |
| $R_{i_2}$ = 77.77 [mm] | 0.74325 | 0.46555 | 0.37382 | 55.74° | 0.38479 | 0.03474 | 0.32523 | 18.82° |
| $R_2$ = 66.66 [mm] | 0.53423 | 0.42400 | 0.32500 | 90° | 0.42400 | 0.05758 | 0.35937 | 25.54° |

Fig. 1.8: Table of values calculated for the absolute flow path

### 1.3.3 Blade geometry

In order to be able to design a correct Cross Flow runner, it is indispensable to determine the blade geometry, and in doing this, it is assumed that the following parameters have been chosen based on hydraulic considerations and the desired velocity triangles:

| | |
|---|---|
| $R_1$ | the outer radius of the runner |
| $R_2$ | the inner radius of the runner, locus of the end of the skeleton lines of the blades |
| $\beta_1$ | the outer blade angle |
| $\beta_2$ | the inner blade angle |

It is further assumed, that the skeleton line of the blade is the segment of a circle, as is normally the case in Cross Flow turbines. Other geometrical parameters of interest are:

| | |
|---|---|
| $r_b$ | the curvature radius of the blade |
| $r_p$ | the pitch circle radius |
| $\delta$ | the segment angle of the blade |

To express the geometrical relationship among the parameters $R_1$, $R_2$, $\beta_1$, $\beta_2$ and $r_b$, $r_p$ and $\delta$, a number of additional parameters need to be introduced as shown in fig. 1.9: $\varepsilon$, $\xi$, $\phi$, c, d

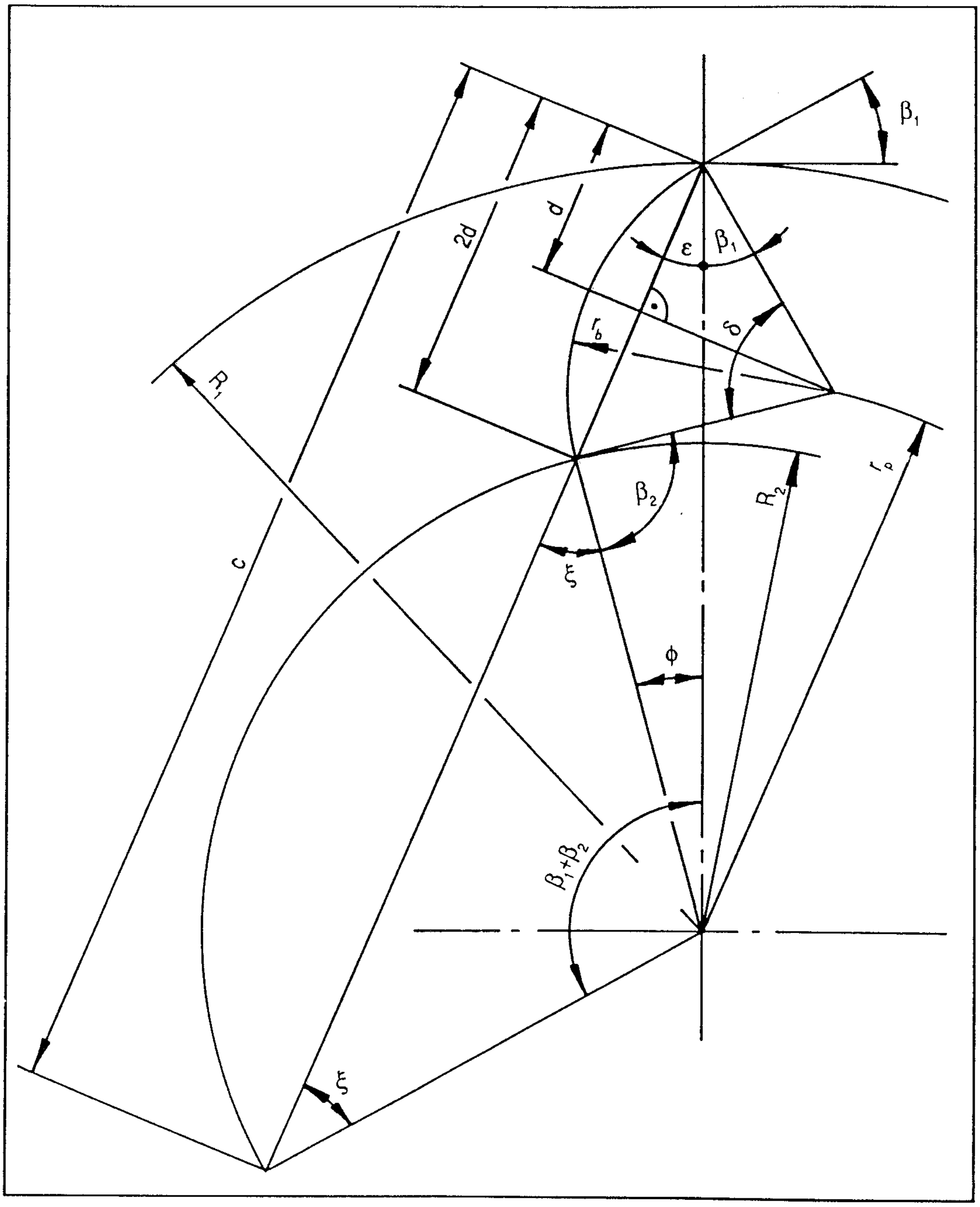


Fig. 1.9 : Construction of blade geometry

Fig. 1.9 also represents the graphical solution to the problem: the angle ($\beta_1 + \beta_2$), is drawn from the center of the runner, so that one vector intersects the radius $R_1$ and the other vector intersects the radius $R_2$. The connecting line from the intersection point on $R_1$ to the intersection point on $R_2$, represents c. The line c intersects the circle of radius $R_2$ at a distance of 2d from the intersection point on the circle with radius $R_1$. Errecting the mean perpendicular on 2d, we find the line on which the center of the radius of curvature $r_b$ of the blade is situated. Drawing a line at an angle of $\beta_1$ from the intersection point of the circle with radius $R_1$, we find an intersection with the previously errected mean perpendicular which is the center of the radius of curvature $r_b$ of the runner blade, at a distance of the pitch circle radius $r_p$ from the center of the runner. Tracing the radius of curvature $r_b$ upto the intersection with the inner circle of the radius $R_2$, and connecting the found intersection point with the center of radius $r_b$, we establish the angle $\delta$. Connecting the intersection point of the circle with $r_b$ and the circle with $R_2$ with the center of the runner, we determine the angle $\phi$, thereby also establishing other remaining angles as shown.

The following formulae are listed in the required order for calculating the parameters $\delta$, $r_b$ and $r_p$, based on the known parameters $R_1$, $R_2$, $\beta_1$ and $\beta_2$. The graphical construction of the blade geometry may be used to verify the calculated values.

**{1.24}** $$c = \sqrt{R_1^2 + R_2^2 - 2R_1R_2 \cos(\beta_1 + \beta_2)}$$

**{1.25}** $$\varepsilon = \arcsin\left[\frac{R_2 \sin(\beta_1 + \beta_2)}{c}\right]$$

**{1.26}** $$\xi = 180° - (\beta_1 + \beta_2 + \varepsilon)$$

**{1.27}** $$\phi = \beta_1 + \beta_2 - (180° - 2\xi)$$

**{1.28}** $$d = \frac{R_1 \sin\phi}{2 \sin(180° - \xi)}$$

**{1.29}** $$\delta = 180° - 2(\beta_1 + \varepsilon)$$

**{1.30}** $$r_b = \frac{d}{\cos(\beta_1 + \varepsilon)}$$

**{1.31}** $$r_p = \sqrt{r_b^2 + R_1^2 - 2 r_b R_1 \cos\beta_1}$$

**Example:**

Given: $R_1 = 200$ [mm], $R_2 = 136$ [mm], $\beta_1 = 30°$, $\beta_2 = 90°$

to be solved for: $\delta$, $r_b$, $r_p$

Step 1: calculation of c:

$$c = \sqrt{200^2 + 136^2 - 2 \cdot 200 \cdot 136 \cdot \cos(30° + 90°)}$$

$$= 292.74 \text{ [mm]}$$

Step 2: calculation of $\varepsilon$:

$$\varepsilon = \arcsin\left[\frac{136 \cdot \sin(30° + 90°)}{292.74}\right] = 23{,}72°$$

Step 3: calculation of $\xi$:

$$\xi = 180° - (30° + 90° + 23.72°) = 36.28°$$

Step 4: calculation of $\phi$:

$$\phi = 30° + 90° - (180° - 2 \cdot 36.28°) = 12.55°$$

Step 5: calculation of d:

$$d = \frac{200 \cdot \sin 12.55°}{2 \sin(180° - 36.28°)} = 36.73 \text{ [mm]}$$

Step 6: calculation of the segment angle $\delta$ of the blade:

$$\delta = 180° - 2(30° + 23.72°) = 72.55°$$

Step 7: calculation of the curvature radius $r_b$ of the blade:

$$r_b = \frac{36.73}{\cos(30° + 23.72°)} = 62.08 \text{ [mm]}$$

Step 8: calculation of the pitch circle radius $r_p$:

$$r_p = \sqrt{62.08^2 + 200^2 - 2 \cdot 62.08 \cdot 200 \cdot \cos 30°}$$

$$= 149.5 \text{ [mm]}$$

## 1.3.4 The inlet curve

The water conveyed to the turbine passes through the penstock with a circular cross-section and then enters the adapter, where the cross section is transformed from circular to the rectangular cross-section of the turbine inlet housing. Before reaching the runner, flow has to be transformed once more, in order that ideally each stream line should fulfil the specific entrance conditions to the runner, such as:

the correct absolute velocity $c_0$

the correct absolute entrance angle $\alpha_0$

Fig. 1.10 shows the different cross-sections of the water flow on its path from the penstock to the runner of the turbine. The turbine inlet serves the purpose of transforming the flow at the end of the rectangular adapter to the optimal flow pattern in the admission area of the runner.

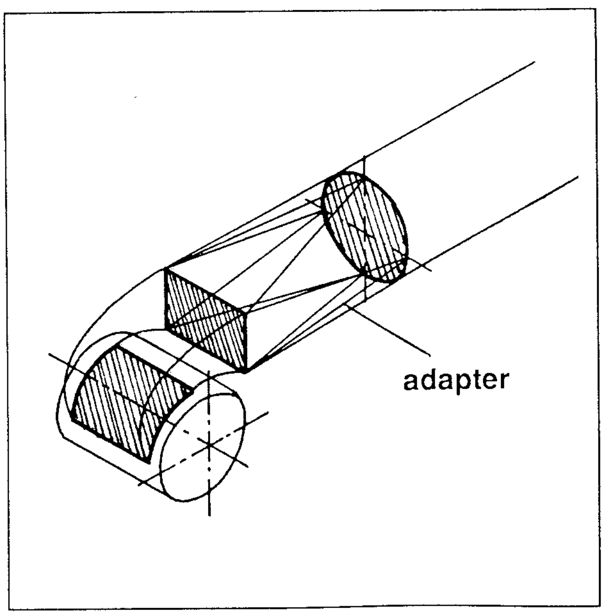


**Fig. 1.10: Cross-sections of flow at the inlet of Cross Flow turbines**

Fig. 1.11 illustrates the desired flow pattern, where all stream lines have the correct velocity and angle of admission at any radius r, so that the following condition is valid:

$$r \cdot c_u = \text{constant}$$

Assuming this condition is fulfilled, all stream lines will enter the runner at $R_1$ having equal velocity

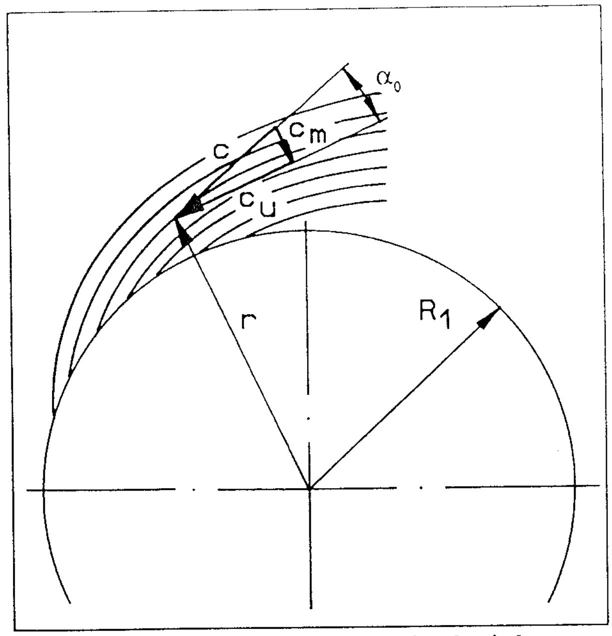


**Fig. 1.11: Ideal flow conditions in the inlet**

components in peripheral direction $c_{u0}$. If it is further assumed that the entire pressure energy has already been converted into kinetic energy at the end of the inlet, the absolute velocity c of each stream line approaching $R_1$ corresponds to the free jet velocity

$$c_0 \text{ proportional to } \sqrt{2\,g\,H}$$

If $c_u$ and c have constant values along the entrance arc on $R_1$, the absolute velocity angle $\alpha_0$ at the entrance to the runner is constant as well. The inlet curve therefore is ideally a line forming a constant angle between the tangent of a point on the inlet curve and its radius vector to the origin of the inlet curve, as shown in fig. 1.12.

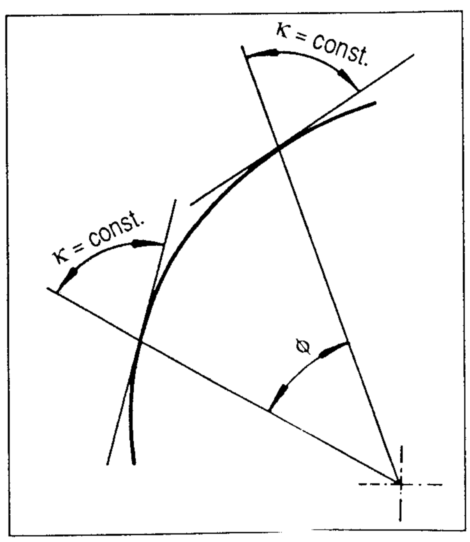


**Fig. 1.12: Constant angle of the ideal inlet curve**

The only curve in which the feature of forming a constant angle between its tangent and the line to its origin is inherent, is the logarithmical spiral.

The logarithmical spiral is expressed by the formula:

$$\boxed{\begin{aligned} r_\phi &= e^{k\phi} \\ k &= \cot\kappa \end{aligned}} \quad (k > 0) \qquad \{1.32\}$$

where:

$r_\phi$ = the distance of a point on the angle from the origin

e = the natural logarithm = 2.7183

k = cot κ = cotangent of the angle between the tangent to the logarithmical spiral and its radius vector to the origin of the spiral = tan $\alpha_0$ (fig. 1.13)

$\phi$ = the angle expressed in radians between two points on the spiral and the origin of the spiral

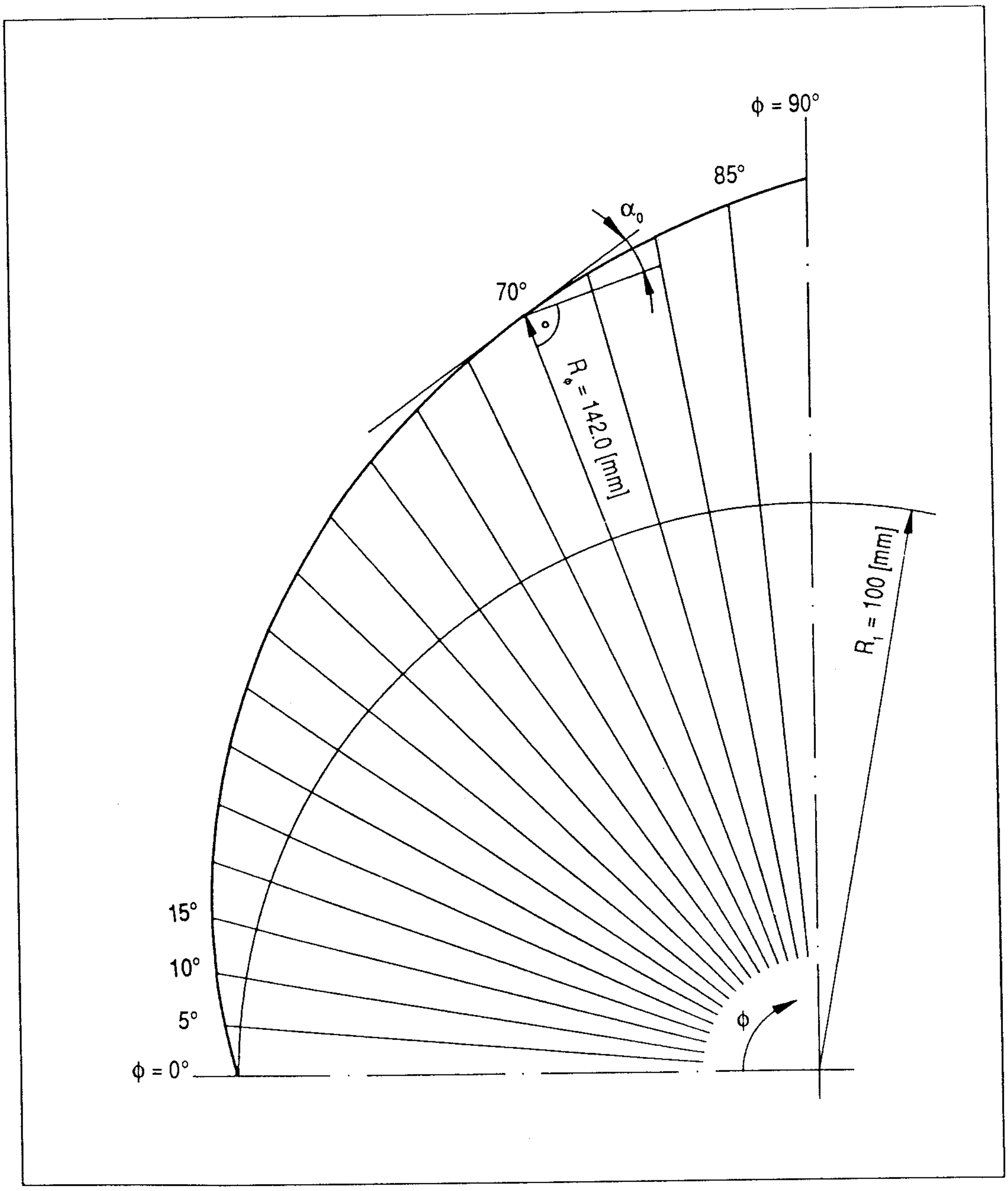


**Fig. 1.13: Design of the logarithmical inlet spiral**

**Example:**

The inlet curve of a Cross Flow turbine is to be drawn with the following given parameters:

$R_1$ = 100 [mm], the outer runner radius
$\alpha_0$ = 16° [deg], the absolute entrance angle
$\phi$ = 90° [deg], the admission arc for which the spiral is to be designed

The radius $r_\phi$ shall be calculated for every step of 5° between $\phi = 0°$ and $\phi = 90°$.

Step 1: calculation of k:

$\kappa = 90° - \alpha_0 \Rightarrow k = \tan \alpha_0 = 0.287$

Step 2: converting $\phi$ every 5° from 0° to 90° into radians

$360° \triangleq 2\pi$

Step 3: calculation of $r_\phi$ :

$r_\phi = e^{\tan\alpha_0 \phi \text{ [rad.]}}$

Step 4: calculation of $R_\phi$ :

$R_\phi = r_\phi \cdot R_1$

| $360° \triangleq 2\pi$ | | $r_\phi = e^{\tan\alpha_0 \phi \text{ [rad.]}}$ | $r_\phi \cdot R_1$ |
|---|---|---|---|
| $\phi$ deg. | rad. | $r_\phi$ | $R_\phi$ |
| 0 | 0 | 1.000 | 100.0 |
| 5 | 0.087 | 1.025 | 102.5 |
| 10 | 0.175 | 1.051 | 105.1 |
| 15 | 0.262 | 1.078 | 107.8 |
| 20 | 0.349 | 1.105 | 110.5 |
| 25 | 0.436 | 1.133 | 113.3 |
| 30 | 0.524 | 1.162 | 116.2 |
| 35 | 0.611 | 1.191 | 119.1 |
| 40 | 0.698 | 1.222 | 122.2 |
| 45 | $\frac{\pi}{4}$ | 1.253 | 125.3 |
| 50 | 0.873 | 1.284 | 128.4 |
| 55 | 0.960 | 1.317 | 131.7 |
| 60 | 1.047 | 1.350 | 135.0 |
| 65 | 1.134 | 1.384 | 138.4 |
| 70 | 1.222 | 1.420 | 142.0 |
| 75 | 1.309 | 1.455 | 145.5 |
| 80 | 1.396 | 1.492 | 149.2 |
| 85 | 1.484 | 1.530 | 153.0 |
| 90 | $\frac{\pi}{2}$ | 1.569 | 156.9 |

## 1.3.5 The runner diameter and inlet width

The flow admission area is the product of the inlet width $b_0$ and the length L of the admission arc, as shown in fig. 1.14

{1.33} $$\boxed{A = b_0 \cdot L}$$

where the length of the admission arc L is determined by the admission arc angle $\phi$[°], and the runner diameter $D = 2 \cdot R_1$

{1.34} $$\boxed{L = \frac{2 \cdot R_1 \cdot \pi \cdot \phi°}{360°}}$$

The required flow admission area depends on the desired flow through the turbine under specific head conditions, according to equation {1.35}:

{1.35} $$\boxed{Q = A \cdot v}$$

where:
Q = discharge through the turbine [m³/s]
A = flow admission area [m²]
v = the flow velocity in perpendicular direction to the flow admission area [m/s]

The velocity component perpendicular to the flow admission area is equivalent to the absolute velocity component in meridional direction $c_m$, and therefore:

{1.36} $$\boxed{Q = A \cdot c_m}$$

The absolute velocity component in meridional direction $c_m$ may also be expressed by the relation:

{1.37} $$\boxed{c_m = c \cdot \sin \alpha}$$

where: $\alpha$ = absolute velocity angle
c = absolute velocity

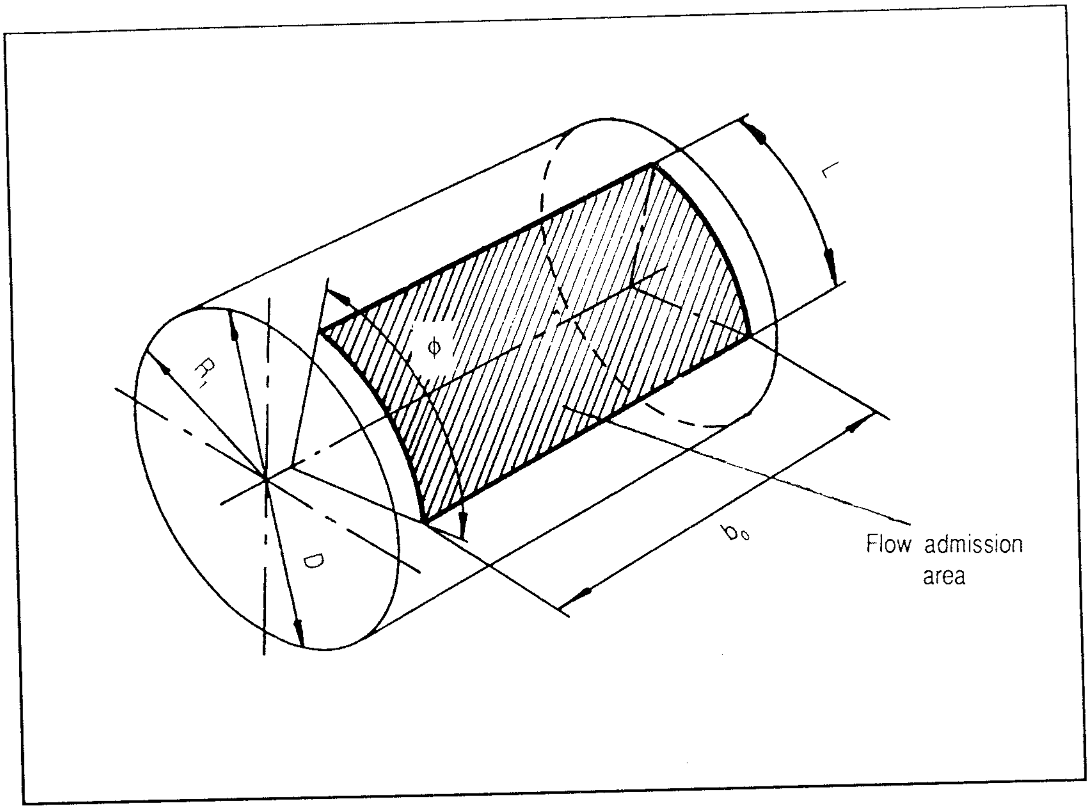


**Fig. 1.14: Flow admission area of a Cross Flow turbine**

If we substitute the absolute velocity component with the corresponding free jet velocity, neglecting any head losses due to friction of flow, c may be expressed as:

{1.38} $$c = \sqrt{2\,g\,H}$$

where: g = gravitational constant
H = net head

therefore, the discharge through the turbine may be written in different ways, using the above substitutions:

$$Q = A \cdot c_m$$

$$Q = b_0 \cdot L \cdot c_m$$

$$Q = \frac{b_0 \cdot 2R_1 \cdot \pi \cdot \phi° \cdot c_m}{360°}$$

$$Q = \frac{b_0 \cdot 2R_1 \cdot \pi \cdot \phi° \cdot c \,\sin\alpha}{360°}$$

{1.39} $$Q = \frac{b_0 \;\; 2R_1 \;\; \pi \;\; \phi° \; \sqrt{2gH} \;\; \sin\alpha}{360°}$$

Equation {1.39} contains all relevant parameters influencing the discharge through the turbine, namely:

- $b_0$ the inlet width
- $R_1$ the radius or diameter $D = 2R_1$ of the runner
- $\phi°$ the admission arc angle
- $\sqrt{H}$ the square root of the net head
- sin $\alpha$ the sinus of the absolute velocity angle at the entrance to the runner

Further, it becomes evident, that the inlet width $b_0$ and the runner radius $R_1$ have an equal and linear influence on the discharge capacity of a Cross Flow turbine. Put in other words, a turbine with an inlet width of $b_0 = 300$ [mm] and with a runner diameter of $D = 400$ [mm], would have the same discharge capacity as a turbine with an inlet width $b_0 = 400$ [mm] and diameter of the runner of $D = 300$ [mm], provided both machines work under the same net head and have an equal absolute velocity angle $\alpha$, as well as equal admission arc angles $\phi°$. Speed of the two machines on the other hand, would be different, due to equal peripheral velocities but different diameters of the respective runner.

# Chapter 2 : Selected nomograms and diagrams

## 2.1. Why nomograms and diagrams?

In the past, nomograms were widely used by engineers as a graphical calculation aid for solving repeatedly occuring engineering problems. Little imagination is needed to understand the popularity of nomograms at the time electronic calculators and PCs were not yet available, but why should we be using nomograms and diagrams today?

There are some very good reasons:

The unique advantage of nomograms is its visualizing of the relationship of involved parameters. This offers the possibility of playing around with new values and different assumptions and of optimizing solutions in an iterative process in line with actual requirements. A further advantage of nomograms is that it doesn't matter which parameter is unknown. A solution may therefore be found from different angles.

Using the same nomogram for a specific type of problem again and again allows you to develop a feeling for the optimal solution.

Furthermore, nomograms prevent you from calculation mistakes, but require careful scale reading.

Similarly, diagrams have the advantage of showing a specific point and its relation to other possible solutions.

Diagrams as well as nomograms define the range of application and therefore provide guidelines as to the validity of assumptions made.

However, nomograms should not be used blindly, under no circumstances it exempts you to understand what you are doing.

## 2.2. Some useful nomograms and diagrams for micro hydro engineers

The discharge nomogram of STRICKLER in its general form as presented under 2.2.1 allows in many cases a first approximation of the available discharge in a river.

The nomogram under 2.2.2 deals with the dimensioning of rectangular canals, as the nomograms under 2.2.3 and 2.2.4 do for trapezoidal canal cross sections.

Further, the nomogram for discharge measurement with weirs under 2.2.5 is meant as an aid when effectively conducting discharge measurements.

When dimensioning a penstock, several or all of the following nomograms/diagrams may be needed: The nomogram for head losses in penstocks under 2.2.6, the diagram for the pre-selection of the economically optimal penstock diameter under 2.2.7, the nomogram for the pre-selection of the minimal required wall thickness of the penstock pipe under 2.2.8 and the ALLIEVI-chart for the examination of water hammer effects under 2.2.9.

The diagram for the pre-selection of the turbine type under 2.2.10 clarifies the question of which type of turbine is to be chosen under specific conditions of head and flow, as well as for a preferred turbine speed.

## 2.2.1 Discharge Nomogram of STRICKLER

This nomogram serves to estimate the discharge in a river or a canal.
The nomogram is based on the formula:

$$\{2.1\} \quad \boxed{Q = k\, s^{1/2} \frac{A^{5/3}}{U^{2/3}}}$$

where:
- k = friction coefficient [ - ]
- s = slope [ - ]
- A = wetted, cross sectional area [ $m^2$ ]
- U = wetted perimeter [ m ]
- Q = river discharge [ $m^3/s$ ]

STRICKLER also established a formula for the determination of the friction coefficient **k** :

$$\{2.2\} \quad \boxed{k = \frac{21.1}{d^{1/6}}}$$

where: d = size of gravel or boulders [ m ]

For values of **k** refer to the table in Figure 2.1:

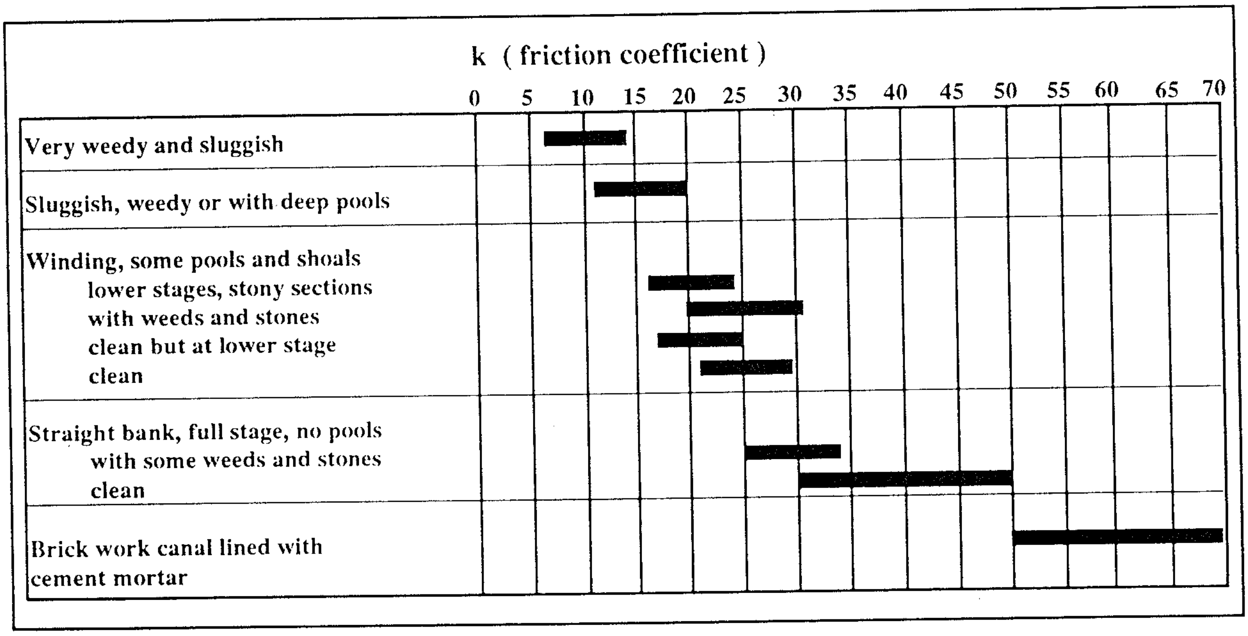


**Fig. 2.1: Friction coefficients k of STRICKLER**

### Example of how to use the nomogram

A sluggish, weedy river bed with a few stony sections and a slope of 1 ‰ shows a wetted cross sectional area of 125 $m^2$ and a wetted perimeter of 64 m.

$$\left.\begin{array}{l} k = 30 \\ s = 1\ ‰ \\ A = 125\ m^2 \\ U = 64\ m \end{array}\right\} \Rightarrow Q = 185\ m^3/s$$

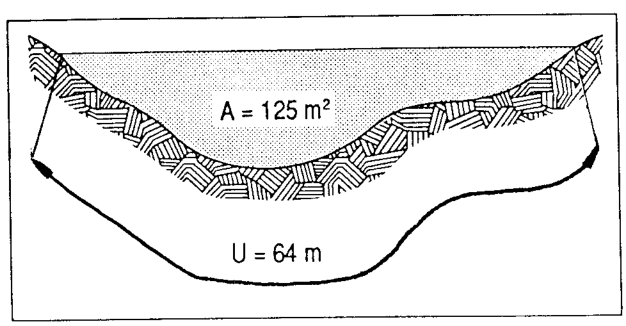


Illustration from: Inversin [3]
page 13

The STRICKLER nomogram is of a complex nature. Because there are 5 variables, two reference lines (1) and (2) are required. Reference line (1) is to be used in combination with the A-scale and the U-scale to the right hand side of the nomogram, while reference line (2) is to be used in combination with the Q-scale and the k-scale, and finally, both reference lines (1) and (2) are to be used in combination with the s-scale. For the example given, in the following way:

- Find 64 m on the U-scale and 125 $m^2$ on the A-scale and draw a line through the points found upto the intersection with reference line (1).
- Continue by drawing a line from the intersection point on reference line (1) to the value 1 ‰ on the s-scale, thereby determining an intersection point on reference line (2).
- From the value 60 on the k-scale, draw a line through the intersection point on reference line (2) upto the Q-scale, thereby finding the value of 370 $m^3/s$. Be aware that scales are logarithmic as in most nomograms and avoid scale-reading errors.
- If other values are given than in the example shown, use the nomogram likewise, keeping in mind the relationship of scales and reference lines.

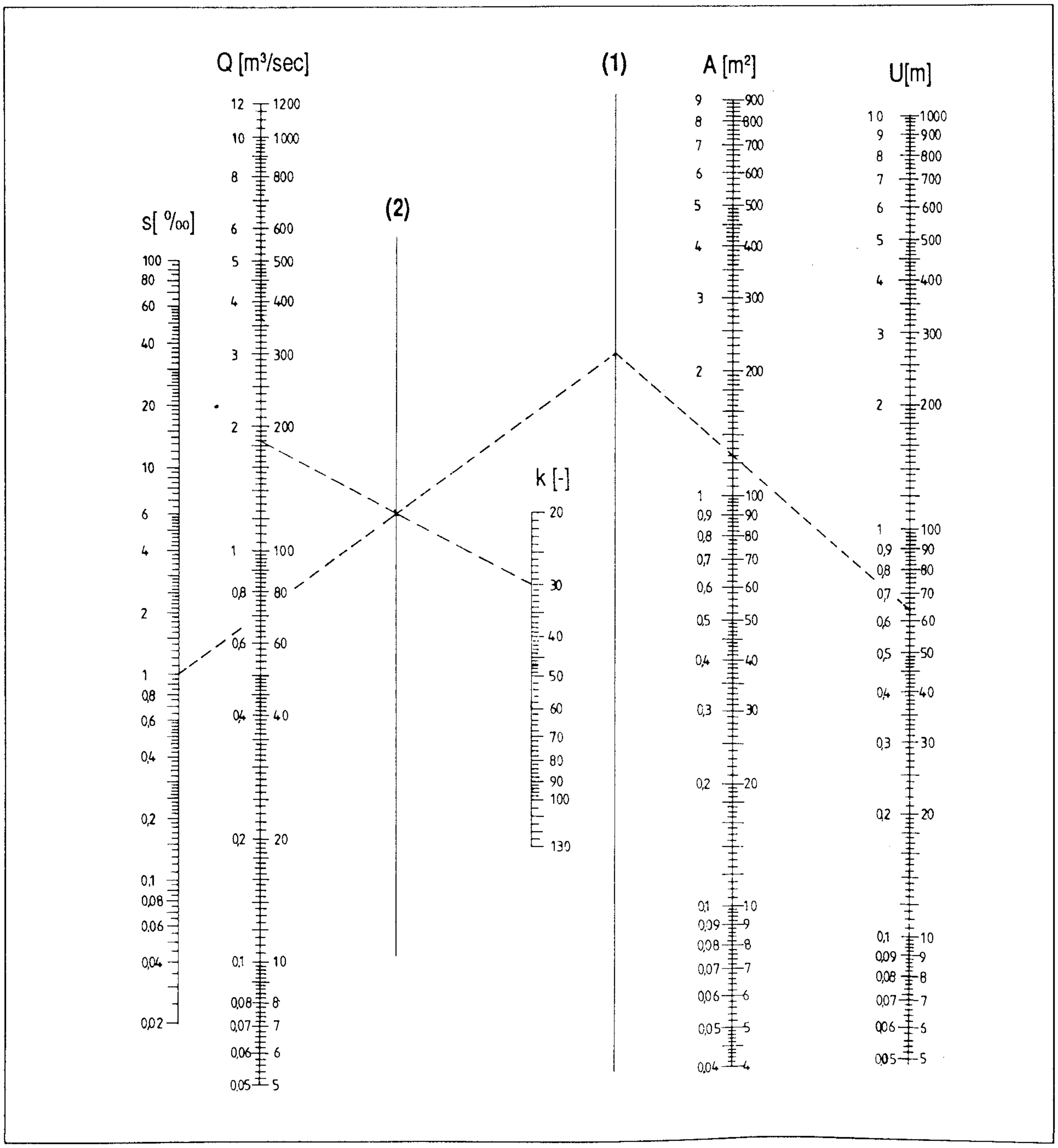


Figure 2.2: STRICKLER Nomogram

## 2.2.2 Flow in rectangular canal cross-sections

Channels with rectangular cross-sections, which implies vertical side walls, are commonly used where it is for some reason not convenient to build channels with a hydraulically better trapezoidal cross-section. The main advantage of rectangular canals is relative ease of construction and a smaller width required for the same flow as compared to trapezoidal canals. Disadvantages chiefly are higher structural stress due to pressure on the side walls and a higher risk of caving in if used in unlined earth construction.

There are four parameters which influence flow in rectangular cross-sections, identical to the relation of STRICKLER {2.1} valid for any cross-section:

{2.1} $$Q = k\ s^{1/2}\ \frac{A^{5/3}}{U^{2/3}} \quad [m^3/s]$$

where: k = friction coefficient of STRICKLER [-] (refer to the note at the top of page 33)
s = the slope or gradient of the channel [-]
A = cross-sectional area [$m^2$]
U = wetted perimeter [m]

For the special case of rectangular cross-sections, A and U may be expressed by the relation of the channel width **B** [m] and the water depth **h**:

{2.3} $$A = B\ h \quad [m^2]$$

{2.4} $$U = B + 2h \quad [m]$$

resulting in equation {2.5}:

{2.5} $$Q = k\ s^{1/2}\ \frac{(B\ h)^{5/3}}{(B + 2\ h)^{2/3}} \quad [m^3/s]$$

The nomogram in fig. 2.3 contains the flow Q and the four parameters s, **k**, **B**, and the relation **h/B**. If any four of the five are known, it is possible to find the solution to the missing parameter, as shown in the example.

**Example:**
find the water depth h if Q = 0.22 [$m^3/s$], k = 70, s = 10‰ and B = 0.5 [m].

Solution: trace a line from the value 0.22 on the Q-scale to 70 on the k-scale, thereby establishing an intersection point on reference line (2). Trace a line from the value of 10 on the s-scale through the intersection point previously found, upto reference line (1). Complete the task by tracing a line from the intersection point on reference line (1) through the value of 0.5 on the B-scale and upto the scale **h/B**. The solution found is h/B = 0.50, and multiplying this value by B = 0.5, gives h = 0.25 [m] for the resulting water depth.

Note: the friction coefficient k of STRICKLER is not to be confused with roughness coefficients used in other equations by other authors. Throughout this manual, STRICKLER's friction coefficient is used, which has proven to be adequate and simple to apply. For in depth study of fluid friction under various flow conditions, many specialised books exist, such as for instance [2] by Hunter ROUSE and [5] by D.S.MILLER.

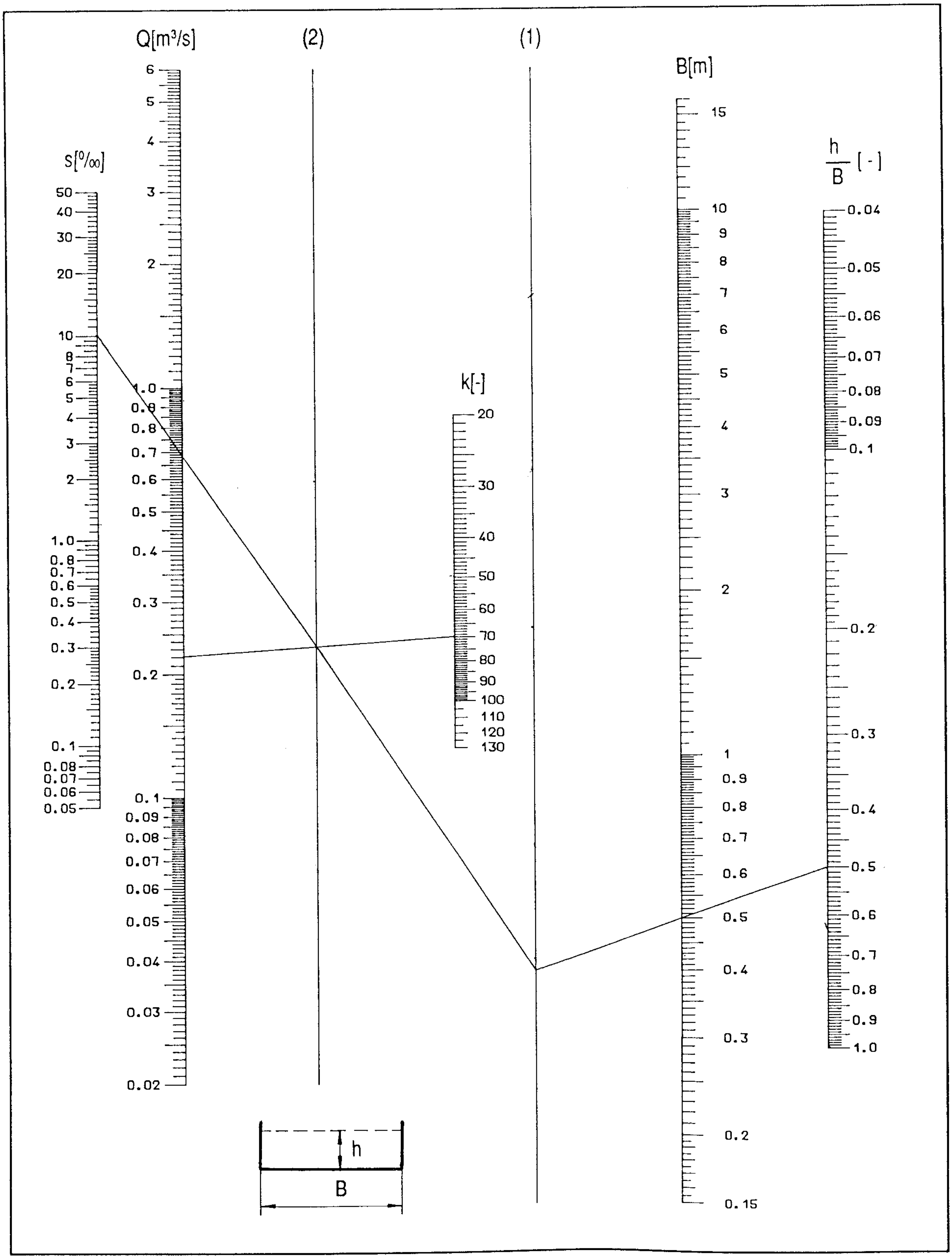


Fig. 2.3 : Flow in rectangular canal cross sections

## 2.2.3 Hydraulically well designed shapes for trapezoidal canal cross sections

What means hydraulically well designed ?

Definition: Among all possible channel cross sections having an equal cross-sectional area, the same surface roughness and the same channel slope, the one having the highest water discharge per unit of time is hydraulically the best.

This means when choosing a suitable channel cross section that we are aiming at a maximum flow velocity. This is the case, if the wetted perimeter is a minimum.

The flow velocity can be expressed by the formula :

$$v = k\, s^{1/2} \frac{A^{2/3}}{U^{2/3}} \qquad \{2.6\}$$

v = flow velocity [m/s]
s = slope [ - ]
A= cross sectional area [$m^2$]
U= wetted perimeter [ m ]

Among all curves, the circle encloses the biggest area for a given perimeter. Therefore the circle is the hydraulically best shape for closed conduits, the semi-circle the best for open channels.
As rectangular and trapezoidal channel cross sections are common, it is of interest to know the optimal dimensions for such channel cross sections. For rectangular cross sections, the optimal width and depth are found if the following relation is observed:

$$b_{opt} = 2\,h \qquad \{2.7\}$$

b = channel bottom width [m]
h = channel depth [m]

For trapezoidal cross sections, the optimal relation of channel width and side wall slope to channel depth is somewhat more complex and needs to satisfy the formula:

$$h = \sqrt{\frac{A \sin\alpha}{2 - \cos\alpha}} = \frac{b}{2} \cdot \frac{1}{\sqrt{1 + \cot^2\alpha} - \cot\alpha} \qquad \{2.8\}$$

h = water depth [ m ]
b = canal bottom width [ m ]
1 : n = tan α = tangent of side wall slope
(cot α = n )

**Example**

The slope of the channel side wall has been chosen to be 1 : 2, wich means n = 2 and therefore α the slope angle = 26,56° (arc tan 0,5). The water depth shall be 3 m ( h = 3m ).
What is the optimal channel bottom width ( b = ? ), in order to obtain the hydraulically best possible channel cross section ?

Solution :

Use the nomogram in fig. 2.4 and connect the point 3 [ m ] on the h-scale with the point 2 on the n-scale and read the value of the intersection point on the b-scale : ⇨ b = 1,42 m

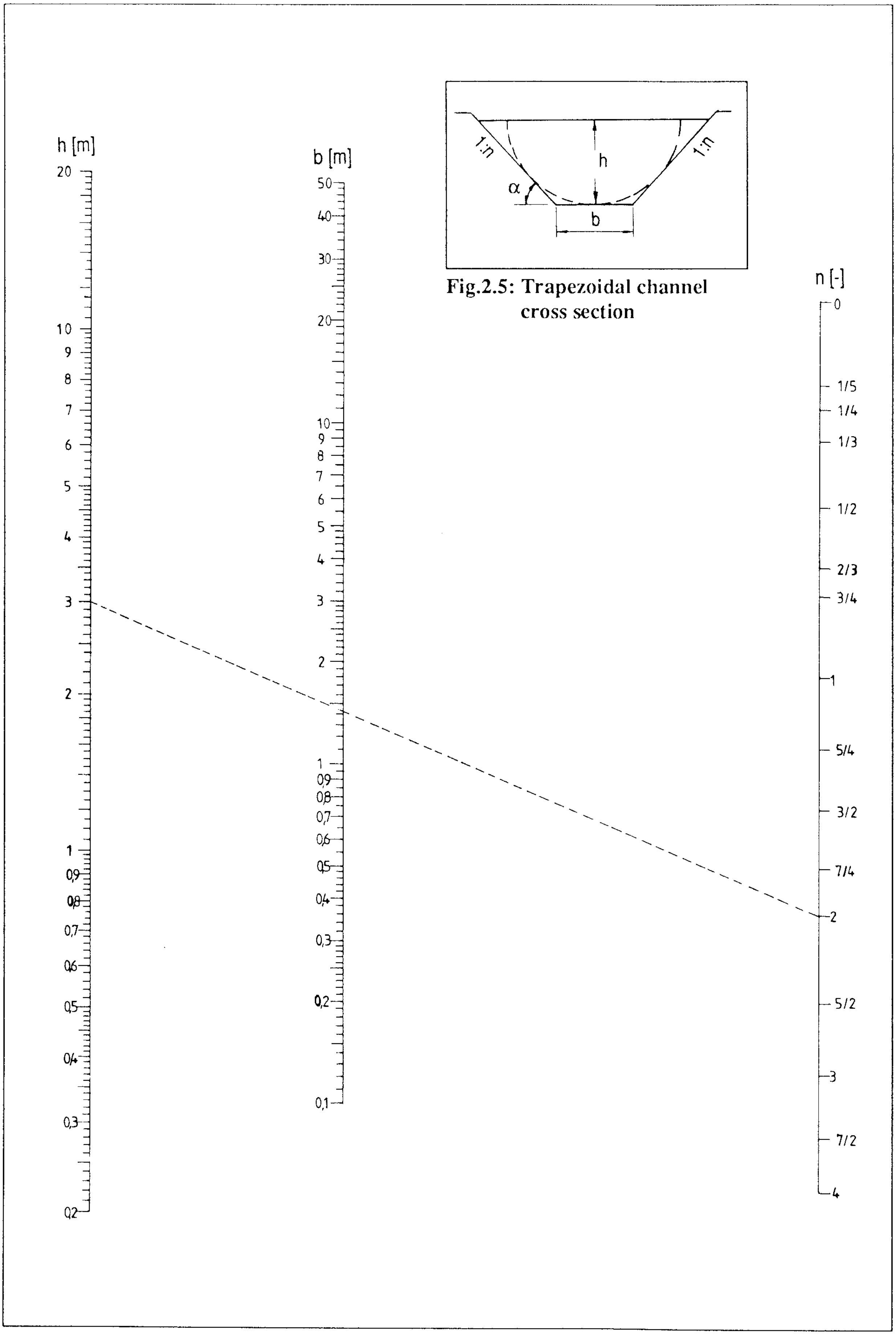


Fig.2.5: Trapezoidal channel cross section

Fig. 2.4: Nomogram for optimal channel sections

## 2.2.4 Nomogram for trapezoidal channel cross-sections

This nomogram is very versatile. It shows the relationship of discharge, flow velocity and the geometrical shape of trapezoidal channel cross-sections. It is preferrably used in conjunction with the discharge nomogram of STRICKLER in section 2.2.1, which is for the pre-selection of the slope of a channel in order to obtain a certain discharge with a given cross-sectional area, or vice versa. When using the nomogram, reference should also be made to the nomogram for hydraulically well designed shapes for trapezoidal channels, in section 2.2.3. The nomogram in fig. 2.6 is based on the following formulae:

{2.9}
$$Q = v \cdot A$$

where: Q = discharge [m³/s],
v = flow velocity [m/s],
A = cross-sectional area [m²]

{2.10}
$$A = b\,h + h^2\,n$$

where: b = channel bottom width [m],
h = water depth [m],
n = cotangent of the side wall slope [-]

{2.11}
$$h = \frac{1}{2}\left[\sqrt{\left(\frac{b}{n}\right)^2 + \frac{4A}{n}} - \frac{b}{n}\right]$$

**Example:**

The task is to design a trapezoidal channel having the following properties:
- design discharge Q = 1.335 [m³/s],
- flow velocity in the channel v = 1.5 [m/s]
- cotangent α of the side wall slope n = 2 [-]
- friction coefficient k = 30 [-]

Solution:

Step 1: find the cross-sectional area A [m²] in the nomogram in fig. 2.6: trace a line from the $\frac{Q}{n}$-scale at the value of $\frac{1.335}{2} = 0.668$, to the value of 1.5 [m/s] on the v-scale and extending the line upto the $\frac{A}{n}$-scale. The result reads 0.445, and as n = 2 ➪ A = 2 • 0.445 = 0.890 [m²].

Step 2: find the optimal water depth h [m] for hydraulically well designed shapes of trapezoidal channels: since the bottom width b is not known for the moment, none of the nomograms can be used directly. The depth h must be calculated by the formula:

{2.12}
$$h = \sqrt{\frac{A \sin\alpha}{2 - \cos\alpha}}$$

where: α is the side wall angle of the channel and as the cotangent α = 2, ➪ angle α = 26.565°

$$h = \sqrt{\frac{0.89 \sin 26.565}{2 - \cos 26.565}} = 0.6 \text{ [m]}$$

Step 3: find the canal bottom width b [m]: by using the nomogram in fig. 2.6, trace a line starting on the $\frac{A}{n}$ -scale at the value of 0.445, intersecting the h-scale at the value of 0.6 and extending upto the $\frac{b}{n}$ -scale, where the value of 0.1415 is found. Since n = 2 ⇒ b = 0.1415 · 2 = 0.283 [m].

Note: Further explanations regarding the use of nomograms 2.2 and 2.4 in combination with this exercise are given on page 38 .

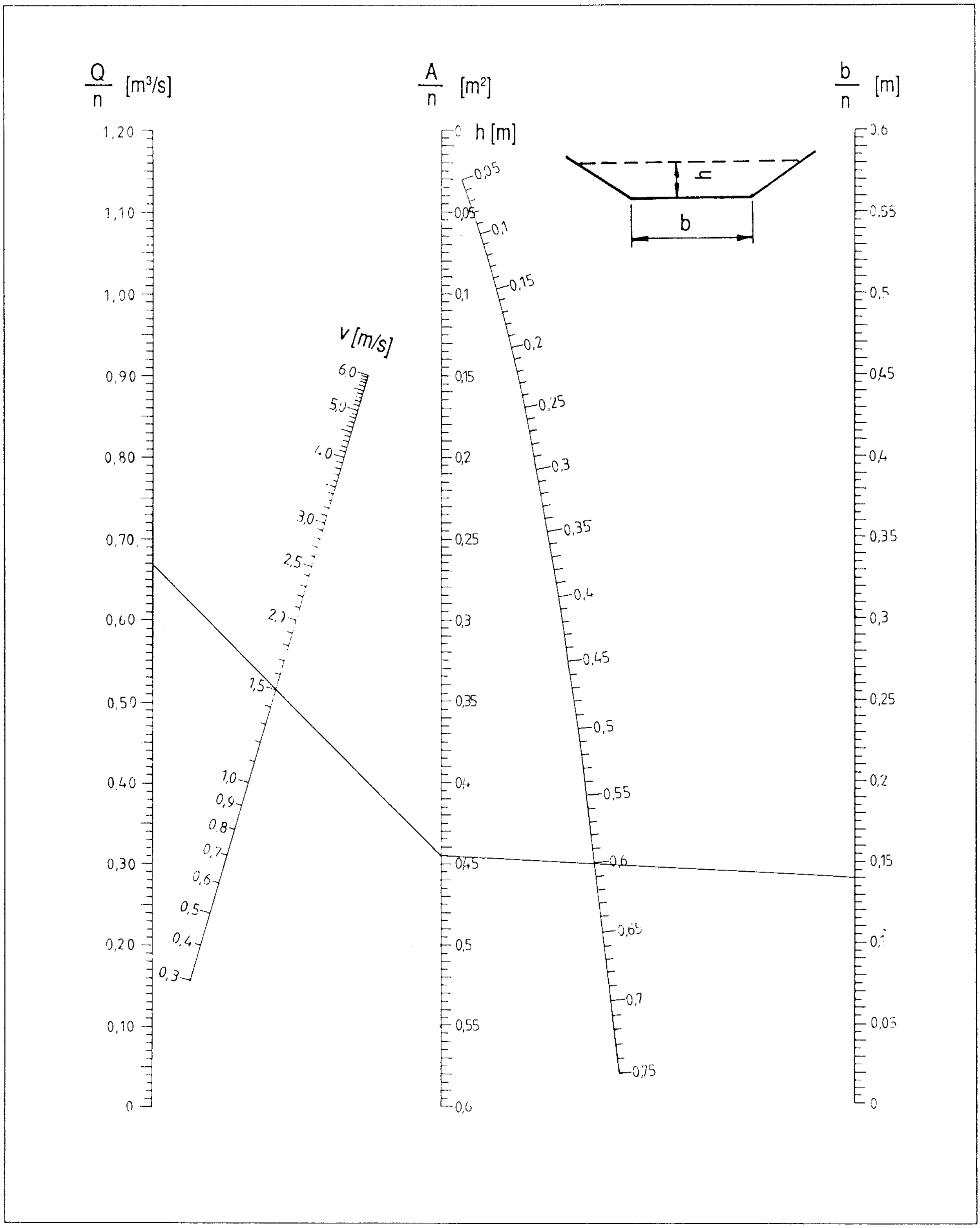


Fig. 2.6: Nomogram for trapezoidal channel cross sections

As an alternative to using nomogram 2.6 to find the optimal channel bottom width b, nomogram 2.4 (page 35) may also be used: by connecting the value of 0.6 on the h-scale with the value of 2 on the n-scale, b may be read from the b-scale, showing a value of 0.283 [m].

It is also possible to calculate the value of b with the equation:

$$b = 2h\left(\sqrt{1 + \cot^2 \alpha} - \cot \alpha\right) \tag{2.13}$$

$$b = 2 \cdot 0.6\left(\sqrt{1 + 2^2} - 2\right) = 0.283 \text{ [m]}.$$

To also find the required gradient of the channel in order to achieve a flow velocity of v = 1.5 [m/s] as given for the example, two further steps are required.

Step 4: calculate the wetted perimeter U of the canal cross-section:

$$U = b + 2\left(\frac{h}{\sin \alpha}\right) \tag{2.14}$$

$$U = 0.283 + 2\left(\frac{0.6}{\sin 26.565}\right) = 2.966 \text{ [m]} \cong 3.0 \text{ [m]}$$

Step 5: find the required channel gradient s, by means of the nomogram in fig. 2.2 on page 31 :

a) determine the intersection point on reference line (1) by connecting the value of 3 on the U-scale with the value of 0.89 on the A-scale.

b) determine the intersection point on reference line (2) by connecting the value of 1.335 on the Q-scale with the value of 30 on the k-scale:

c) find the value of s by tracing a line from the intersection point on reference line (1), through the intersection point on reference line (2), to the s-scale; we find 12.45, which is the solution, and means that the channel drops 12.45 meters per 1000 m of length.

## 2.2.5 Nomogram for discharge measurement with weirs

The type of weir used in this nomogram is the so called rectangular thin-plate weir. It is a flow measuring method utilising an artificial control section with defined geometrical dimensions. The application of a discharge formula and the measurement of the water level permit to determine the discharge without the need for prior calibration.

For correct results, it is important that the plate is smooth and plane and perpendicular to the main axis of the channel. The structure must be sealed properly to ensure that the entire amount of water passes the weir notch. The upstream edges of the weir notch must be sharp and the downstream edges chamfered under at least 45° if the plate is thicker than 3 mm, which is likely as the plate has to withstand the water pressure resulting from the level difference of water on the upstream and the dowstream side. The discharge nappe must be fully ventilated and must not be submerged, in order to achieve free fall of water. In case of a full-width weir, where the length of the crest is equal to the width of the channel, this requires special provision for ventilation of the nappe, such as a ventilation pipe on each side of the channel.

The recommended location for the head measurement is upstream of the weir at a distance equal to three to four times the maximum head to be measured.

The nomogram is based on the discharge formula :

{2.15}

$$Q = \frac{2}{3} \mu \ b \ h \sqrt{2gh}$$

where: Q = discharge [m³/s],
b = crest width [m]
h = piezometric head of the upstream water surface above crest level [m]
g = gravitational constant = 9.81 [m/s²]
μ = discharge coefficient [m]

For the case of a full-width weir where B = b, BUNTSCHU has given a value of approximation for the discharge coefficient μ as:

{2.16}

$$\mu = \sqrt{\frac{1}{3}} = 0.577$$

The nomogram in fig. 2.8 is valid for weirs of b = 1.0 [m], either full-width with the value of μ as in equation {2.16} or with different values of μ for partially contracted weirs. The latter are recommended for accurate measurements and μ must be calculated with equation {2.17}, which has been specified by the Swiss Association of Standards:

{2.17}

$$\mu = \left\{0.578 + 0.037 \left(\frac{b}{B}\right)^2 + \frac{0.00365 - 0.0030\left(\frac{b}{B}\right)^2}{h + 0.0016}\right\} \cdot \left\{1 + 0.5\left(\frac{b}{B}\right)^4 \left(\frac{h}{h+P}\right)^2\right\}$$

where: b = crest width [m]
B = channel width [m]
h = piezometric head [m]
P = weir height [m]

and the following limitations are strictly observed:
- h/p shall not exceed 1.0
- the head h shall exceed 0.025 · b/B [m], but shall be less than 0.8 [m]according to fig. 2.7
- b/B shall not be less than 0.3
- the weir height P shall be at least 0.3 [m]

**Example on how to use the nomogram in fig. 2.8:**

Given data: $\mu$ = 0.577 [ - ]
h = 0.06 [m]
b = 1.0 [m]

Result:

Q = 25 [l/s], since b is 1 [m] in the nomogram. For other widths b of weir, Q is a proportional multiple or fraction of b. for example, if the nomogram is to be used for a weir width of 2.0 [m], the value for Q read from the nomogram must be multiplied by a factor of 2. Be aware that the limitations mentioned at the bottom of page 39 are still valid.

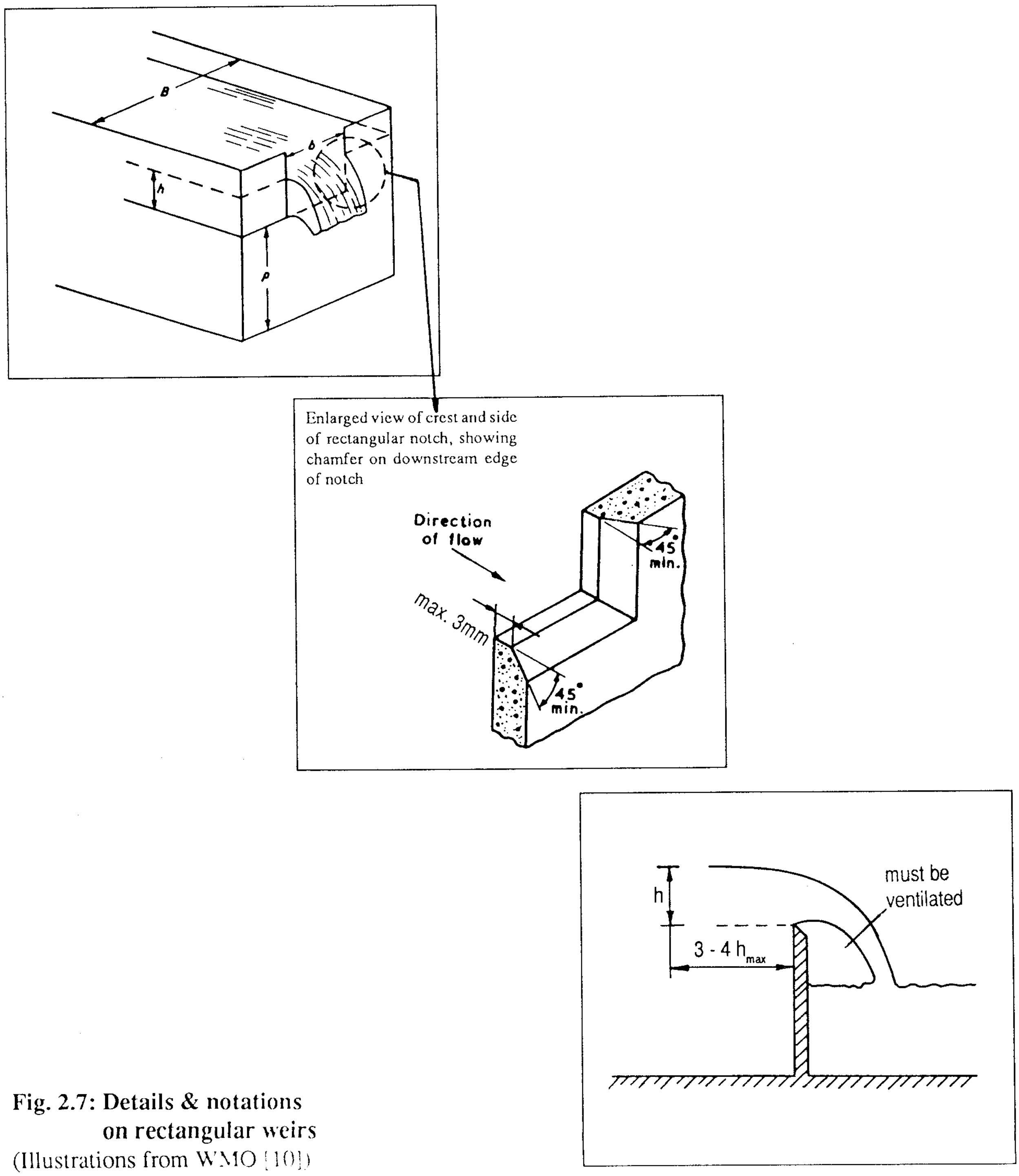


**Fig. 2.7: Details & notations on rectangular weirs**
(Illustrations from WMO [10])

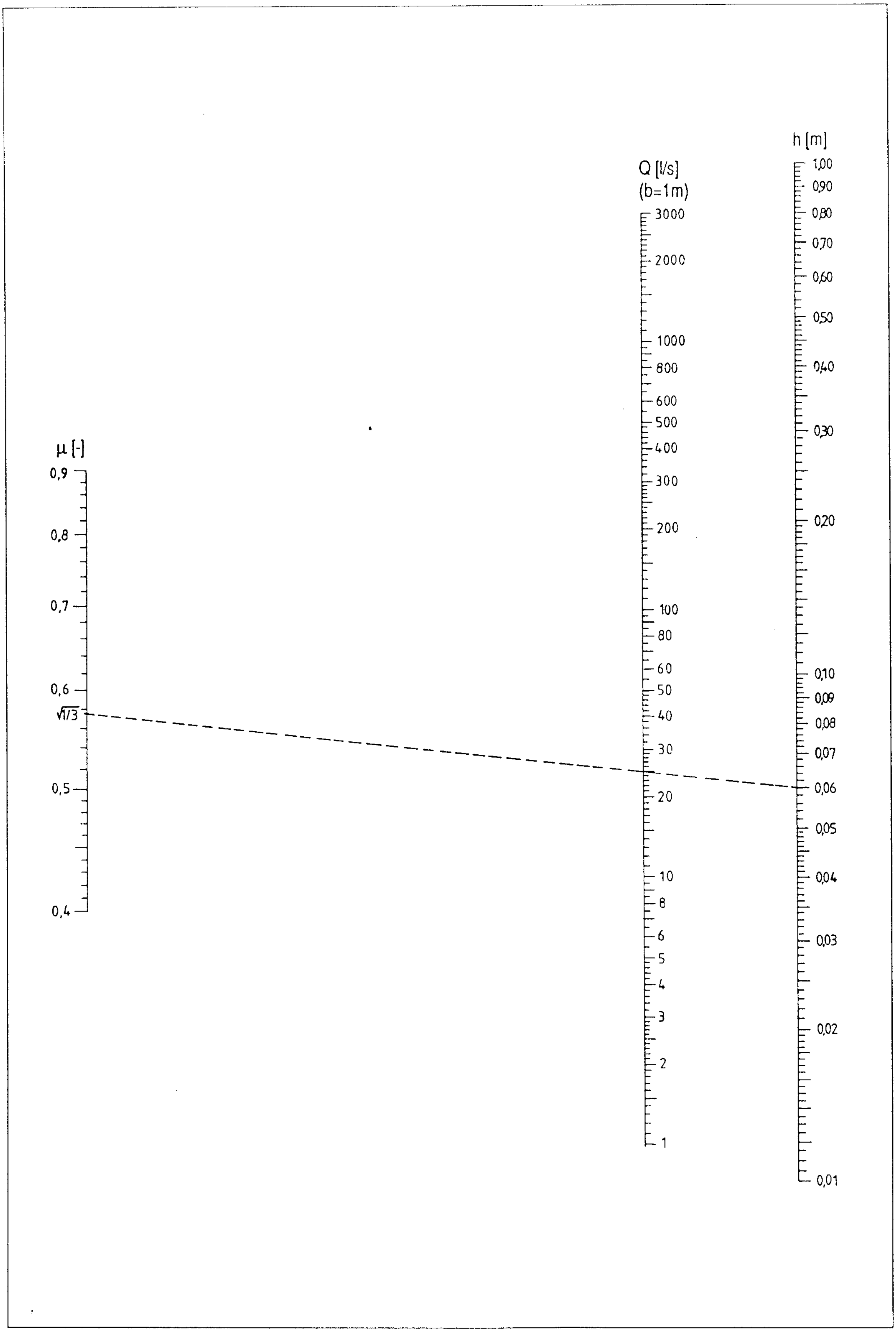


Fig.2.8: Nomogram for discharge measurement with weirs

## 2.2.6 Head losses in penstocks and related other losses

### 2.2.6.1 Nomogram for head losses in penstocks

For successful micro hydropower projects, it is essential to know head losses $\Delta H$ due to friction in the penstock as well as elsewhere in the waterway at an early stage because the actual turbine working head $H_{net}$ is a key parameter in turbine selection and design, affecting the operating speed, discharge through the turbine and power output.

The actual working head or net head $H_{net}$ may be calculated by substracting total head losses $\Delta H_{tot}$ from the geodetic head H, where $\Delta H_{tot}$ consists of total losses due to friction in the penstock plus all other losses applying.

{2.18}

$$H_{net} = H - \Delta H_{tot} \quad [m]$$

Head losses in the penstock H may be calculated by equation {2.19} :

{2.19}

$$\Delta H = \frac{4^{10/3}}{\pi^2} \frac{Q^2 L}{k^2 D^{16/3}} \quad [m]$$

where: $\pi$ = 3 .141593
Q = discharge through the penstock [m³/s]
L = straight length of the penstock [m]
D = the inside diameter of the penstock [m]
k = the fricition coefficient used [-], according to STRICKLER

For convenience, the formula may also be written as:

{2.20}

$$\Delta H = 10.294 \frac{Q^2 L}{k^2 D^{5.33}} \quad [m]$$

In order to be able to deduct head losses from gross head as a basis for further calculations, units shown are usually in meters. This, however is not strictly correct. Proper units are mkg/s², which are energy units, which head losses actually represent. The following facts become apparent when looking at equation {2.20}
- The influence of penstock length L is directly proportional to head losses.
- The influence of discharge Q is proportional to the second power of Q, i.e. doubling the discharge results in a four-fold increase of head losses.
- The influence of friction k is reciprocally proportional to the second power of k, i.e. double the k-number results in head losses of 25% of the original value.
- The influence of diameter D is reciprocally proportional to the power of 5.33 of the diameter, i.e. doubling the diameter results in head losses of $1/2^{5.33}$ = 2.5% of the original value. Reducing the diameter to half, increases head losses about fourty times.

The nomogram in fig. 2.9 may conveniently be used to find one of the head loss related values, if the three other parameters are given.

**Example:**
Find the head loss $\Delta H$ for a penstock in the following situation:
Discharge Q=0.3 [m³/s], material of penstock: welded steel, diameter D of penstock = 0.3 [m] and the length of the penstock L = 15 [m].

Solution:
As a first step, the friction coefficient k for the material used must be determined.
We use k = 80 from the table in fig. 2.10.
Using the nomogram: by tracing a line from the value of 80 on the k-scale to the value of 300 (= 0.3 $m^3$/s) on the Q-scale, we determine an intersection point on the reference line. By subsequently tracing a line from the value of 0.3 on the D-scale, through the intersection point on the reference line and upto the ΔH-scale, we determine the head loss in meters per one meter length of penstock ΔH = 0.089. Multiplied by the penstock length L = 15 [m], we get:

$$\Delta H = 0.089 \quad 15 = 1.335 \text{ [m]}.$$

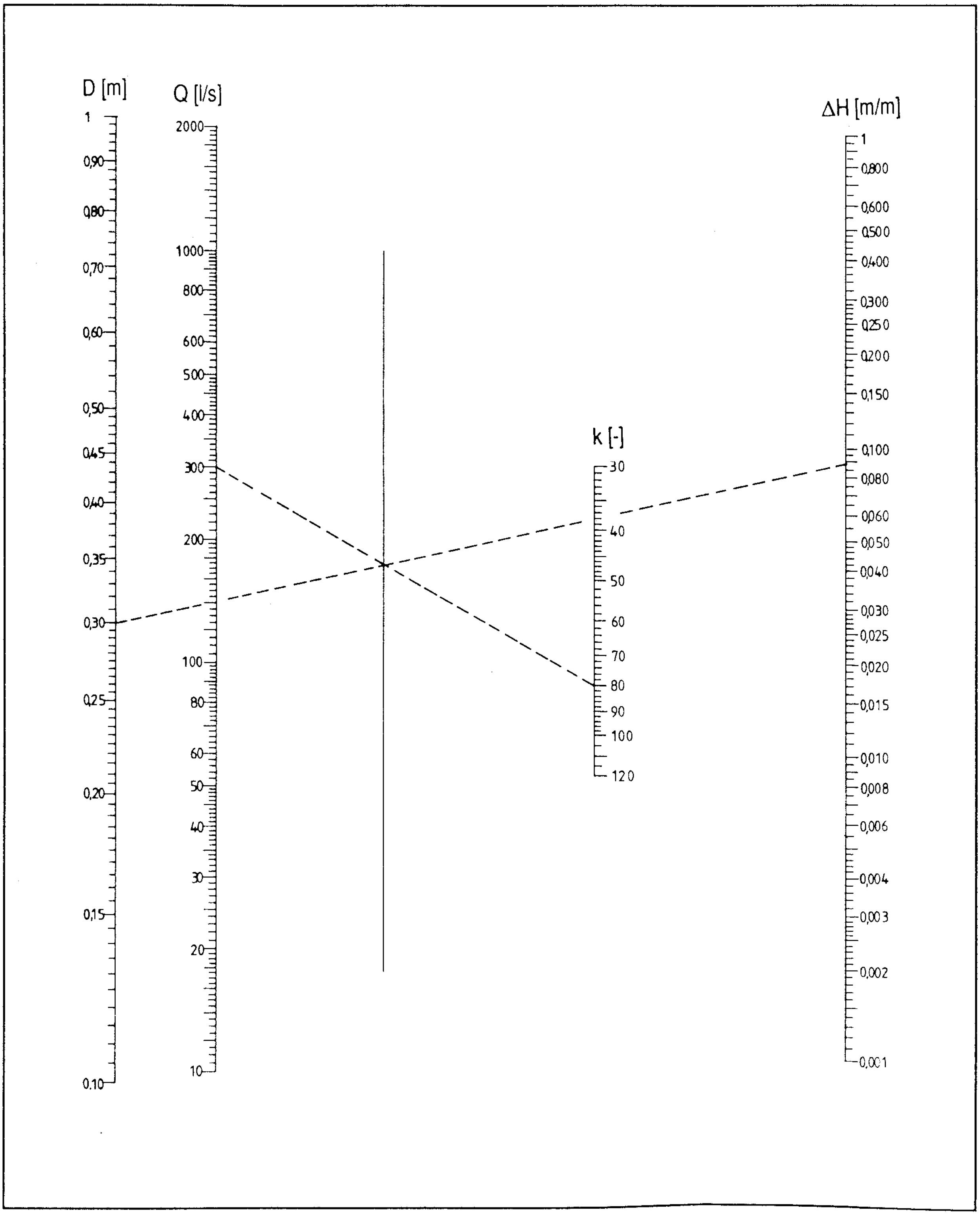


Fig. 2.9 : Nomogram for head losses in penstock

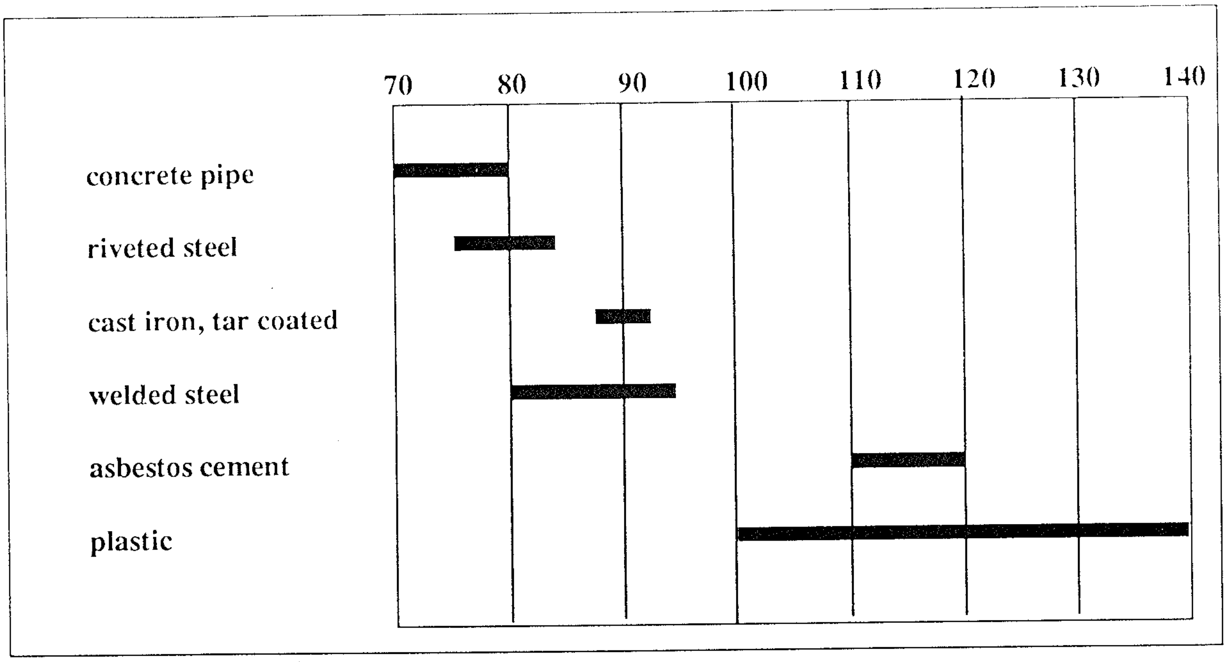


**Fig. 2.10 : Friction coefficients k for penstock materials according to STRICKLER (note that higher k-numbers mean lower losses)**

### 2.2.6.2 Related other head losses

Minor losses occur at the penstock entrance and due to penstock joints and bends. To account for such losses for the calculation of the net head, it is convenient to introduce the coefficient of resistence $\zeta$, according to formula 2.21:

$$\boxed{\Delta h = \zeta \frac{v^2}{2g} \quad [m]} \qquad \{2.21\}$$

Where: $\Delta h$ = head loss [m]
$\zeta$ = the coefficient of resistance applicable
v = the exit velocity at the cross sectional area under consideration [m/s]

The values of the coefficient of resistance have been empirically established for many situations. A few relevant cases are shown in figure 2.11:

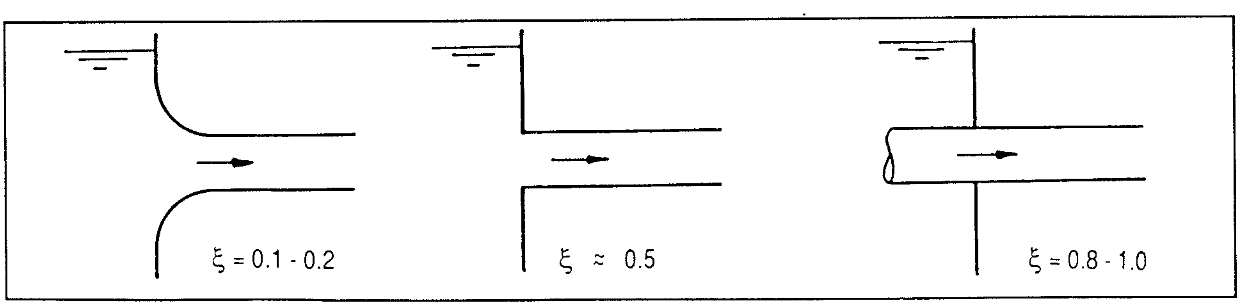


**Fig. 2.11: Entrance loss resistance coefficients**

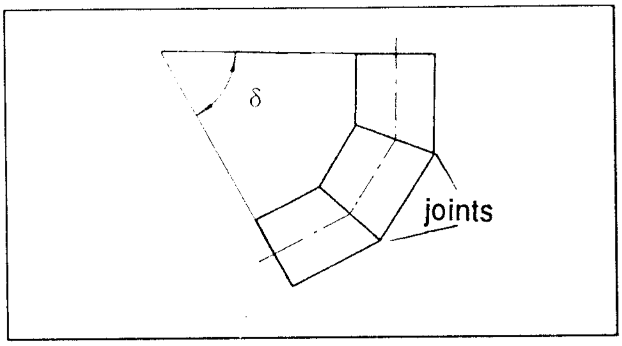


| δ | 15° | 22.5° | 30° | 45° | 60° | 90° |
|---|---|---|---|---|---|---|
| Number of joints | 1 | 1 | 2 | 2 | 3 | 3 |
| ζ | 0.08 | 0.10 | 0.12 | 0.18 | 0.25 | 0.31 |

Fig. 2.12: Resistance coefficients at bends

### 2.2.6.3 Several penstocks in parallel

Depending on circumstances, one may also consider to design two or more penstocks in parallel of a smaller diameter, instead of one large-diameter penstock. To investigate such alternatives, it is useful to know the basic hydraulic relationship for the comparison of a single penstock and several (n) penstocks in parallel for a given discharge. For this purpose, the table in figure 2.13 shows the hydraulic relations for the three different cases of interest:

case a: a single penstock
case b: n-number of penstocks for the same flow or velocity as in case a
case c: n-number of penstocks for the same head loss as in case a

| | case a | case b | case c |
|---|---|---|---|
| discharge per penstock | $Q$ | $\frac{Q}{n}$ | $\frac{Q}{n}$ |
| internal penstock diameter | $d$ | $\frac{d}{\sqrt{n}}$ | $\frac{d}{\sqrt[5]{n^2}}$ |
| flow velocity in the pipe | $v$ | $v$ | $\frac{v}{\sqrt[5]{n}}$ |
| head loss per meter length of pipe | $h$ | $\sqrt{n} \cdot h$ | $h$ |
| wetted perimeter of all penstocks | $U$ | $\sqrt{n} \cdot U$ | $\sqrt[5]{n^3} \cdot U$ |
| penstock wall thickness | $t$ | $\frac{t}{\sqrt{n}}$ | $\frac{t}{\sqrt[5]{n^2}}$ |
| total weight of all penstocks per meter length | $W$ | $W$ | $\sqrt[5]{n} \cdot W$ |

Fig. 2.13: Hydraulic comparison of different penstock arrangements

## 2.2.7 Diagram for the pre-selection of the economically optimal penstock diameter

For a given discharge, penstocks with a large diameter have lower flow velocities and consequently a low head loss due to friction, as compared to smaller diameters where the head loss is higher. On the other hand, large diameters incur higher costs than small diameters.

Friction losses in the penstock reduce the potential energy production of the plant during its working life. Since head losses increase with smaller penstocks, the potential energy production loss increases. Selecting the economically optimal penstock diameter is therefore an optimization process, where the initial investment cost and resulting operating cost are to be considered versus the potential energy production loss and the resulting reduction of total income from the sale of energy.

In general terms, a penstock is economically optimal, if the sum of yearly operating costs of the penstock, including maintenance, interest payable for the investment and depreciation plus the price of yearly energy production losses, is a minimum.

In the planning process of micro hydropower stations, the economical diameter of the penstock, including possibly sections of different material thickness, may be calculated, once the size and situation of the power plant and its operating mode and the profile of the penstock, are established. Static pressure in the penstock is given for each point of the penstock by its geodetic head with reference to the lowest point. In order to calculate the required thickness of the penstock, dynamic pressure resulting from various operating conditions, including possible water-hammer effects, must be added to arrive at the total pressure p for which the penstock must be safe. Refer to section 2.2.9 for resolving the question of the maximum pressure. Economic parameters shall be discussed here in detail.

The energy losses consist chiefly of the friction losses incurred due to water flowing through the penstock, and are expressed in the corresponding loss of head $\Delta H$ [m], according to equation {2.22}, per meter of penstock length:

{2.22}
$$\Delta H = \frac{v^2}{k\ D\ 2g} \quad [m]$$

where:
- k = friction coefficient according to the pipe material used [-]
- D = the inside diameter of the penstock [m]
- v = the flow velocity in the penstock [m/s]
- g = the gravitational constant = 9.81 [m/s$^2$]

by substituting:

{2.23}
$$v = \frac{4\,Q}{\pi\,D^2} \quad [m/s]$$

where:

Q = the discharge at full load [m$^3$/s]
$\pi$ = 3.14159...

we get the value of the loss of head reciprocally proportional to the fifth power of the diameter:

{2.24}
$$\Delta H = \frac{8\,Q^2}{\pi^2\,g\,k\,D^5} \quad [m]$$

Based on this, the resulting energy loss is also reciprocally proportional to the fifth power of the diameter, and is equal to:

{2.25} $$\Delta P = \frac{\eta\, Q\, \Delta H}{102} \quad [kW]$$

where: $\Delta P$ = energy loss of the plant [kW]
$\eta$ = the overall plant efficiency [-]
$\Delta H$ = head loss according to equation {2.24} [m]

If we further introduce yearly full load operating hours calculated by dividing kW-hours produced by installed capacity = **S** [h], and an average energy price per kWh **a**, the cost of energy lost is:

{2.26} $$\text{Cost of energy lost} = S \cdot a \cdot \Delta P$$

The capital invested, on the other hand, is proportional to the weight of the penstock. By using the hoop stress formula (page 50{2.32}) for the calculation of the required penstock thickness **t** [m], the weight **W** [kg] per meter of penstock length is established according to equation {2.27}:

{2.27} $$W = \frac{\rho\, \pi\, D_m^{\,2}\, p}{2\, \sigma_{perm}} \quad [kg]$$

where: W = the weight [kg], per meter length
p = the operating pressure [kgf/cm²]
$D_m$ = the mean diameter of the penstock = inside diameter D + wall thickness t
$\sigma_{perm}$ = the permissible stress [kgf/cm²]
$\rho$ = the density of material used [kg/m³]

In addition to the penstock material, costs of flanges, anchors and supports as far as related to the diameter, are taken care of by a factor of **n** > 1. The capital invested in the penstock is then calculated by taking the price per ton **T**, ex-works, plus freight, assembly at site and corrosion protection. The yearly costs for interest, depreciation, maintenance, and other costs are represented by a factor **b** as a percentage of the capital invested. Since yearly costs are thus proportional to the weight and the weight is proportional to $D^2$, yearly costs **b** are also proportional to $D^2$, it is eventually possible to solve the entire equation for D with formula {2.28}:

* {2.28} $$D = 0.77 \sqrt[7]{\frac{\eta\, \sigma_{perm}\, a\, Q^3\, S}{k\, p\, n\, T\, b}} \quad [m]$$

*The above equation and its derivation is based on chapter 1.4 of the book ''Druckrohrleitungen neuzeitlicher Wasserkraftwerke'' [6]

Based on experience, the following ranges of values are thereby appropriate:

$\eta$ = overall plant efficiency = 0.6 ... 0.7
k = friction coefficient = 80 ... 100 (according to fig. 2.10, on page 44)
$\sigma_{perm}$ = permissible hoop stress at operating pressure = 1000 ... 2000 [kgf/cm²]
a = price of energy generated = 0.05 ... 0.15 [U.S.$/kWh]
T = price per tonne of penstock, assembled = 1'200 ... 2'000 [U.S.$/ton]
b = yearly cost factor of the capital invested = 0.08 ... 0.15 [-]
n = factor for additional costs of accessories = 1.05 ... 1.1
p = operating pressure, which is always > net head H, and is expressed in [kgf/cm²]

To facilitate using the equation, it may also be written as:

$$\{2.29\} \quad D = \left(0.77 \sqrt[7]{\frac{\eta\, \sigma_{perm}\, a\, S}{k\, n\, T\, b}}\right) \cdot \sqrt[7]{Q^3} \cdot \sqrt[7]{\frac{1}{p}} \qquad [m]$$

and if we substitute A for the first term, B for the second term and C for the third term of the equation, we get:

$$\{2.30\} \quad D = A \cdot B \cdot C$$

where: $A = f(\kappa)$,

$$\{2.31\} \quad \kappa = \frac{\eta\, \sigma_{perm}\, a\, S}{k\, n\, T\, b} \quad \Rightarrow A = 0.77\, \kappa^{0.1429}$$

$B = f(Q) = Q^{0.4286}$
$C = f(p) = p^{-0.1429}$

The diagram in fig. 2.14 shows curves and the values of A, B and C on the vertical scale, in relation to $\kappa$, Q and p respectively. For each situation, p and Q are determined elsewhere in the design process and calculation work here is reduced to calculating appropriate values. The optimal diameter may then be calculated by multiplying the graphically obtained values of A, B, and C according to formula {2.30}.

**Example:**
Find the optimal penstock diameter for a plant with a static head H of **40** [m] and an operating pressure calculated at p = **5.2** [kgf/cm$^2$], a discharge of Q = **0.26** [m$^3$/s], where the following other factors are assumed:

- overall efficiency $\eta$ = 0.6 [ - ]
- permissible material stress $\sigma_{perm}$ = 1100 [kgf/cm$^2$]
- average price of energy generated a = 0.08 [U.S.$/kWh]
- unit cost of penstock T = 1800 [U.S.$/ton]
- yearly full load operating hours S = 2000 [hrs/year]
- capital cost factor; interest, depr, O+M b = 0.12 [ - ]
- factor for accessory costs n = 1.1 [ - ]
- welded steel penstock: friction coefficient k = 80

Solution:
As a first step, the factor $\kappa$ must be calculated using equation {2.31}, we find:

$$\kappa = \frac{\eta\, \sigma_{perm}\, a\, S}{k\, n\, T\, b} = \frac{0.6 \cdot 1100 \cdot 0.08 \cdot 2000}{80 \cdot 1.1 \cdot 1800 \cdot 0.12} = 5.55$$

Then, by using the diagram in fig. 2.14, find the values of A, B and C on the vertical scale:

⇨ A = 0.984; intersection of $\kappa$ = 5.55 on the curve A = f($\kappa$)
⇨ B = 0.56 ; intersection of Q = 0.26 on the curve B = f(Q)
⇨ C = 0.79 ; intersection of p = 5.2 on the curve C = f(p)

With formula {2.30}, the optimal diameter D may now be calculated:

$D = A\ B\ C = 0.984 \cdot 0.56 \cdot 0.79 = 0.43$ [m] ,representing the optimal diameter for the parameters assumed

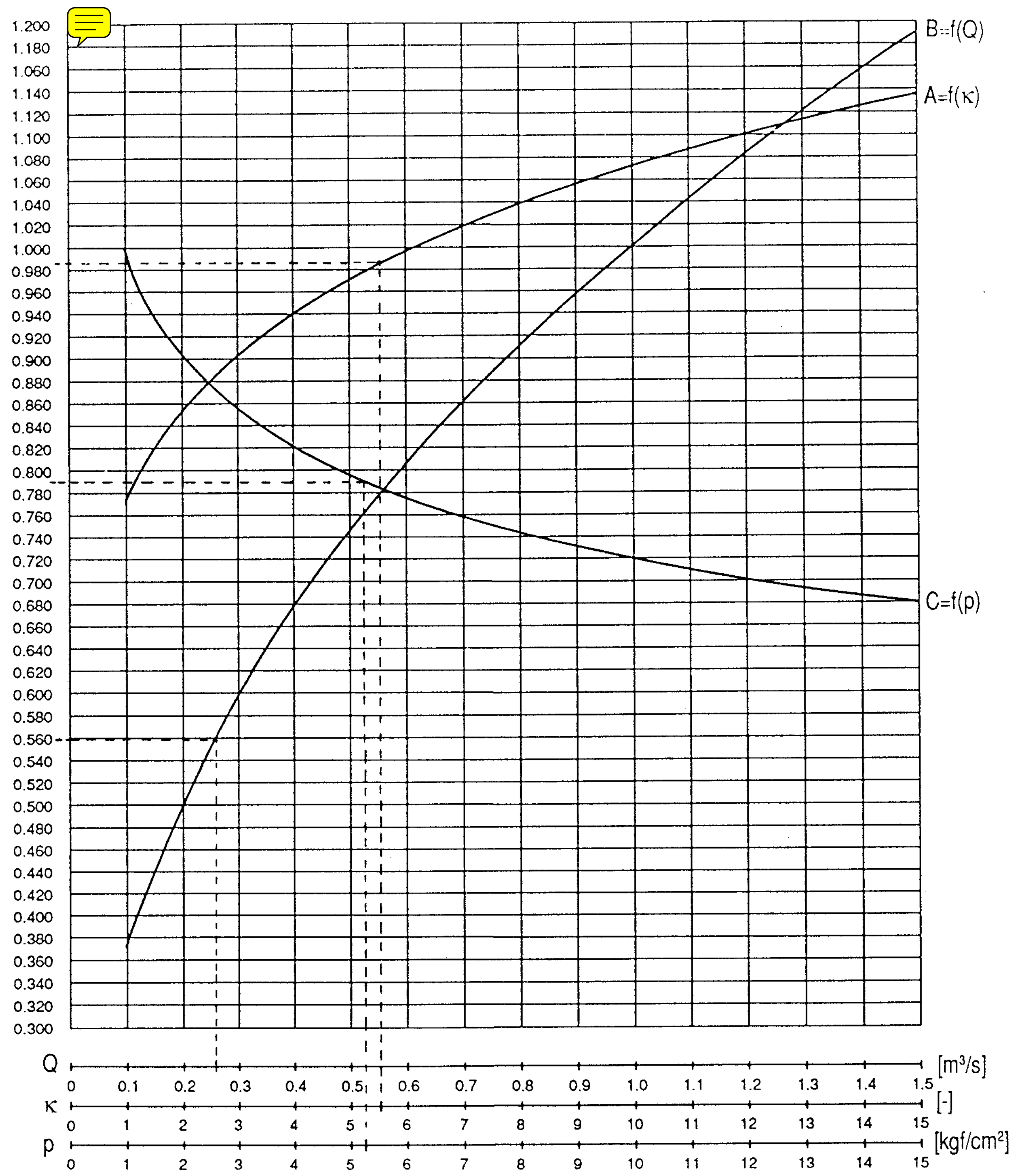


**Fig. 2.14: Diagram for the pre-selection of the economically optimal penstock diameter**

# ERRATA page 47 to 49

In formula {2.28} and {2.29}, an error has been introduced because it was wrongly assumed, that the friction coefficient of STRICKLER $k = 1/\lambda$, where $\lambda$ is the friction/roughness coefficient of the MOODY diagram. In fact, the relationship between k and $\lambda$ is more complex.

The diagram in fig. 2.14 incorporates this error and its magnitude depends on the penstock diameter D and the STRICKLER coefficient k used. The result found must therefore be multiplied by the correction factor f of the diagram provided here, which is found using the obtained value of D and the value of k applied.

The correct diameter D is:

$$\boxed{D = A\ B\ C\ f}$$

where A, B and C are from formula {2.30} on page 48 in the handbook, and f is the factor obtained from the diagram provided on this errata sheet.

For the diameter of 0.43 m found in the example in the handbook and with k = 80, the correction factor found is 1.11 and the correct diameter therefore is 11% larger: 0.43 x 1.11 = 0.48 m.

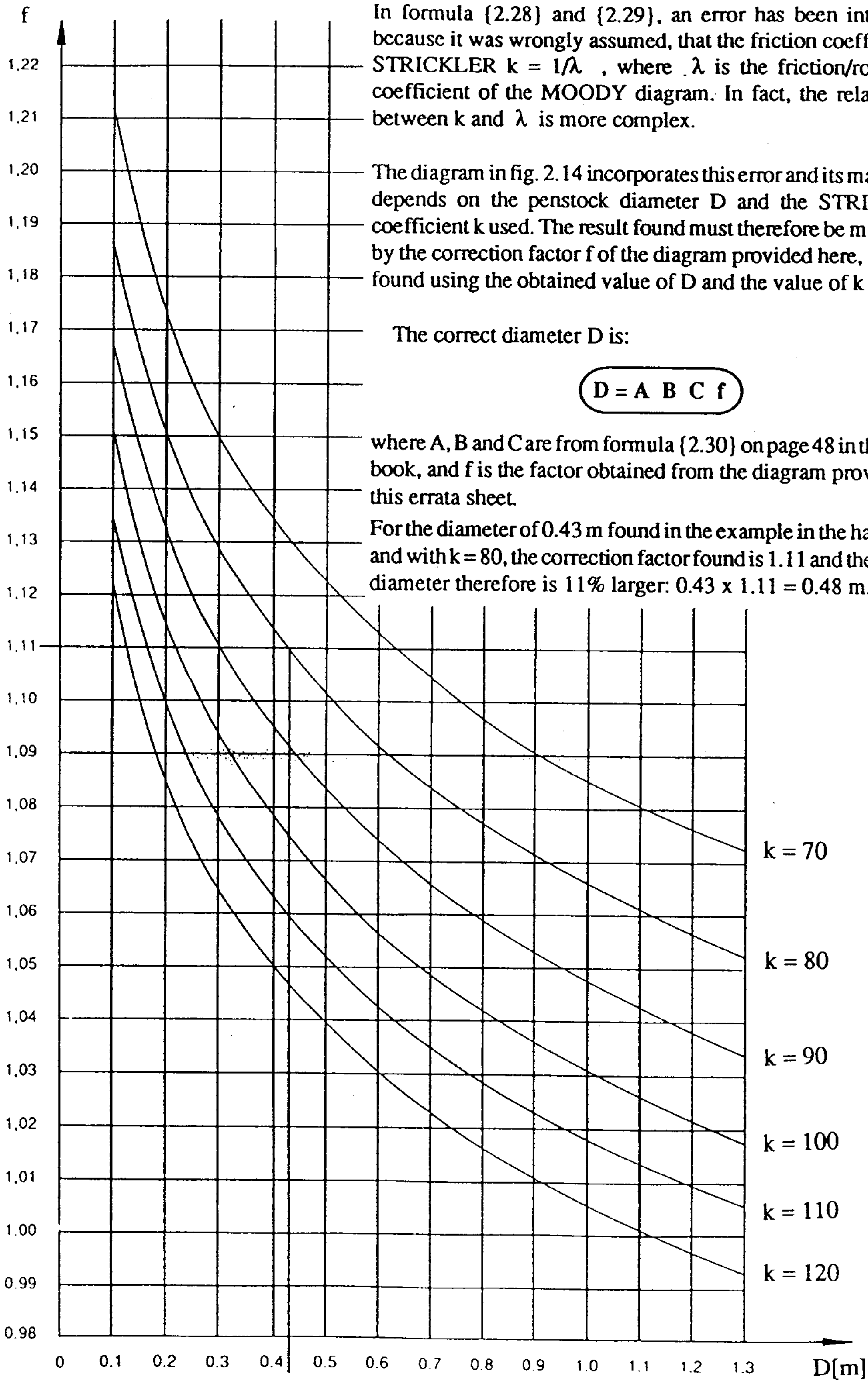

## 2.2.8 Nomogram for the pre-selection of the minimal required wall thickness for a penstock pipe.

The wall thickness selected for a penstock pipe mainly depends on the following parameters:

- the material selected for the penstock
- the diameter of the pipe
- the operating pressure

When selecting the material for a penstock, it is of interest to know the permissible hoop stress, the ultimate tensile bending stress and stresses due to thermal expansion. To calculate the latter, we need to know YOUNGs Modulus of Elasticity, and of interest is also the question of corrosion and weldability of the material used..

The selection of the pipe diameter depends primarily on the design discharge, the length of the penstock and the acceptable head losses as well as economical considerations.
The operating pressure depends not only on the static head of the installation, but also on transient surge pressure effects. It is understood, that the penstock must withstand the maximum operating pressure occuring.
Each term, the pressure p, the permissible stress σ and the penstock diameter D need to be carefully evaluated before using these data for the determination of the wall thickness t. Further, after having determined the wall thickness, the result needs to be reviewed by incorporating a reasonable safety-factor.

The nomogram in figure 2.16 provides minimum values for the wall thickness, not including safety and corrosion allowances. It is based on the hoop-stress formula:

$$t = \frac{p\,D}{2\,\sigma_{perm}} \quad [cm] \tag{2.32}$$

where:

- $t$ = wall thickness of penstock pipe in cm
- $p$ = operating pressure in kgf per cm$^2$
- $D$ = internal diameter of penstock in cm
- $\sigma_{perm}$ = permissible stress in kgf per cm$^2$

| | |
|---|---|
| 1 kgf/cm$^2$ | = 10 m of water column |
| 1 kgf | = 9.81 Newton |

**Example:**

operating pressure: 16 kgf / cm$^2$
permissible stress: 1200 kgf / cm$^2$
internal penstock diamter: 150 cm

} required minimum wall thickness = 10 mm, with a safety factor of $\frac{3500}{1200} = 2.9$

The table below lists properties of materials used in the manufacture of penstock pipes

| Material | YOUNGs modulus of elasticity E (kgf / cm²) | Coefficient of linear expansion a ( m/m °C) | Ultimate tensile stregtth (kgf / cm²) | Density (kgf / m³) |
|---|---|---|---|---|
| Steel | 21 $10^5$ | 12 $10^{-6}$ | 3500 | 7900 |
| Polyvinyle chloride (PVC) | 0.28 $10^5$ | 54 $10^{-6}$ | 280 * | 1400 |
| Polyethylene | 0.02-0.08 $10^5$ | 140 $10^{-6}$ | 60 - 90 * | 940 |
| Concrete | 2 $10^5$ | 10 $10^{-6}$ | | 1800-2500 |
| Asbestos cement | | 8.1 $10^{-6}$ | | 1600-2100 |
| Cast iron | 8 $10^5$ | 10 $10^{-6}$ | 1400 | 7200 |
| Ductile iron | 17 $10^5$ | 11 $10^{-6}$ | 3500 | 7300 |

**Fig.: 2.15: Properties of penstock materials (source: Inversin, [3], p.126)**

* Hydrostatic design basis

Solution:

-Connect values on the D-scale and on the p-scale to find the intersection point on the reference line.

-Connect the value on the σ-scale with the intersection point and extend the line up to the t-scale.

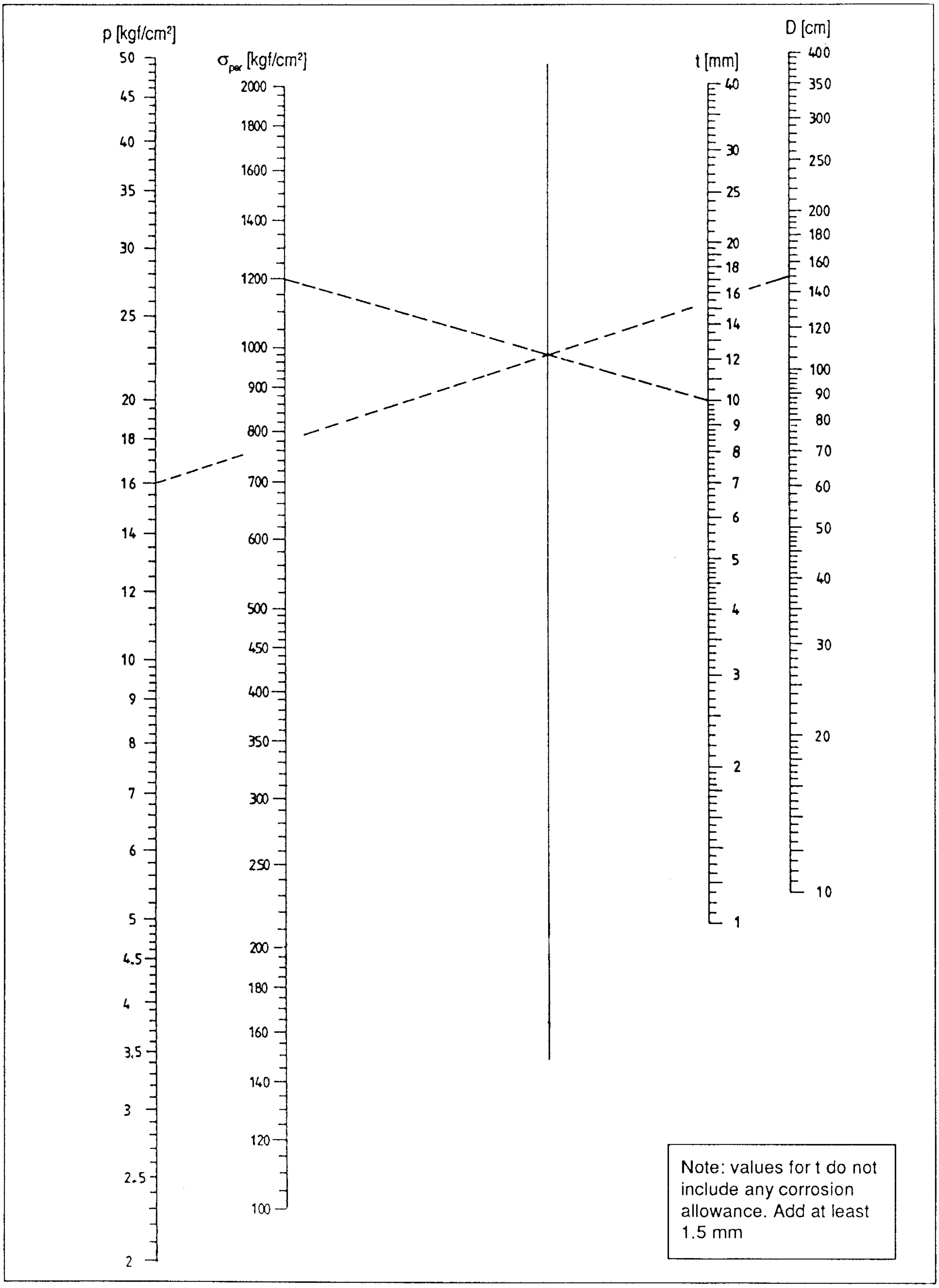


Fig.: 2.16: Nomogram for minimal penstock thickness

## 2.2.9 ALLIEVI chart for the examination of the water-hammer effect

Whenever the discharge rate through a penstock is varied, for instance by changing the gate opening at the end of the penstock, the mean flow velocity of the water changes, resulting in fluctuations of pressure.

In case of sudden gate closure at the end of a penstock, the pressure may rise to a significantly higher value. This effect is called water-hammer. Similarly, in case of sudden valve opening, the pressure may drop. The water-hammer effect is related to the conversion of the kinetic energy of the flowing water in the penstock to the work absorbed in stretching the penstock wall and compressing the water column. The theory behind the water-hammer effect is very complex and not easily understood.

Rather than trying to explain the phenomena of positive and negative pressure waves travelling up and down the penstock at the propagation speed of sound, an attempt is made here to provide a tool for the preliminary assessment of the water-hammer effect. Refer to RICH [11] for further reading. Charts 2.17 - 2.20 from [11].

Such a tool are the ALLIEVI charts, named after Lorenzo ALLIEVI, the great Italian pioneer in water-hammer investigation. These charts are based on the assumption that the closing motion of the gate is uniform, that the diameter of the penstock is equal along its total length, and that friction losses are not taken into account. These simplifications are acceptable as long as the use of the charts is for preliminary studies.

The coordinate axes of the ALLIEVI chart are:

the $\rho$ **axis** which stands for **the penstock parameter** $\rho$ [–] and
the $\theta$ **axis** which stands for **the valve operation parameter** $\theta$ [–]

The penstock parameter $\rho$ ist expressed by the formula:

{2.33} $$\boxed{\rho = \frac{a\ v_0}{2\,g\,H_0}}$$

where: $a$ = wave velocity [ m/s ]
$v_0$ = flow velocity in the penstock [ m/s]
$g$ = gravitational constant, 9.81 [ $m/s^2$ ]
$H_0$ = steady state head [ m ]

The valve operation parameter $\theta$ is expressed by the formula:

{2.34} $$\boxed{\theta = \frac{a\,t_c}{2\,L}}$$

where: $a$ = wave velocity [ m/s ]
$t_c$ = closing or opening time of the valve [ s ]
$L$ = length of the penstock [ m ]

The **wave velocity a** which needs to be known for the calculation of $\rho$ as well as of $\theta$ is expressed by the formula:

{2.35} $$\boxed{a = \frac{1425}{\sqrt{1 + \frac{E_w\,D}{E\ t}}}}$$

where: $E_w$ = modulus of elasticity of water = 2030 [ $N / mm^2$ ]
$D$ = internal diameter of penstock [ m ]
$E$ = YOUNG's modulus of elasticity of the penstock material [ $N / mm^2$ ]
$t$ = wall thickness of penstock pipe [ m ]

The value $Z^2$, which stands for **the pressure rise factor**, may be read from the ALLIEVI chart once values for $\rho$ and $\theta$ are determined.
The pressure rise factor is expressed by the formula :

$$\{2.36\} \qquad \boxed{Z^2 = \frac{H}{H_0}}$$

where: $H$ = pressure head [ m ]
$H_0$ = steady state pressure [ m ] (net head)

The following four examples demonstrate the practical use of the ALLIEVI chart.

## Example 1

The following data of a typical micro hydro site are given:

| | | |
|---|---|---|
| - net head of the installation | $H_0 = 10$ | [ m ] |
| - length of the penstock | $L = 30$ | [ m ] |
| - internal diameter of penstock pipe | $D = 0.3$ | [ m ] |
| - wall thickness of penstock pipe | $t = 0.004$ | [ m ] |
| - flow velocity in the penstock | $v_0 = 2.8$ | [ m/s ] |
| - penstock material: mild steel with a YOUNG's modulus of elasticity | $E = 210'000$ | [ $N/mm^2$ ] |

If the closing time of the inlet valve in case of an emergency shut down is to be $t_c = 2.1$ [ s ]

What is the maximum pressure head $H_{max}$ due to water-hammer ?

Step 1: calculation of the wave velocity a [ m/s ] (propagation speed of sound in water)

$$a = \frac{1425}{\sqrt{1 + \frac{E_w D}{E \; t}}}$$

where: $E_w$ = modulus of elasticity of water = 2030 [ $N/mm^2$ ]

$$a = \frac{1425}{\sqrt{1 + \frac{2030 \cdot 0.3}{210'000 \cdot 0.004}}} = 1085 \text{ [ m/s ]}$$

Step 2: calculation of penstock parameter $\rho$ [ - ]

$$\rho = \frac{a \, v_0}{2 \, g \, H_0}$$

where: $g$ = gravitational constant = 9.81 [ $m/s^2$]

$$\rho = \frac{1085 \cdot 2.8}{2 \cdot 9.81 \cdot 10} = 15.5 \text{ [ - ]}$$

Step 3: calculation of the valve operation parameter θ [ - ]

$$\theta = \frac{a\, t_c}{2\, L}$$

$$\theta = \frac{1085 \cdot 2.1}{2 \cdot 30} = 38\ [\ -\ ]$$

Step 4: determination of the pressure rise factor $Z^2$ (ratio $H/H_0$) [ - ] by means of the ALLIEVI chart.

$\left.\begin{array}{l}\rho = 15.5. \\ \theta = 38\end{array}\right\}$ ➪ figure 2.17:ALLIEVI Chart ( large ρ and θ ) ➪ $Z^2 = 1.48$ [ - ]

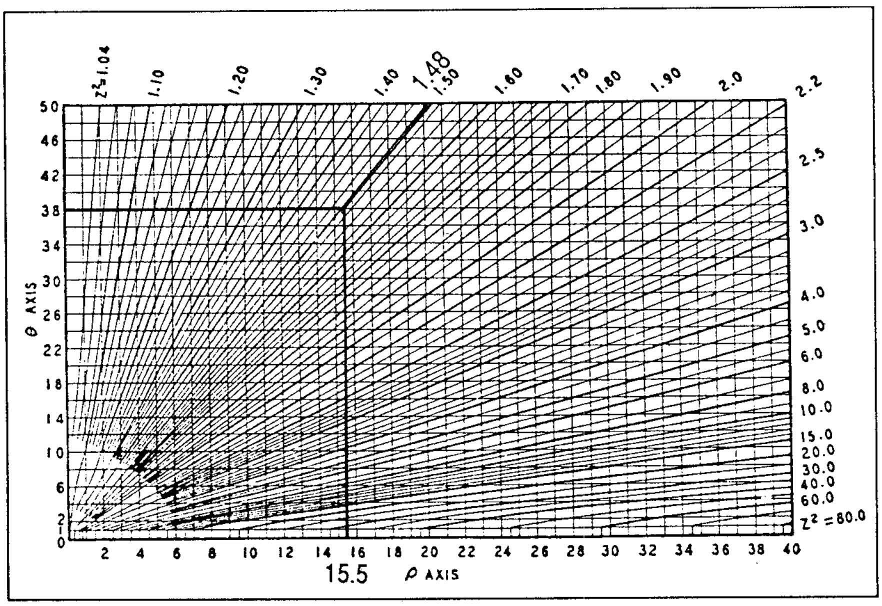


**Fig.: 2.17:ALLIEVI chart: pressure rise for uniform gate closure and simple conduits ( large ρ and θ )**

Step 5: calculation of the maximum pressure head $H_{max}$ [ m ] due to water-hammer

$$Z^2 = \frac{H}{H_0}$$

where : H = total head (water-hammer plus steady state head) [ m ]

therefore :

$$H_{max} = H_0 \cdot Z^2$$
$$= 10 \cdot 1.48 = 14.8\ [m]$$

which means the pressure rise due to water-hammer is nearly 50 % of the steady state head.

## Example 2

It is planned to use HD polyethylene pipes for a penstock. The permissible pressure for these pipes is not to exceed 10 bar ( 100 m water column). What is the shortest permissible closing time of the valve at the end of the penstock with the following data:

| | | | |
|---|---|---|---|
| - net head of the installation | $H_0$ | = 67 | [ m ] |
| - length of penstock | L | = 200 | [ m ] |
| - internal diameter of penstock pipe | D | = 0,1 | [ m ] |
| - wall thickness of penstock pipe | t | = 0,01 | [ m ] |
| - flow velocity in the penstock | $v_0$ | = 2.5 | [ m/s ] |
| - maximum permissible pressure head | $H_{max}$ | = 100 | [ m ] |
| - penstock material: HD polyethylene | | | |
| YOUNG's modulus of elasticity | E | = 1500 [ N/mm2 ] | |

Step 1: calculation of pressure rise factor $Z^2$ [ - ]

$$Z^2 = \frac{H_{max}}{H_0} = \frac{100}{67} = 1.49$$

Step 2: calculation of wave propagation velocity a [ m/s ]

$$a = \frac{1425}{\sqrt{1 + \frac{E_w D}{E\ t}}}$$ where: $E_w$ = modulus of elasticity of water = 2030 [ N/mm$^2$ ]

$$a = \frac{1425}{\sqrt{1 + \frac{2030 \cdot 0.1}{1500 \cdot 0.01}}} = 374 \text{ [ m/s ]}$$

Step 3: calculation of penstock parameter ρ [ - ]

$$\rho = \frac{a\ v_0}{2\ g\ H_0}$$ where : g = gravitational constant = 9.81 [ m/s$^2$ ]

$$\rho = \frac{374 \cdot 2.5}{2 \cdot 9.81 \cdot 67} = 0.71 \text{ [ - ]}$$

Step 4: determination of the valve operation parameter θ [ - ] by means of the ALLIEVI chart:

$$\left.\begin{array}{ll} Z^2 & = 1.49 \\ \rho & = 0.71 \end{array}\right\}$$ ➪ figure 2.18 :ALLIEVI chart ( small ρ and θ ) ➪ θ = 2.2

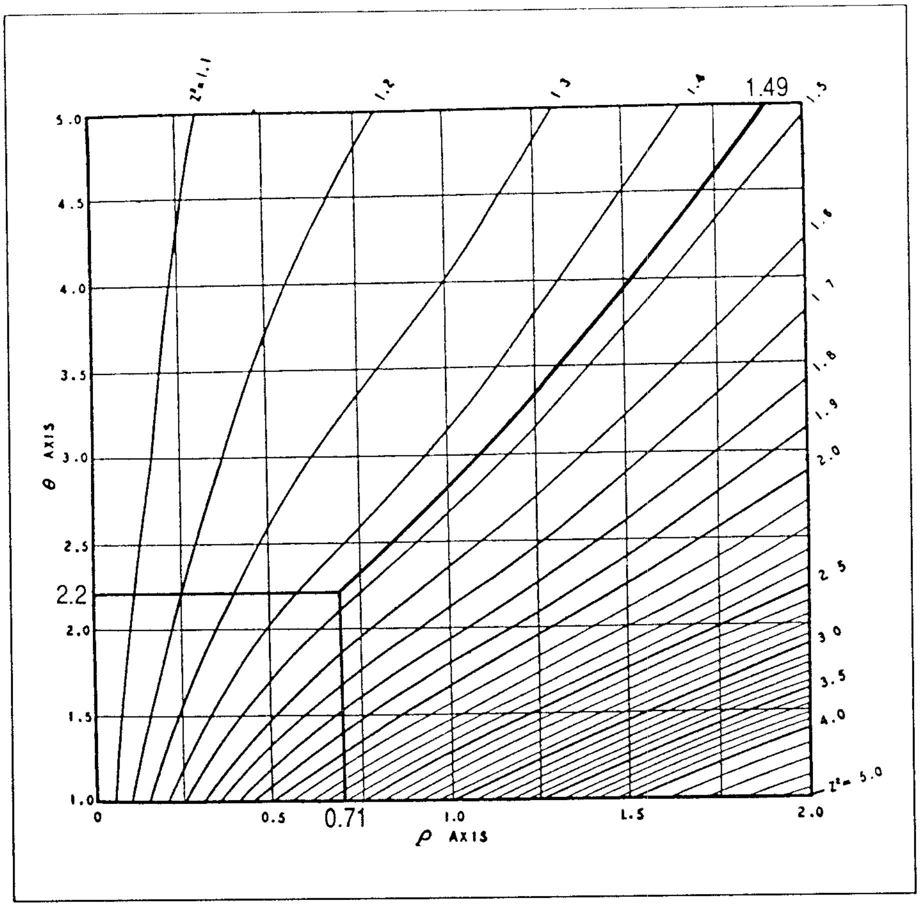


**Fig. 2.18 :ALLIEVI chart: pressure rise for uniform gate closure and simple conduits ( small ρ and θ )**

Step 5: calculation of shortest permissible closing time $t_c$ [ s ]

$$t_c = \frac{\theta\, 2\, L}{a} = \frac{2.2 \cdot 2 \cdot 200}{374} = 2.35 \text{ [ s ]}$$

To keep the pressure rise within the limit of $H_{max}$ = 100 [ m ], the closing time of the gate is not to be less than 2.35 seconds.

**Example 3**

In a scheme with the data given below, the closing time shall be chosen in such a way that the pressure rise does not exceed 20% of the steady state head. Further, it is of interest to find the time after which the wave cycles create the maximum water-hammer.

| | | | |
|---|---|---|---|
| - net head of installation | $H_0$ | = 63.9 | [ m ] |
| - length of penstock | L | = 450 | [ m ] |
| - internal diameter of penstock pipe | D | = 0.3 | [ m ] |
| - wall thickness of penstock | t | = 0.01 | [ m ] |
| - flow velocity in the penstock | $v_0$ | = 2 | [ m/s ] |
| - penstock material: mild steel with a YOUNG's modulus of elasticity | E | = 210'000 | [ N/mm2 ] |

Step1: calculation of the wave velocity a [ m/s ]

$$a = \frac{1425}{\sqrt{1 + \frac{E_w D}{E \; t}}}$$

where: $E_w$ = modulus of elasticity of water = 2030 [ N/mm$^2$ ]

$$a = \frac{1425}{\sqrt{1 + \frac{2030 \cdot 0.3}{210'000 \cdot 0.01}}} = 1255 \text{ [ m/s ]}$$

Step 2: calculation of penstock parameter ρ [ - ]

$$\rho = \frac{a\, v_0}{2\, g\, H_0}$$

where: g = gravitational constant = 9.81 [ m/s$^2$ ]

$$\rho = \frac{1255 \cdot 2}{2 \cdot 9.81 \cdot 63.9} = 2 \text{ [ - ]}$$

Step 3: calculation of pressure rise factor $Z^2$ [ - ] : pressure rise = 20 % ➪ $Z^2 = 1.2$ [ - ]

Step 4: determination of the valve operation parameter θ [ - ] by means of the ALLIEVI chart.

$$\left.\begin{array}{l} \rho = 2 \\ Z^2 = 1.2 \end{array}\right\}$$ ➪ figure 2.19:ALLIEVI chart ( medium ρ and θ ) ➪ θ = 11 [ - ]

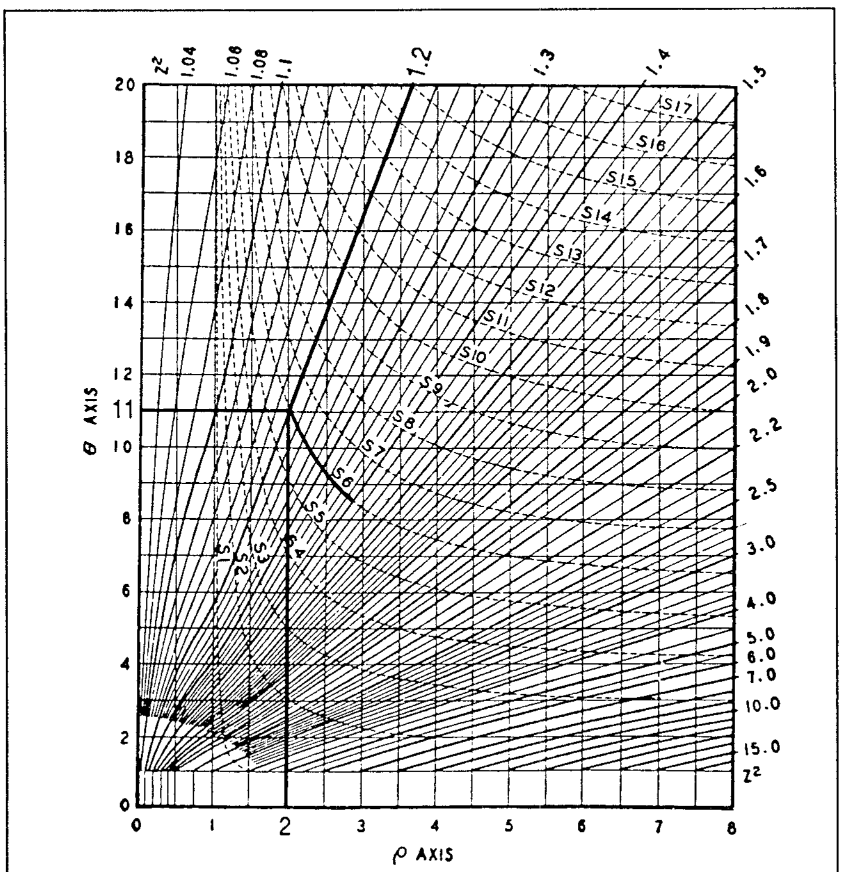


Fig. 2.19: ALLIEVI chart: pressure rise (medium ρ and θ ) and wave cycle curves

Step 5: calculation of gate closing time tc [ s ]

$$t_c = \frac{\theta\, 2\, L}{a} = \frac{11 \cdot 2 \cdot 450}{1255} = 7.9\ [\ s\ ]$$

With a gate closing time of 7.9 seconds the pressure rise remains within the limit of 20% of head.

Step 6: determination of the time required by the wave cycles to reach maximum water-hammer.

from the ALLIEVI chart (fig. 2.19) we see that the maximum pressure rise is reached after six wave cycles ( $s_6$ ) .

The time for one wave cycle through the entire penstock length is:

$$\{2.37\} \quad \boxed{t_{wc} = \frac{4\, L}{a}} = \frac{4 \cdot 450}{1255} = 1.43\ [\ s\ ]$$

As six cycles occur to reach maximum water-hammer, the total time required is:

$$t_{tot} = s_6\ t$$

$$t_{tot} = 6 \cdot 1.43 = 8.6\ [\ s\ ]$$

After 8.6 seconds the peak pressure is reached.

## Example 4

In the same way that closing a gate at the end of a penstock initiates a presssure rise, so does opening a gate create a pressure drop. It is therefore of interest to calculate the permissible opening time of a gate for a given pressure drop limit under specific conditions.

| | | | |
|---|---|---|---|
| -net head of the installation | $H_0$ | = 4.4 | [ m ] |
| -length of the penstock | L | = 380 | [ m ] |
| -internal diameter of pipe | D | = 1.1 | [ m ] |
| -wall thickness of penstock pipe | t | = 0.005 | [ m ] |
| -flow velocity in the penstock | $v_0$ | = 1.5 | [ m/s ] |
| -penstock material: mild steel | | | |
| YOUNG's modulus of elasticity | E | = 210'000 | [ N/mm$^2$ ] |
| -permissible minimum pressure | $H_{min}$ | = 2.2 | [ m ] |

Step 1: calculation of pressure drop factor $Z^2$ [ - ]

$$Z^2 = \frac{H_{min}}{H_0}$$

$$Z^2 = \frac{2.2}{4.4} = 0.5$$

Step 2: calculation of wave velocity a [ m/s ]

$$a = \frac{1425}{\sqrt{1 + \frac{E_w d}{E\ s}}}$$

where $E_w$ = modulus of elasticity of water = 2030 [ N/mm2 ]

$$a = \frac{1425}{\sqrt{1 + \frac{2030 \cdot 1.1}{210'000 \cdot 0.005}}} = 806 \text{ [ m/s ]}$$

Step 3: calculation of penstock parameter ρ [ - ]

$$\rho = \frac{a\, v_0}{2\, g\, H_0}$$

where: g = gravitational constant = 9.81 [ $m/s^2$ ]

$$\rho = \frac{806 \cdot 1.5}{2 \cdot 9.81 \cdot 4.4} = 14$$

Step 4: determination of the valve operation parameter θ [ - ] by means of the ALLIEVI chart, fig. 2.20

$$\left.\begin{array}{l} Z^2 = 0.5 \\ \rho = 14 \end{array}\right\} \Rightarrow \text{ALLIEVI chart} \Rightarrow \theta = 40$$

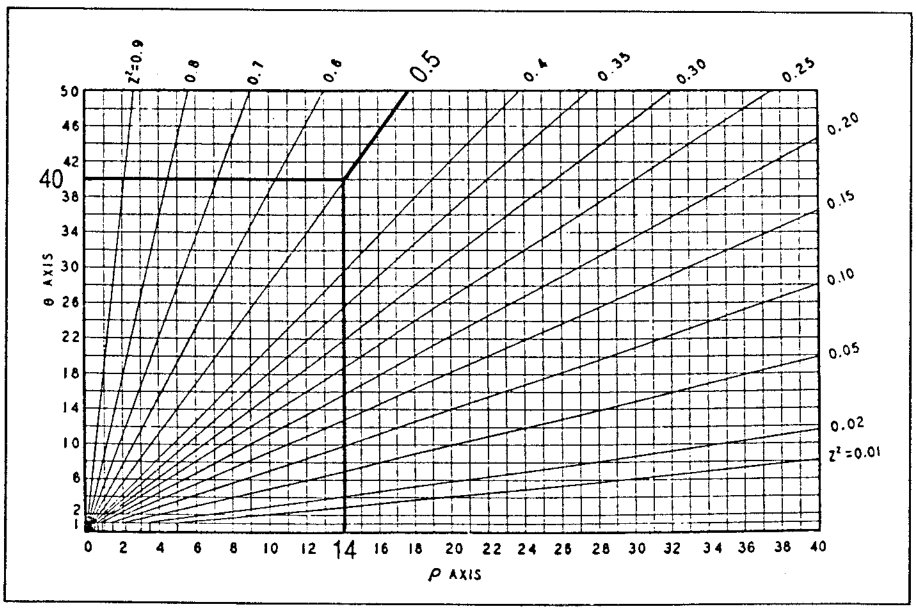


**Fig. 2.20: ALLIEVI chart : pressure drop**

Step 5: calculation of shortest permissible opening time $t_c$ [ s ]

$$t_c = \frac{\theta\, 2\, L}{a} = \frac{40 \cdot 2 \cdot 380}{806} = 37.7 \text{ [ s ]}$$

If the pressure is not to drop below 2.2 [ m ] the opening time of the gate is to be at least 37.7 seconds.

## Illustration of the water-hammer effect

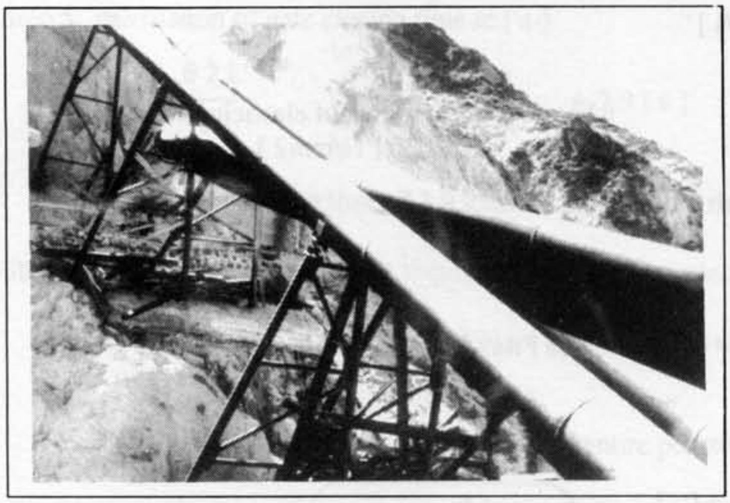

Fig. 2.21

Fig. 2.22

photographs by W. Roth

Fig. 2.23

The above photographs drastically illustrate the fatal consequences of the water-hammer effect: The entire penstock of a powerstation was totally destroyed due to a malfunctioning inlet valve.

## 2.2.10 Diagram for the pre-selection of the turbine type

In most cases the expression of the specific speed $n_s$ helps to make a sensible choice among different types of turbines such as Pelton, Francis, Propeller or Cross Flow.

The specific speed $n_s$ is a term used to classify turbines on the basis of their performance and dimensional proportions, regardless of their actual size or the speed at which they operate. The specific speed is the speed expressed in revolutions per minute (rpm) of an imaginary turbine, geometrically similar in every respect to the actual turbine under consideration, and capable of lifting 75 kg of water per second to a height of 1 m (effective output 1 metric HP). The mathematical formula for calculating the specific speed reads:

$$\{2.38\} \qquad \boxed{n_s = 3.65\ n\ \frac{\sqrt{Q}}{H^{3/4}}}$$

where Q ist to be inserted in $m^3/s$ and H in m and n (turbine speed) in rpm .

The same formula may be written as:

$$\{2.39\} \qquad \boxed{n_s = \frac{n\sqrt{P}}{H^{5/4}}}$$

where P is the theoretical turbine output in HP $\left( P = \frac{Q\,H}{75} \right)$

Note: Above formulae for $n_s$ are classical and still widely in use, however as they base on metric Horse Power, they do not comply with the SI-units.
If SI-units are applied, the conversion factor of 1.36 ( HP/kW) is to be considered as otherwise the obtained $n_s$-value would be 14 % smaller. Hence, for calculating $n_s$ based on HP but using power in kW, the following formula is derived:

$$n_s = n\,H^{-5/4}\ (1.36\ P_{[kW]})^{1/2} = 1.166\,n\,H^{-5/4}\,P_{[kW]}^{1/2}$$

True metric specific speed is denoted $N_s$ and is getting more and more popular. However, diagram 2.24 is based on HP-related $n_s$.

For a specific application where operating head, flow and a preferred speed of the turbine are known, the specific speed may be found in diagram in figure 2.24 . For a given task the specific speed of a turbine can easily be determined in the same diagram.

The turbine type may then be found by using diagram in figure 2.25, using the specific speed and the actual working head.

**Example:**

There is a site with a discharge of 100 l/s and a head of 30 m. The turbine speed is preferably 750 rpm . Which turbine type is appropriate ?

Step 1: determine $n_s$ either by using above formula or the diagramm for the data:

$$\left.\begin{array}{l} Q = 100 \text{ l/s ;} \\ H = 30\text{m ;} \\ n = 750 \text{ r p m} \end{array}\right\} \Rightarrow n_s = 67.5$$

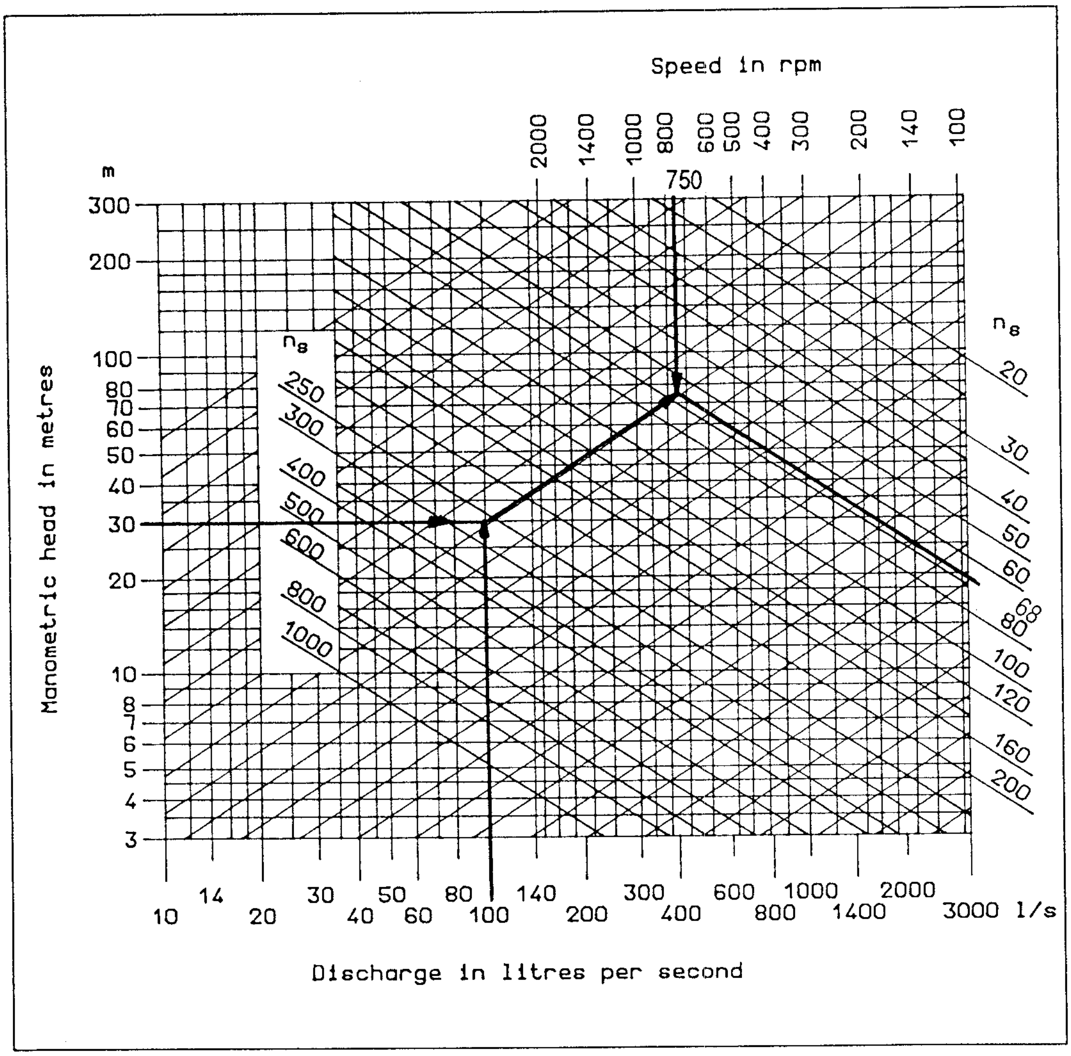


**Fig. 2.24: Specific speeds**

In the diagram, find the intersection point of H and Q and from the point found, move along the nearest reference line towards the upper right or the lower left upto the intersection with the selected speed.
Read / interpolate $n_s \cong 68$

Step 2: determine the turbine type by using the diagram 2.25 on the opposite page for the data:

$$\left.\begin{array}{l} n_s = 68 \\ H = 30 \text{ m} \end{array}\right\} \Rightarrow \text{Cross flow turbine}$$

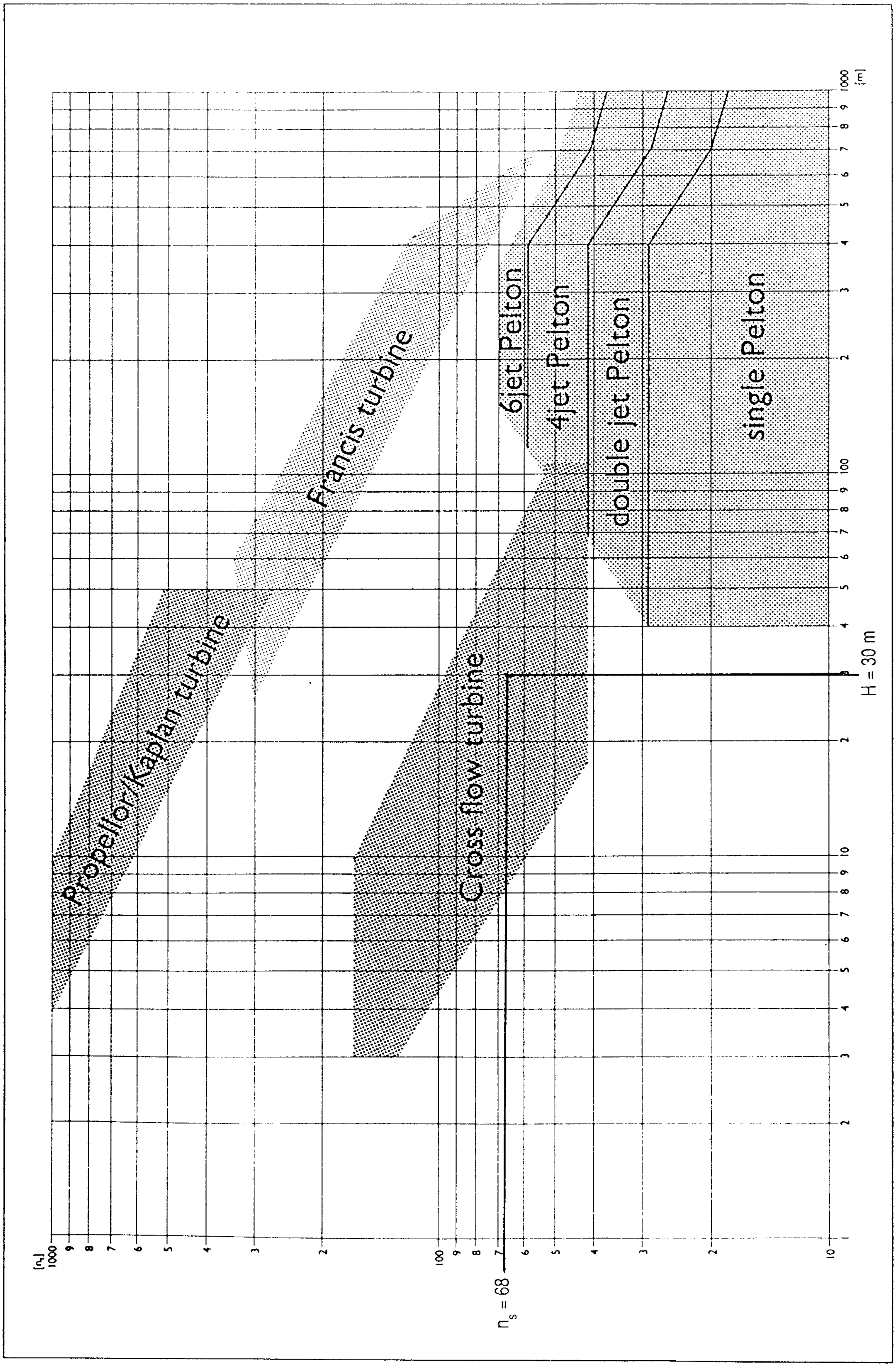


Fig. 2.25: Turbine application ranges

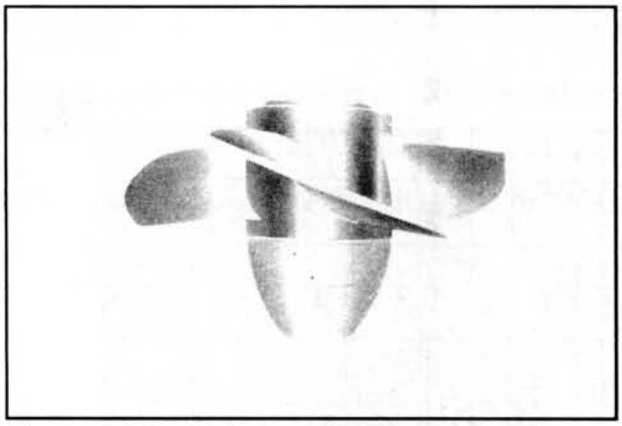

Fig. 2.26: Kaplan/Propeller Runner

$n_s$: 270 .... 1000
$N_s$: 230 .... 860

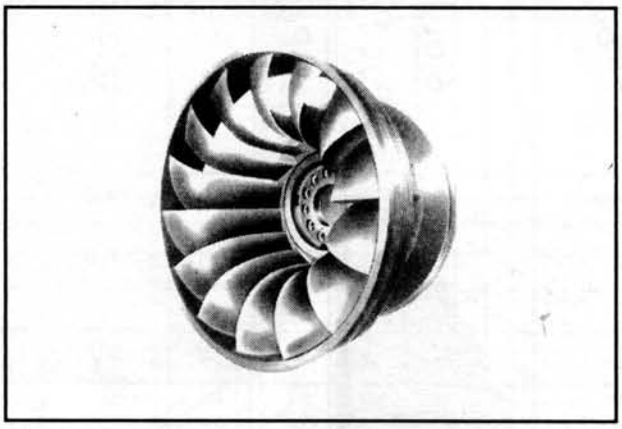

Fig. 2.27: Francis Runner

$n_s$: 60 .... 350
$N_s$:50 .... 300

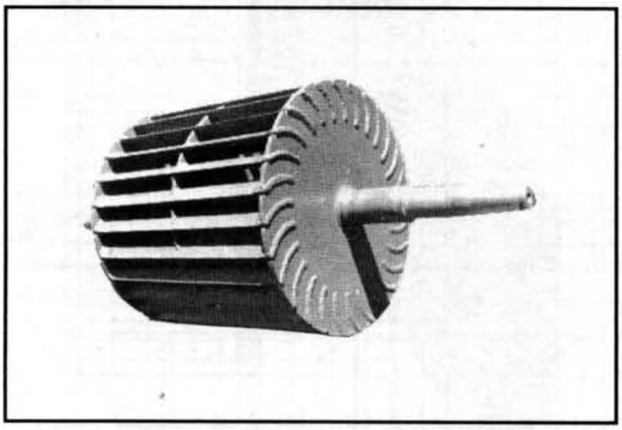

Fig. 2.28: Cross Flow Runner

$n_s$: 42 .... 170
$N_s$:36 .... 146

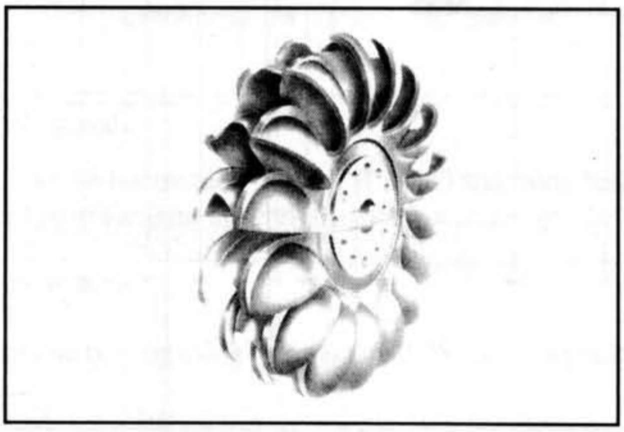

Fig. 2.29: Pelton Runner

$n_s$: 8 .... 72
$N_s$: 7 .... 62

$$N_s = 0.86 \cdot n_s$$

# Chapter 3 : Performance tests on Cross Flow turbines

## 3.1 Why performance tests

In general, performance tests serve the purpose to verify predicted data. Obtained test data tell you the actual performance characteristics of the investigated machine, and also permit to evaluate the accuracy of a prediction made. Both is equally important. At the time of working out a quotation, the turbine manufacturer normally specifies maximum output and discharge through the turbine under a given head. A reputed supplier may guarantee data such as part load efficiency and runaway speed. In order to reliably provide such data, it is indispensable to perform tests to establish the performance characteristics of a similar machine in advance. The art of turbine manufacturing is to know the behaviour of the turbine before having built it. The tool to master this art, is performance testing.

Furthermore, it is evident that any design modifications need a measuring stick, allowing to judge whether progress has been made or not. Such investigations also require performance tests.

Another aspect of performance tests is its significance concerning the reputation of the turbine manufacturer. If the customer knows that the turbine offered is based on a tested design, his confidence for having made the right choice is understandably higher. The risk of facing a calamity the day the turbine goes in operation, is reasonably small if the machine is based on a tested design.

### 3.1.1 Possible consequences of unknown turbine characteristics

If the turbine performance characteristics is unknown, the ultimate plant performance becomes a lucky draw. Concurrence of actual plant performance with predicitions made, may be achieved by chance. More common is the following case: the responsible person for the size selection of the turbine knows that the performance of the turbine is unknown.
He may conceal this fact and have a natural tendency to make assumptions on the safe side. To give an example: if the customer insists on a maximum output of 100 kW under nominal head, and the stated turbine efficiency of 82% is questioned by the manufacturer to be unrealistic, a machine may be specified absorbing a higher discharge to produce 110 kW in order to reach the guaranteed output, even if the efficiency should be 75 % only. In other words, the machine is intentionally being oversized in order to compensate for a possibly lower efficiency and/or inaccurate assessment of the discharge through the machine.

There are basically two possible problems with unknown turbine characteristics:

**case a:** the turbine size is too small, the turbine is not absorbing the design discharge under nominal head.

**consequences**: the planned plant output will never be reached, as the turbine even at full opening can not take the required amount of water. The turbine needs to be replaced, or else the plant maximum output is lower than intended.

**case b:** the turbine size is too large, resulting in turbine operation at part load when absorbing the design discharge under nominal head.

**consequences**: the turbine will produce the expected output but will require a greater amount of water compared to a properly sized machine. Due to the increased discharge through the turbine and through the penstock, head losses in the penstock are increased, resulting in a reduction of the working head of the turbine. As the optimal speed of the turbine is a function of the square root of head, it is evident that a reduced working head means operating the machine at a higher than optimal speed. However, as long as there is sufficient water available, the turbine will produce the expected output but at at an unexpected low efficiency.

The case becomes critical if the amount of water available is limited, which is very common (e.g. in the yearly dry season).

The following diagrams visualize the situation when oversizing the turbine.

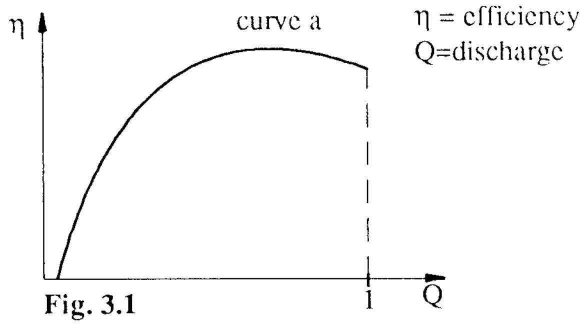


**Fig. 3.1**

turbine characteristics of a properly sized machine for a maximum discharge of Q = 1.

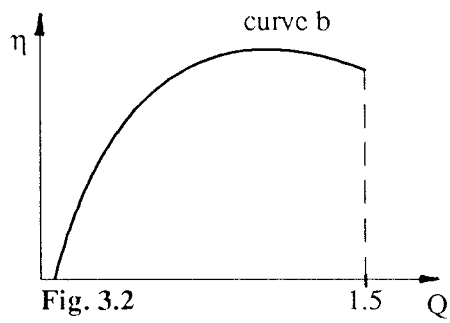


**Fig. 3.2**

turbine characteristics of a properly sized machine for a maximum discharge of Q = 1.5 .

Except for the size, the two machines are identical and therefore show the same efficiency curve. The machine having the characteristic as per sketch a is as good as the turbine having the characteristics as per sketch b for the respective maximum discharge of Q = 1 and Q = 1.5. Curve a and curve b in the diagrams above are the same, but the scales on the axis showing the discharge Q are different by a ratio of 1 : 1.5.

In a next step, curve b is plotted again, using the same scale for the discharge axis as in diagram a. Every point on curve b is shifted along the horizontal axis by a factor of 1.5, without altering its vertical position.

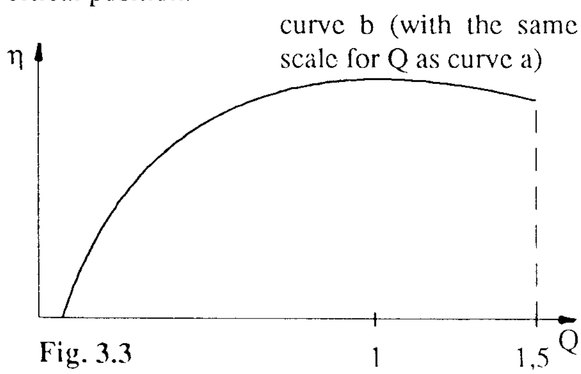


**Fig. 3.3**

As now the two curves a and b have the same scales, we may incorporte both into one diagram which will permit a direct comparison.

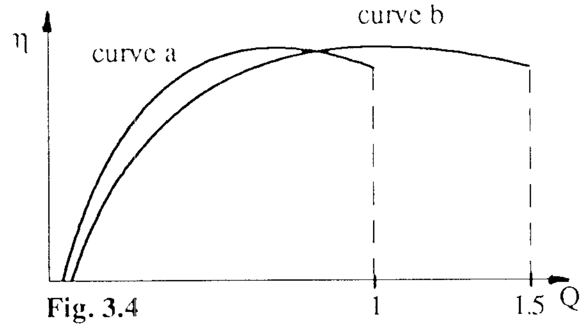


**Fig. 3.4**

It is now evident, that curve b represents the turbine characteristics of a 50% oversized machine as compared to curve a. Which machine is the better choice only depends on the available discharge Q.

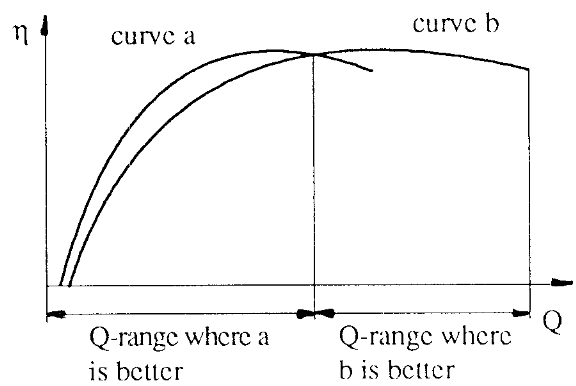


**Fig. 3.5**

The following example shows dry season conditions where only a limited amount of water is available. In such a case, the efficiency drop of an oversized machine as compared to a properly sized one may be significant and may possibly mean a temporary shut down of the entire plant.

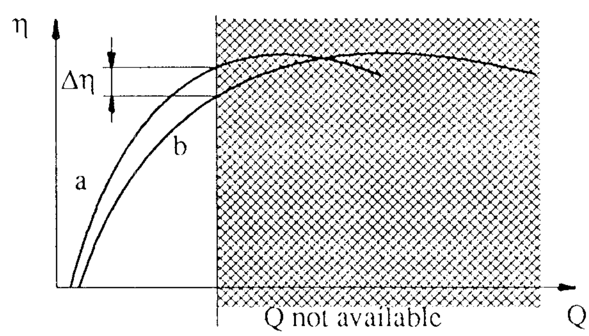


**Fig. 3.6** (no water due to dry season)

The explanations given also make it clear why turbine designers try hard to develop machines with a flat efficiency curve. The object being to achieve a high efficiency over a wide range of discharge.

# 3.2 Laboratory tests

## 3.2.1 Turbine test facility

In establishing a laboratory test facility, headroom limitations and cost may inhibit the installation of high head supply tanks and a pump with a low level sump tank is often adopted for head/flow generation. A variable speed pump is more versatile, with a sump capacity as large as practicable. The turbine supply pipe should be as long and straight as possible and the inclusion of a pressure tank in the system helps to improve flow steadiness. The turbine discharges directly into the sump and this aerates the water considerably. Baffles in the sump tank are therefore necessary to prevent air from being drawn into the pump.

A typical installation, suitable for testing machines of a few kilowatts power output and operating under heads of up to 20m, was developed at the Hong Kong Polytechnic and is shown in Fig. 3.7.
The test facility shown is relatively unsophisticated and can be readily constructed inexpensively.

### 3.2.1.1 Head measurement

The simplest and most fundamental method of measuring pressure heads is by means of a mercury manometer which is suitable for heads up to 20m of water. If the head is above 20m, the manometer would become too large, and a pressure transducer would be more appropriate. For more accurate measurement, a four tapping ring arrangement should be used, as shown in Fig. 3.8 , which minimises errors due to sensing hole burrs and misalignment.

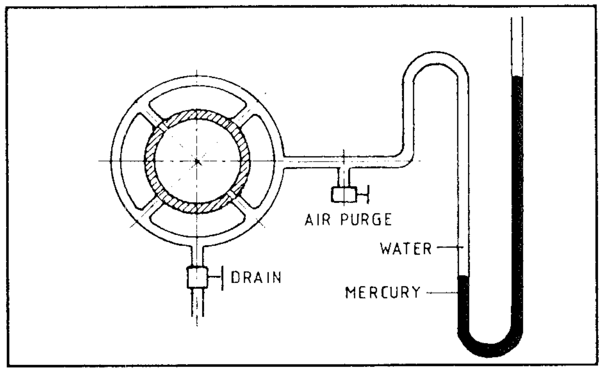


**Fig. 3.8: Static pressure measurement in a pipe**

A practical arrangement for an individual tapping is shown in Fig. 3.9, where it is important to have a "high quality" sensing hole connected to the manometer through a metal tube insert. Air entrainment in the manometer is very common and it is convenient to have a small purge valve in the line. The manometer pressure can then be used to calculate the pipe pressure and the turbine inlet total head H can be determined from the equation:

$$H = \frac{p}{\rho g} + \frac{v^2}{2g} + z$$

The velocity v is found from the flow rate and turbine inlet pipe cross sectional area and Z is the height difference between the pipe and shaft centre lines.

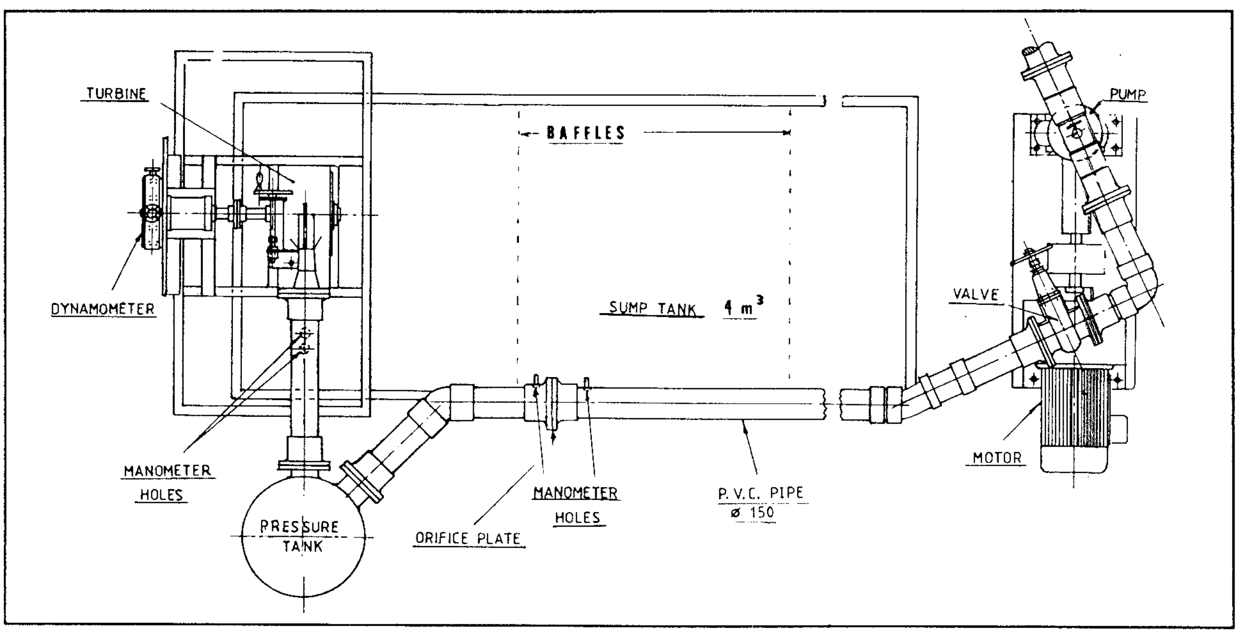


Fig. 3.7: Plan view of turbine test rig layout

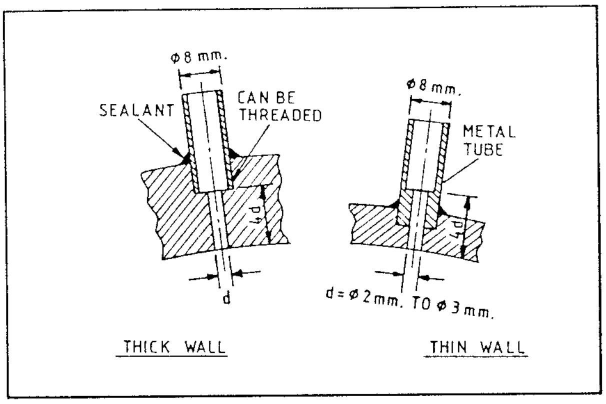


**Fig. 3.9 : Single pressure tapping in PVC pipe**

### 3.2.1.2 Flow rate measurement

The accurate determination of flow rate is perhaps the most difficult parameter to measure and considerable care and attention to detail is required. There are many methods of flow measurement including orifice plates and venturi meters, electromagnetic and turbine flow meters for pipe flows, and notches and weirs for external flows. In the case of internal flow systems, it is very important to have a long straight pipe upstream, and to a lesser extent downstream of the flowmeter, in order that the flow is hydrodynamically fully developed and that secondary flows and swirl effects have been dissipated. In the test rig in Fig. 3.7 an orifice plate was used, designed to B.S.1042 (ISO 5167) specification. The orifice size chosen was as large as permitted in the standard but with a significant pressure head difference to allow accurate measurement by manometer. The orifice is easy to manufacture and can be fitted into a standard PVC pipe/flange arrangement as shown in Fig. 3.10 .

The above arrangement allows the orifice plate to be centred accurately. The plate must be made according to the standard in regard to size and surface finish and non-ferrous metals such as brass or aluminium alloys should preferably be used from a corrosion resistance viewpoint. Providing the above conditions are met, the measurement accuracy can be confidently established.

### 3.2.1.3 Speed measurement

The shaft rotational speed can be measured by a variety of methods including revolution counters, mechanical tachometers or tachogenerators. A convenient method however, is by means of an optical tachometer. This type of instrument gives a direct

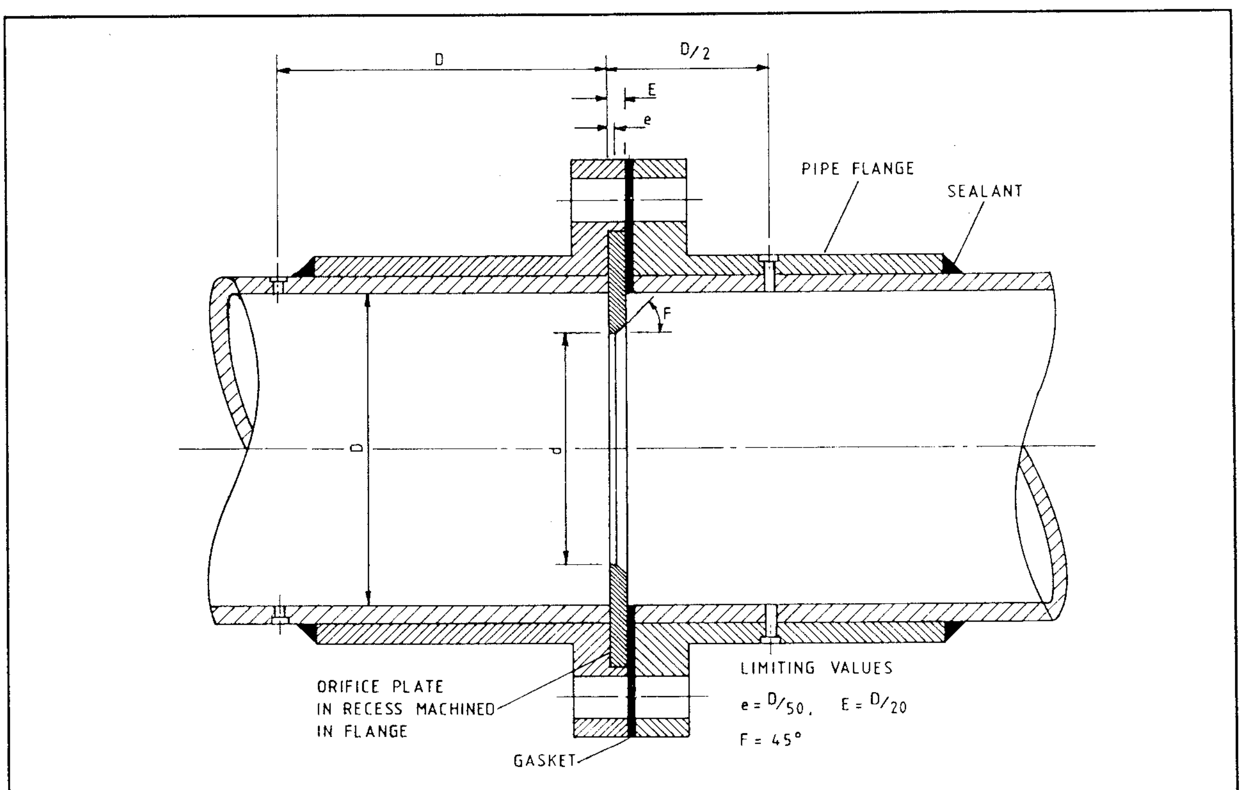


**Fig 3.10 : Orifice meter in PVC pipe**

digital read out of rotational speed or number of revolutions. A small piece of reflective tape is fixed to the turbine output shaft onto which the instrument light beam is directed. An optical sensor detects each pulse from the reflected beam and displays the consequent rotational speed digitally.

### 3.2.1.4 Torque measurement

The torque produced by the turbine can be measured by torque meter and brake, hydraulic or electrical dynamometer. A brake dynamometer is suitable for the testing of micropower turbines using brake pads and drum, as shown in Fig. 3.11 in which water is used to overcome the frictional heating of the drum.

To improve the accuracy, the brake arms, with dead weight hangers, should be as wide as possible, and the sensitivity can be increased by having fine and coarse adjustment of the brake pad tensioning system. To equalize loads on the bearings, equal weights should be used and thin piano wire is suitable for supporting the hangers. Running-in of the brake pads is necessary before testing to ensure even contact which prevents snatching.

## 3.2.2 Test procedure

The experienced engineer should adopt a skeptical attitude towards testing, and should calibrate all instruments and equipment, and check all readings for repeatability.

### 3.2.2.1 Calibration

The measurement of pressure head by manometer is a fundamental method, however checks should be made at all connections. Dirty tubes and air bubbles lead to large errors, and careful examination of the transparent tubing must be made after purging. It is sometimes useful to have an additional pressure gauge, calibrated with a dead weight tester, as a direct indicator during the pre-test period.

Once a particular device has been chosen for flow measurement, it is generally difficult to calibrate in situ and, if necessary, should be sent to the nearest standards laboratory for calibration prior to installation. This is relatively expensive and if a lower accuracy can be tolerated, then by following the appropriate standard exactly and checking the installation carefully, acceptable accuracy can be achieved.

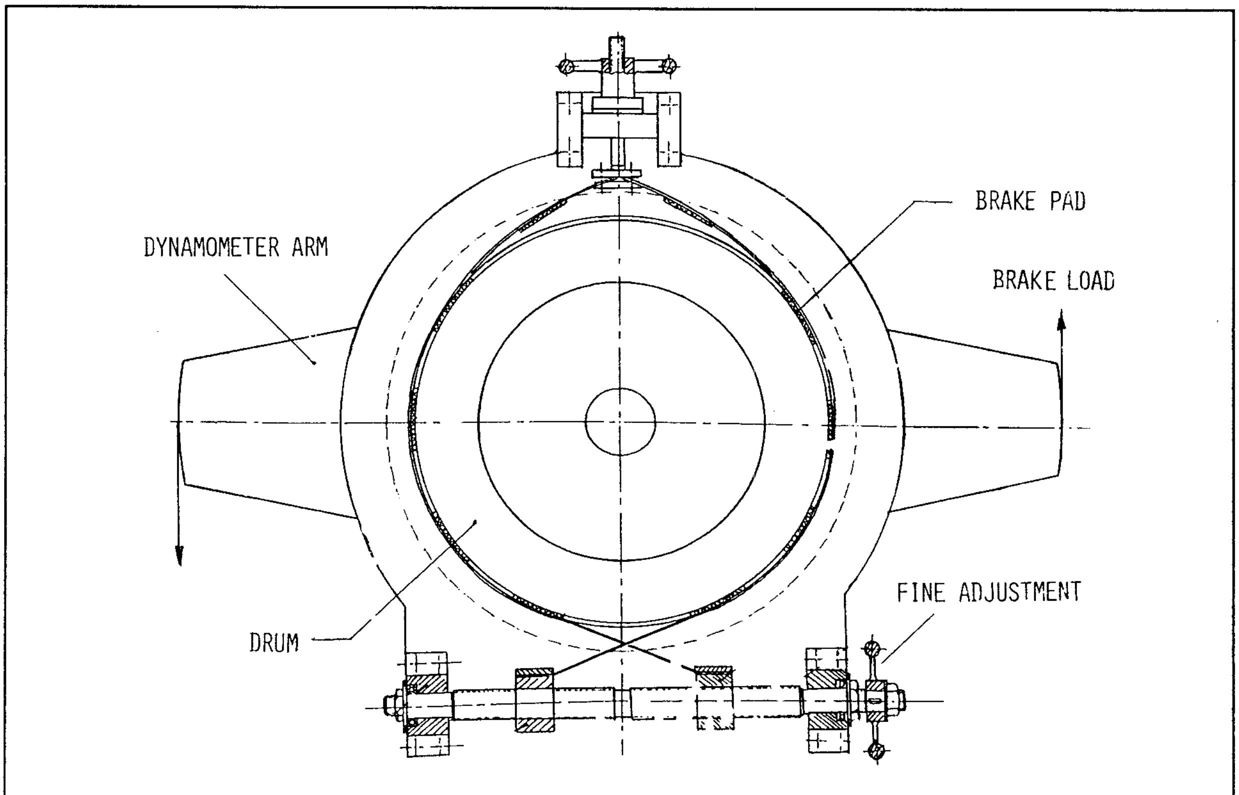


Fig. 3.11: Dynamometer

The speed measurement device can easily be calibrated using a revolution counter and stopwatch or a mechanical tachometer. As many alternatives as are available should be used.

Dynamometer calibration is difficult to achieve. One possibility is to use an electric motor of known characteristics to drive the turbine and to compare the torque input with the dynamometer torque. Dynamometer accuracy is generally satisfactory, particularly if the design has incorporated features to permit high sensitivity. The zero balance position can be established by the use of an appropriate jockey weight.

All dimensions should be accurately measured, and pipe diameters, in particular, should be ckecked in different directions for non circularity.

### 3.2.2.2 Testing

To undertake reliable testing, adequate manpower is necessary, under the direction of the Chief of Test who will be responsible for the conduct, coordination and supervision of the test program. In a non automated laboratory, it is preferrable to have one person in charge of each instrument, with the Chief of Test controlling events and operating the dynamometer brake. A test sheet should be devised in order that experimental results can be easily tabulated and an example of a typical sheet is shown in Fig. 3.12.

Before switching on the pump to start the tests, the dynamometer brake pads should be fully tightened to prevent any rotation of the turbine. When the pump has reached its operating speed, the gate valve can be opened to allow flow through the system. The turbine inlet valve is fully opened, and in this non-rotating condition, all the checks and adjustments can be made to the instruments.

Testing can commence after completing all the checks, and it is convenient to release the brake pads completely and to start testing at the no-load runaway speed, after allowing a sufficient warm up time.

A small weight is then added to each of the weight hangers which unbalances the dynamometer. By adjusting the brake pad tensioning, the dynamometer can be brought back to the equilibrium position. On clear instruction from the Chief of Test, all the instrument readings are recorded simultaneously. Increased weights can be added and the procedure repeated until a very low speed condition is reached whereby the sensitivity is inadequate to achieve an equilibrium condition.

**TEST RECORD SHEET**

DATE: 10.3.86 CONFIGURATION: BYS Cross Flow VALVE SETTING: 100 % TEMP: 23 °C PRESSURE: 765 mmHg

| | | | | | | | | | | | | | |
|---|---|---|---|---|---|---|---|---|---|---|---|---|---|
| Total Brake Load | (kg) | 0 | 2.0 | 3.0 | 4.0 | 4.5 | 5.0 | 6.0 | 7.0 | 8.0 | 9.0 | 10.0 | |
| Speed | (rpm) | 1413 | 1221 | 1132 | 1044 | 991 | 949 | 865 | 782 | 705 | 596 | 465 | |
| Output Power | (W) | 0 | 940.7 | 1308.1 | 1608.6 | 1717.8 | 1827.8 | 1999.2 | 2168.6 | 2172.5 | 2066.2 | 1791.2 | |
| Orifice Manometer ($mH_2O$) | $h_1$ | 1.450 | 1.450 | 1.450 | 1.450 | 1.450 | 1.450 | 1.450 | 1.460 | 1.460 | 1.465 | 1.465 | |
| | $h_2$ | 0.995 | 0.975 | 0.975 | 0.945 | 0.935 | 0.925 | 0.910 | 0.890 | 0.880 | 0.890 | 0.885 | |
| | $\Delta h$ | 0.455 | 0.475 | 0.475 | 0.505 | 0.515 | 0.525 | 0.540 | 0.570 | 0.580 | 0.575 | 0.580 | |
| Flow Rate | ($m^3/s$) | 0.0225 | 0.0230 | 0.0230 | 0.0237 | 0.0239 | 0.0242 | 0.0245 | 0.0252 | 0.0254 | 0.0253 | 0.0254 | |
| Hg Manometer (mHg) | $h_3$ | 1.290 | 1.275 | 1.270 | 1.265 | 1.260 | 1.260 | 1.255 | 1.245 | 1.245 | 1.245 | 1.245 | |
| | $h_4$ | 0.245 | 0.260 | 0.265 | 0.270 | 0.275 | 0.275 | 0.280 | 0.290 | 0.290 | 0.290 | 0.290 | |
| | $\Delta h$ | 1.045 | 1.015 | 1.005 | 0.995 | 0.985 | 0.975 | 0.975 | 0.955 | 0.955 | 0.955 | 0.955 | |
| Inlet Head | ($mH_20$) | 13.53 | 13.41 | 13.00 | 12.87 | 12.74 | 12.74 | 12.61 | 12.35 | 12.35 | 12.35 | 12.35 | |
| Net Head | ($mH_2O$) | 13.80 | 13.41 | 13.27 | 13.15 | 13.02 | 12.89 | 12.64 | 12.64 | 12.64 | 12.64 | 12.64 | |
| Water Power | (W) | 3046.0 | 3025.7 | 2994.1 | 3057.3 | 3052.7 | 3091.0 | 3098.0 | 3124.8 | 3149.6 | 3137.2 | 3149.6 | |
| $\eta_{overall}$ | (-) | 0 | 0.311 | 0.437 | 0.526 | 0.563 | 0.591 | 0.645 | 0.694 | 0.689 | 0.659 | 0.569 | |
| $n_s$ ($rpm \cdot kW^{1/2} \cdot m^{-5/4}$) | | 0 | 46.15 | 51.12 | 52.88 | 52.52 | 51.88 | 50.07 | 48.32 | 43.60 | 35.95 | 26.11 | |
| $C_w$ | (rad) | 2.883 | 2.527 | 2.355 | 2.182 | 2.082 | 1.993 | 1.826 | 1.667 | 1.503 | 1.271 | 0.991 | |
| $C_Q$ | (-) | 0.0376 | 0.0390 | 0.0396 | 0.0406 | 0.0411 | 0.0417 | 0.0424 | 0.0440 | 0.0444 | 0.0442 | 0.0444 | |

Fig. 3.12: Test record sheet

The above procedure will give all the required performance data at the fully open inlet valve setting. Tests should be carried out at other settings, typically in 5% or 10% decrements until the half open setting is reached. This range should enable sufficent data to be obtained to give the full performance characteristics over the useful operating range.

### 3.2.2.3 Data reduction

It is preferrable to use a computer to convert the measured data into turbine performance parameters, and a small personal computer is quite suitable for this purpose. Hand calculations can be undertaken, however a lot of data is generated by the tests and is therefore very time consuming. The following quantities are to be determined from the test data.

| | | |
|---|---|---|
| Output power | $P_o$ | [watts] |
| Input power | $P_i$ | [watts] |
| Efficiency | $\eta$ | [ - ] |
| Specific speed | $N_s$ | [rpm $kW^{1/2}m^{-5/4}$] |
| Speed coefficient | $c_\omega$ | [rads] |
| Flow coefficient | $c_Q$ | [-] |
| Specific speed coefficient | $c_{\omega s}$ | [rads] |

The dimensionless quantities are recommended as confusion over units is avoided.

## 3.2.3 Data analysis

This section deals with the accuracy of the data obtained and the methods of graphical presentation.

### 3.2.3.1 Error analysis

Each quantity measured is subject to uncertainty and in very accurate work many readings should be taken and the standard deviation obtained. In the testing of small turbines in the manner described, it may not be feasible to acquire multiple data, and estimates of the individual errors $\Delta x$ of each quantity **x** should be considered. If the quantity **x** is, for example, flow rate **Q**, then the accuracy of this quantity will depend on the other variables involved in the orifice plate formulation.

If $x = f(x_1 x_2 \cdots x_n)$, then the propagation of errors can be determined by the **equation {3.1}**, where $\Delta x_1$, $\Delta x_2$ etc. are the standard deviations or errors in the variables.

If the efficiency $\eta$ is considered as an example where $\eta = T\omega(\rho\, g\, Q\, H)^{-1}$, then differentiating the variables partially, non-dimensionalizing and assuming no errors in density and gravity gives **equation {3.2}**.

Errors in each of the above variables can be estimated at the best efficiency condition from the measurement discrimination and unsteadiness of the reading. The most significant error is in the flow rate for considerable care and skill is needed to reduce the uncertainity below 1.5%. However an overall accuracy in efficiency determination of 2% is an achievable objective in the system shown in Fig. 3.7.

### 3.2.3.2 Graphical presentation

The test data is best presented graphically in non dimensional form. The starting point is usually the efficiency $\eta$ against $c_\omega$ plot and several curves can be shown for different turbine inlet valve settings. (see fig. 3.13 ). The $c_Q$ variation with $c_\omega$ can then be plotted (see fig. 3.14) and from the two graphs isoefficiency curves can be drawn on a separate $c_Q$ versus $c_\omega$ plot as shown in fig. 3.15.

Efficiency $\eta$ against specific speed $N_s$ (or in dimensionless form $c_{\omega s}$ can be plotted directly from the calculated data as shown in fig. 3.16 .

{3.1}: $$\Delta x = \left\{ \left(\frac{\delta x}{\delta x_1}\Delta x_1\right)^2 + \left(\frac{\delta x}{\delta x_2}\Delta x_2\right)^2 + \dots \left(\frac{\delta x}{\delta x_n}\Delta x_n\right)^2 \right\}^{1/2}$$

{3.2}: $$\frac{\Delta\eta}{\eta} = \left\{ \left(\frac{\Delta T}{T}\right)^2 + \left(\frac{\Delta\omega}{\omega}\right)^2 + \left(\frac{\Delta Q}{Q}\right)^2 + \left(\frac{\Delta H}{H}\right)^2 \right\}^{1/2}$$

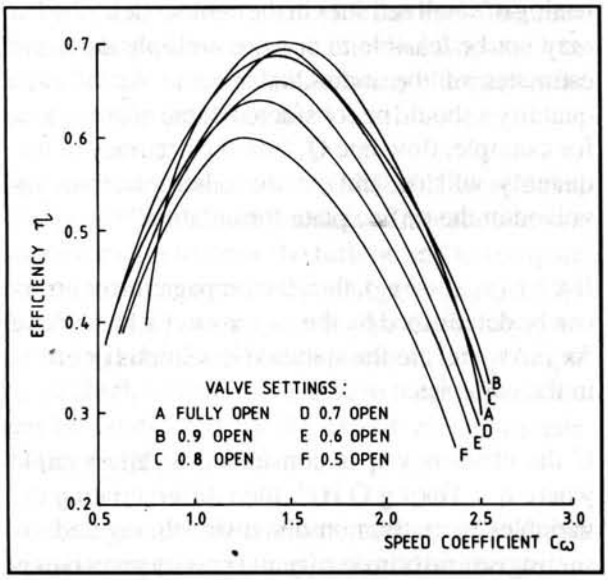


Fig. 3.13: $\eta$ vs $c_{\omega}$

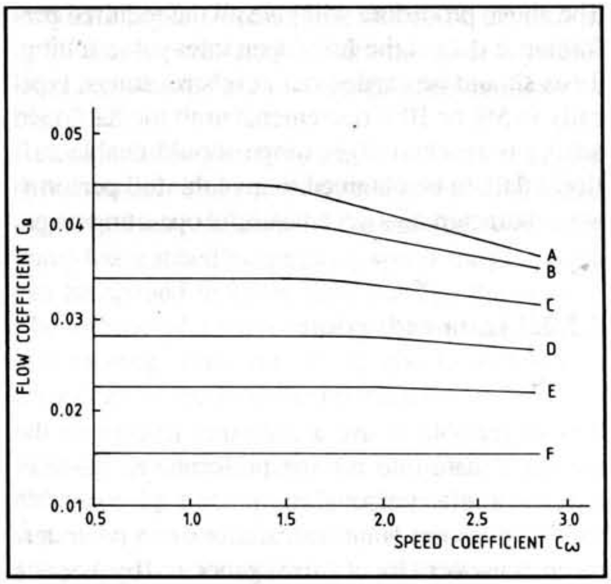


Fig. 3.14: $c_Q$ vs $c_{\omega}$

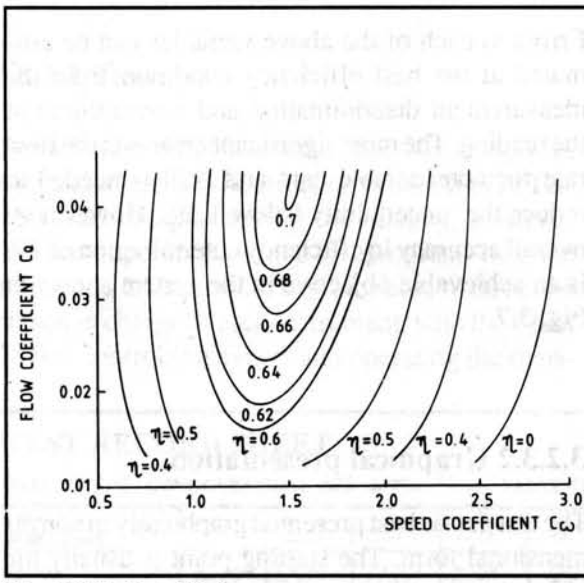


Fig. 3.15: Isoefficiency curves

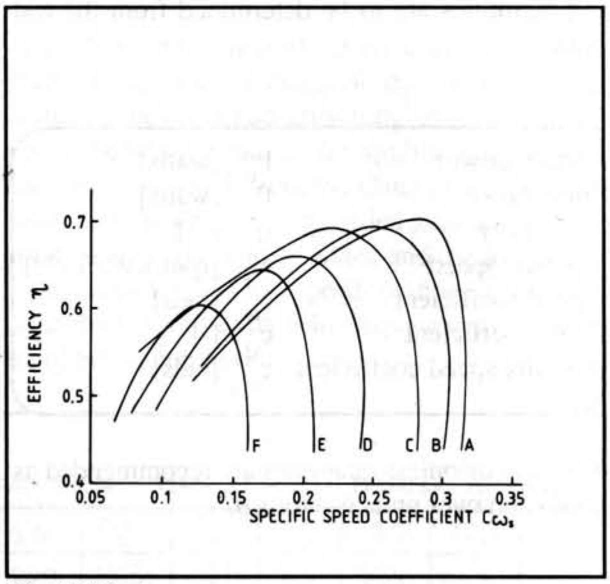


Fig. 3.16: $\eta$ vs $c_{\omega s}$

Fig. 3.17: General view of test rig at the Hong Kong Polytechnic

# List of Literature

[1] BALJE O. E., Turbomachines, John Wiley & Sons, New York 1981

[2] HUNTER Rouse, Elementary Mechanics of Fluids, Wiley Eastern Edition, New Dehli 1946

[3] INVERSIN Allen R., Micro-Hydropower Sourcebook, NRECA, Washington D.C. 1986

[4] MEIER Ueli, Local Experience with Micro-Hydro Technology, Volume 1, SKAT, St. Gallen 1984

[5] MILLER Donald S., Internal Flow Systems, BHRA, Cranfield 1978

[6] MUELLER Walter E., Druckrohrleitungen neuzeitlicher Wasserkraftwerke, Springer Verlag, Berlin 1968

[7] WAGNER S. K., et al, Small Hydro Power Fluid Machinery 1984, ASME, New York 1984

[8] WEBB D. R., et al, Small Hydro Power Fluid Machinery 1982, ASME, New York 1982

[9] VON DER NUELL Werner, Die Kreiselrad-Arbeitsmaschinen, Teubner, Berlin 1937

[10] WORLD METEOROLOGICAL ORGANISATION, Use of Weirs and Flumes in Stream Gauging, Technical Note 117, WMO No. 280, World Met. Organisation, Geneva 1971

[11] RICH G.R., Hydraulic Transients, Dover Publications, New York 1951

# Index

As a supplement to the Hydraulics Engineering Manual, a folder SELECTED NOMOGRAMS AND DIAGRAMS is also available. It contains 11 full-page Nomograms and Diagrams for practical application.
Fill out the attached card and mail today. If card is missing, order directly at SKAT-BOOKSHOP, Tigerbergstr.2, CH-9000 St.Gallen, Switzerland.

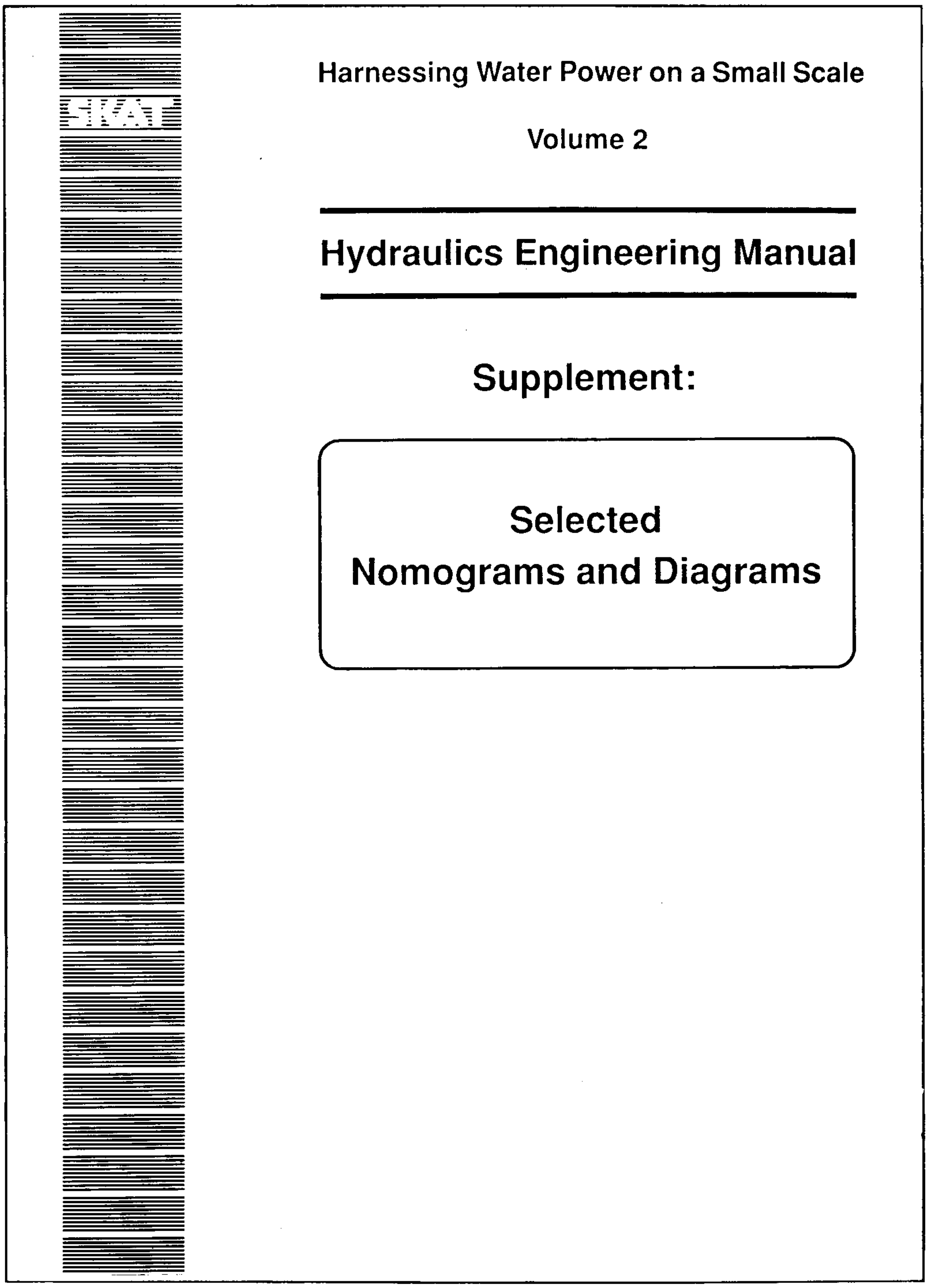


Hydraulics Engineering Manual, Supplement: Selected Nomograms and Diagrams, 4.- SFr.

Volume 2 in the series "Harnessing Water Power on a Small Scale" with the title HYDRAULICS ENGINEERING MANUAL, is based on practical experience in the field of micro-hydropower development in Nepal, and covers the theory required by the hydropower engineer.

The handbook contains the basic theory and fundamental relations of flow systems, the theory of the BANKI turbine and design aspects of Cross Flow Turbines, as well as a number of working tools in the form of nomograms and diagrams for the design of water conduits and for turbine selection. Emphasis is on ready-for-use procedures with many example calculations. The testing of small turbines is also included, based on actual laboratory tests performed.

ISBN 3-908001-13-7